Molecular programs in the venous pole of the developing murine heart

Von der Naturwissenschaftlichen Fakultät
der Gottfried Wilhelm Leibniz Universität Hannover
zur Erlangung des Grades

Doktorin der Naturwissenschaften
(Dr. rer. nat.)

genehmigte Dissertation von

Dipl.-Biotechnol. Julia Norden
geboren am 18.05.1978 in Walsrode

2011

Die vorliegende Arbeit wurde in der Zeit vom 01.10.2006 bis zum 06.05.2011 am Institut für Molekularbiologie der Medizinischen Hochschule Hannover in der Arbeitsgruppe von Prof. Dr. Andreas Kispert angefertigt.

Referent: Prof. Dr. Andreas Kispert

Korreferent: Prof. Dr. Hans-Jörg Jacobsen

Tag der Promotion: 25.07.2011

Für meine Eltern
und Jan.

Summary

At the beginning of mammalian heart development a linear tube is established that is able to undergo peristaltic contractions to pump the blood from a posterior inflow to an anterior outflow region. Further development of this cardiac tube involves the recruitment of highly proliferative, undifferentiated precursor cells at both poles and the subsequent differentiation into cardiomyocytes to form the right ventricle, the outflow tract and the atria. The development of the cardiac venous pole region, which includes the myocardial sleeves of the caval veins inside the pericardial cavity and the sinoatrial node (SAN), depends on the further addition of yet another distinct mesenchymal cell population. These precursor cells are positive for the T-box transcription factor Tbx18, but do not express the cardiac transcription factor *Nkx2-5*. In *Tbx18*-deficient embryos the development of the sinus venosus region is disturbed, the myocardialization of the sinus horns is delayed, the SAN is smaller, and the caval veins are positioned abnormal laterally inside the pleuropericardial membranes (PPMs), which are the precursors of the adult pericardium.

My analysis of mice deficient for the transcription factor *Wt1* revealed that the development of the sinus horns at the cardiac venous pole is coupled with that of the pericardium. A similar interdependence was detected in conditional *beta-catenin* loss- and gain-of-function mutant embryos suggesting that the release of the PPMs from the subcoelomic mesenchyme is essential for the development of a completely closed pericardium. This release depends both on *Wt1* and its downstream effector retinoic acid, as well as on canonical Wnt/beta-catenin signaling. Defects in the detachment of the PPMs from the lateral body wall resulted in pericardial hernia, a phenotype that is also described as a rare congenital human disease.

A second crucial process in the development of a complete pericardium is the closure of the pleuropericardial ducts (PPDs). These canals are necessary during early lung development, but they need to be closed for further pericardial development to occur correctly. In this work, I demonstrate the requirement of *Tbx18* for the attachment of the PPMs to the hilus of the lung and thus for the closure of the PPDs. In *Tbx18*-deficient embryos these canals remain open and a pericardial hernia occurs.

Furthermore, my analysis of conditional *beta-catenin* loss- and gain-of-function mutant embryos revealed the significance of canonical Wnt signaling for the myocardialization of the murine sinus horns. In the distinct *Tbx18*-positive, *Nkx2*-5-negative mesenchymal precursor cells of the sinus horns the canonical Wnt/beta-catenin signaling pathway is crucial for the maintenance of precursor cell proliferation.

In summary, this work provides new insights into the development of the murine venous pole of the heart and reveals the interdependence between sinus horn and pericardial development.

Keywords: murine heart development, pericardium, sinus horn

Zusammenfassung

In Säugetieren entsteht am Anfang der Herzentwicklung ein einfacher linearer Schlauch, der peristaltische Kontraktionen ermöglicht und dadurch das Blut vom posterior gelegenen Einflussbereich zum anterioren Ausflussbereich pumpt. Die weitere Entwicklung des Herzens beruht auf der Rekrutierung von stark proliferierenden, undifferenzierten Vorläuferzellen an beiden Polen des Herzens sowie deren anschließende Differenzierung zu Herzmuskelzellen. Diese bilden den rechten Ventrikel, den Ausflussbereich und die Atrien. Die Entwicklung des venösen Pols des Herzens, welcher das Myokard der Hohlvenen innerhalb der Perikardhöhle und den sinoatrialen Knoten (SAN) beinhaltet, erfolgt durch die spätere Addition einer weiteren mesenchymalen Vorläuferzellpopulation. Diese Vorläuferzellen sind positiv für den T-Box-Transkriptionsfaktor *Tbx18*, exprimieren aber nicht den kardialen Transkriptionsfaktor *Nkx2-5*. In *Tbx18*-Verlustmutanten ist die Entwicklung des Sinus venosus gestört, die Bildung des Myokards der Hohlvenen ist verzögert, der SAN ist verkleinert und die Hohlvenen sind abnormal innerhalb der Pleuroperikardmembranen (PPM), den Vorläufern des adulten Perikards, positioniert.

Meine Untersuchung der *Wt1*-Verlustmutanten ergab, dass die Entwicklung der Sinushörner am venösen Pol des Herzens und des Perikards gekoppelt sind. Eine ähnliche gegenseitige Abhängigkeit wurde in konditionellen *Beta-Catenin*-Verlust- und *Beta-Catenin*-Stabilisierungs-mutanten detektiert. Das deutet darauf hin, dass die Ablösung der PPM von dem subzölomischen Mesenchym für die Entwicklung eines geschlossenen Perikards notwendig ist. Diese Ablösung ist einerseits von *Wt1* und einem nachgeordneten Retinsäure-Signalweg, andererseits vom kanonischen Wnt/Beta-Catenin-Signalweg abhängig. Defekte in der Ablösung der PPM von der seitlichen Körperwand resultieren in einer perikardialen Hernie, einer Öffnung zwischen der Pleurahöhle und der Perikardhöhle. Diese Missbildung ist auch als seltene angeborene Krankheit in Menschen beschrieben.

Ein zweiter wichtiger Prozess bei der Entwicklung eines kompletten Perikards ist der Verschluss der pleuroperikardialen Kanäle (PPD). Diese Kanäle sind in der frühen Entwicklung der Lungen notwendig, müssen danach aber geschlossen werden, damit die Perikardentwicklung korrekt verläuft. In dieser Arbeit zeige ich, dass *Tbx18* für die Anhaftung der PPM an den Lungenhilus und damit für den Verschluss der PPD notwendig ist. In *Tbx18*-Verlustmutanten bleiben diese Kanäle offen und eine perikardiale Hernie entsteht.

Zusätzlich zu der Bedeutung des kanonischen Wnt Signalweges in der Perikardentwicklung weisen meine Analysen der konditionellen *Beta-Catenin*-Mutanten auch auf die Bedeutung des kanonischen Wnt-Signalweges für die Bildung der Herzmuskelzellen der Sinushörner hin. In der spezifischen *Tbx18*-positiven, *Nkx2-5*-negativen mesenchymalen Vorläuferzellpopulation der Sinushörner ist der kanonische Wnt-Signalweg für die Erhaltung der Proliferation der Vorläuferzellen notwendig.

Somit liefert die vorliegende Arbeit neue Erkenntnisse zur Entstehung des venösen Pols des Herzens und verdeutlich die gegenseitige Abhängigkeit der Entwicklung der Sinushörner und des Perikards.

Schlagworte: Herzentwicklung, Maus, Perikard, Sinus Horn

Table of Contents

Introduction

The heart is a highly complex and efficient muscle that will perform its function, the pumping of blood throughout the whole body, continuously during the complete life of its owner. It consists of two atria and two ventricles, which are separated by valves and septa (Figure 1). The superior and inferior caval veins receive the deoxygenated blood from the body and direct it into the right atrium, followed by the transport of the blood into the right ventricle. From here the blood is pumped through the pulmonary artery to the lungs. Afterwards the left atrium receives the oxygenated blood from the pulmonary veins, and conducts it to the left atrium that in turn pumps the blood through the aorta to the arterial circuit of the body.[1,2]

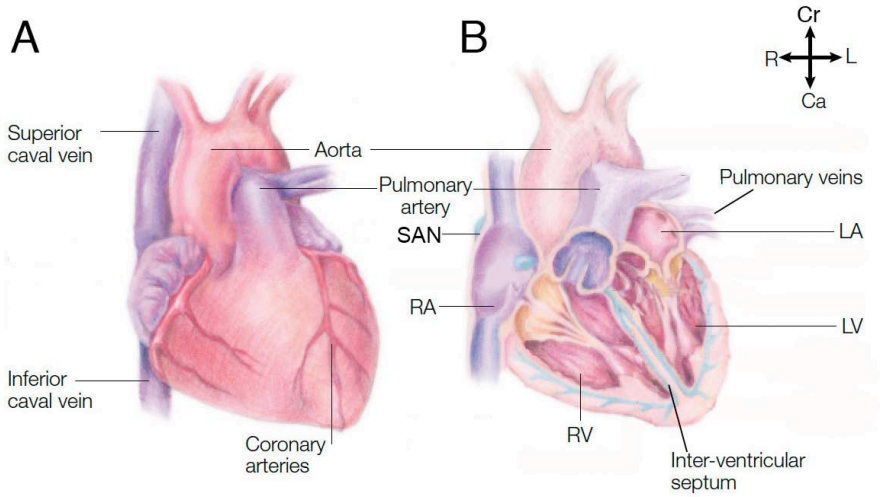

Figure 1. Illustration of an adult human heart. The main components of a whole (**A**) or sectioned (**B**) heart are depicted. LA, left atrium; LV, left ventricle; RA, right atrium; RV, right ventricle; SAN, sinoatrial node; Modified from (2)

To achieve an efficient blood transport, the heartbeat of the atria and ventricles is synchronized by the cardiac conduction system. Its main pacemaker is the sinoatrial node (SAN) that is positioned at the entrance of the superior caval vein into the right atrium. In combination with the right superior caval vein, the inferior caval vein, the persisting left caval vein (the coronary sinus in humans), and the sinus venarum, the SAN represents the systemic venous return of the murine heart.[3]

The heart is a common focus of congenital malformations such as ventricular or atrial septal defects, sinus venosus interatrial communications, patent ductus arteriosus, transposition of the great arteries, or double-outlet right ventricle.[4] Cardiac malformations account for approximately 30% of prenatal death, and congenital heart defects are the main cause for death in the first year after birth.[5,6] Furthermore, atrial arrhythmias in the systemic venous return of the heart often have their origin in genetic deficiencies during heart formation.[7] Therefore, embryonic cardiac

development has to be tightly regulated as marginal alterations may lead to severe congenital heart defects. In the last years the regulatory mechanisms involved in specification of cardiac lineages and cardiac morphogenesis have been studied extensively, but the genetic circuits regulating cardiac development are far from being completely understood.

The formation of the embryonic cavities and cardiac development occur in parallel

The heart is positioned inside the pericardial cavity, which is required for protection and positioning of the heart, throughout embryonic development and adult life. This pericardial cavity develops as part of the intraembryonic cavity, which arises between the somatic and splanchnic mesoderm by the gastrulation movements of the embryo (Figure 2 and Figure 3).[8,9]

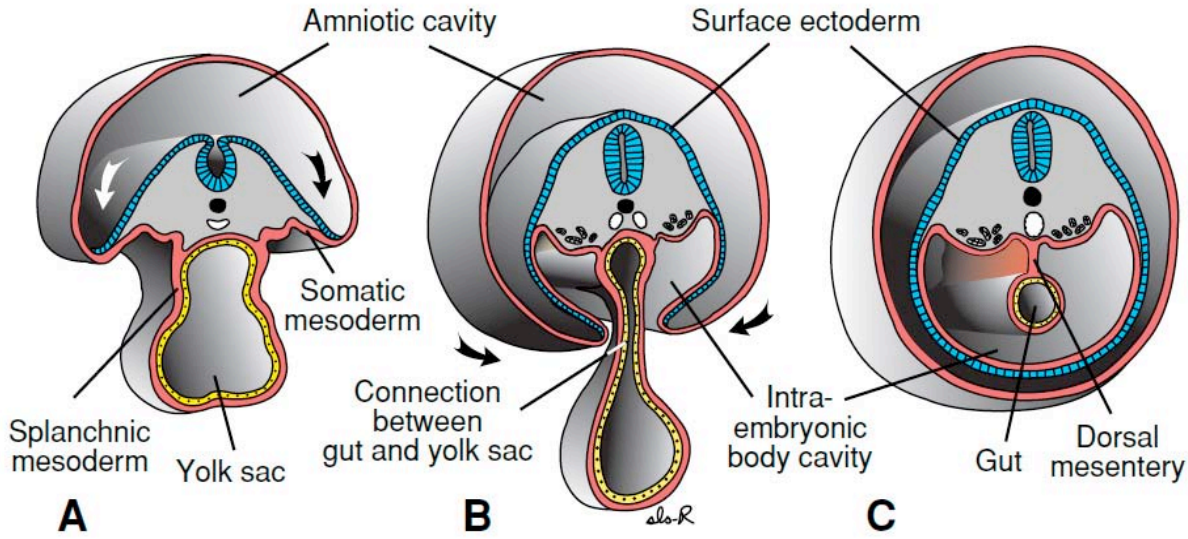

Figure 2. Formation of the intraembryonic cavity during human embryonic development. Transverse section trough different stages of human embryonic development (**A** aged 21 days, **B** in the middle of the 4th week, and **C** at the end of the 4th week) to clarify the establishment of the intraembryonic cavity. Modified from (8).

The intraembryonic coelom is first divided into a peritoneal and a thoracic cavity by the ingrowth of the septum transversum, a thick mesenchymal tissue. This separation is not complete in the early human embryo, but two pericardioperitoneal ducts on each side of the foregut remain to allow the growth of the lung buds inside these canals (Figure 3).

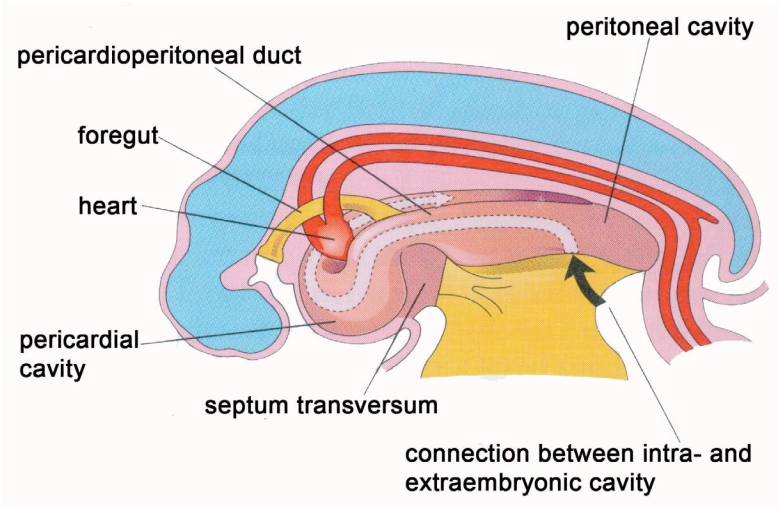

Figure 3. Scheme of the intraembryonic coelom in the 4th week of human embryonic development. At this stage of development the intraembryonic coelom consists of the pericardial and peritoneal cavities, which are connected by the pericardioperitoneal ducts on both sides next to the foregut. Modified from (9).

While the size of the lung increases, the pericardioperitoneal canals expand dorsally, laterally, and ventrally into the subcoelomic mesenchyme. During this process the laterodorsal mesenchyme next to the lung disappears and the pleural cavity expands inside the pericardioperitoneal ducts. Afterwards, the pericardial and pleural cavities are separated by the closure of the pleuropericardial duct and the formation of the pericardium, a double-walled mesothelial sac that completely surrounds the heart and the roots of the great vessels. Furthermore, the development of the diaphragm disconnects the pleural and peritoneal cavities.[8,10,11] These processes, especially the formation of the pericardium, are only partially analyzed in mice until now, and the genetic mechanisms regulating its development have remained unidentified.

Cardiac development also starts during gastrulation, in the middle of the 3rd week in humans, and accordingly in mice at embryonic day (E) 6.5-7.5, by the migration of cardiac progenitor cells into the mesodermal layer of the embryo.[8,12] These cardiac progenitors are separated from the somatic mesoderm by the pericardial cavity (Figure 4A).[1] During further development the cardiac progenitor cells merge across the anterior midline and form the cardiac crescent around E7.75. The cardiac cells continue to move ventrocaudally to form a linear heart tube until E8.25, a process that is connected with the growth of the head folds and the ventral closure of the embryo (Figure 4B). The fully functional linear heart tube consists of two layers, the myocardium and the endocardium, and is connected to the foregut by the dorsal mesocardium. The wall of the thoracic cavity that surrounds the heart tube is named (embryonic) pericardium at this stage. Further development between E8.25 and E10.5 includes the addition of the epicardium to the heart, the elongation of the heart tube and a complex looping process inside the pericardial cavity, which results in a dorsocranial movement of the common atrium and the caval veins.

(Figure 4C). Additionally, the future chambers balloon out of the heart tube[13], and the separation of the chambers starts by the formation of endocardial cushions and the interventricular septum. Further remodeling results in the mature adult heart (Figure 4D).

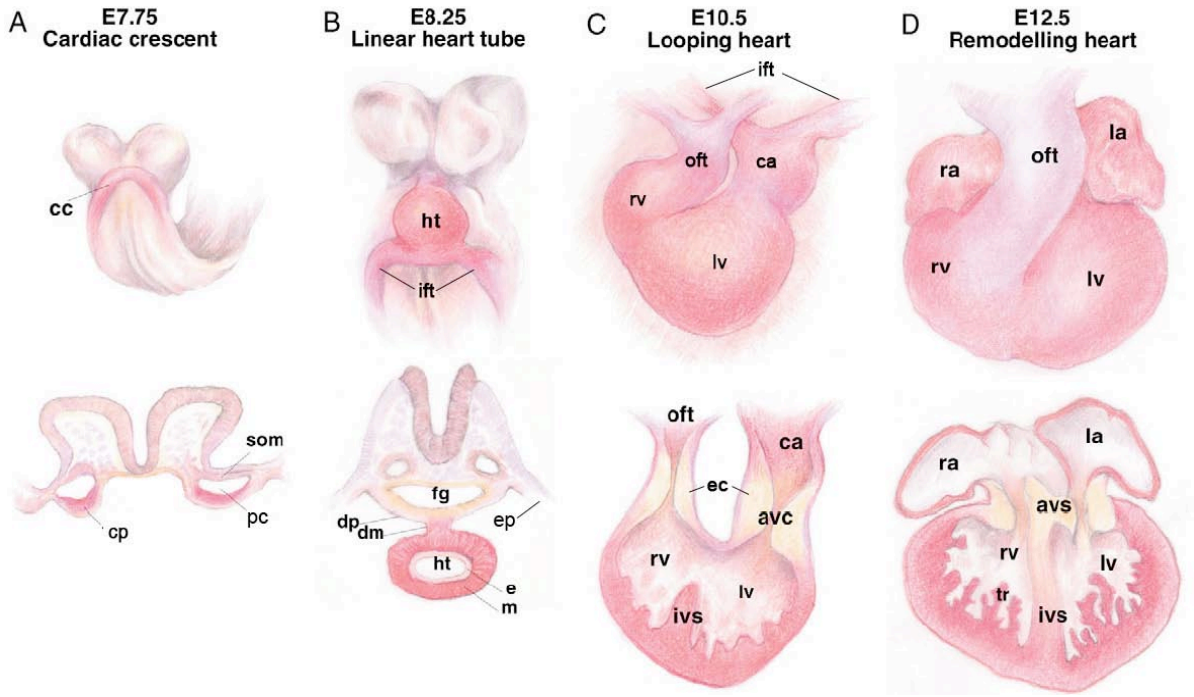

Figure 4. Schematic illustration of murine heart development. A – D, Illustration of different stages of cardiac development at E7.75 (A), E8.25 (B), E10.5 (C), and E12.5 (D). The upper row shows a whole embryo or an isolated heart, a representative section is depicted beneath. See main text for further information. avc, atrioventricular canal; avs, atrioventricular septum; ca, common atrium; cc, cardiac crescent; cp, cardiac progenitor; dm, dorsal mesocardium; dp, dorsal pericardium; e, endocardium; ec, endocardial cushion; ep, embryonic pericardium; fg, foregut; ht, heart tube; ift, inflow tract; ivs, interventricular septum; la, left atrium; lv, left ventricle; m, myocardium; pc, pericardial cavity; oft, outflow tract; ra, right atrium; rv, right ventricle; som, somatic mesoderm; tr, trabeculae. Modified from (1).

Cardiac cells are derived from different precursor cell populations

Two mesodermal progenitor pools contribute cells to the murine developing heart in a spatiotemporally specific manner, both express the cardiac transcription factor *NK2 transcription factor related, locus 5* (*Nkx2-5*) (Figure 5).[14]

The cardiac crescent derives from cells of the so-called first heart field (FHF) and encompasses mainly progenitor cells for the left ventricle and parts of the atria of the mature heart.[12] These cells are marked by an early differentiation into the cardiac lineage, a low proliferation rate, and the expression of *heart and neural crest derivatives expressed transcript 1 (Hand1)*.[12] Precursor cells of the second heart field (SHF), which are positioned posterior and medially to the FHF cells, elongate the early heart tube by addition of progenitor cells on both the anterior (outflow) and the posterior (inflow) pole after E8.5. Therefore the SHF derived cells are the major contributor to the mature heart. Progenitor cells of the SHF are highly proliferative,[15] and remain

undifferentiated until they enter the growing heart. Recent findings revealed the existence of distinctive subpopulations inside the SHF that can be distinguished by gene expression profiles and their positioning next to the developing heart tube (Figure 5).[14]

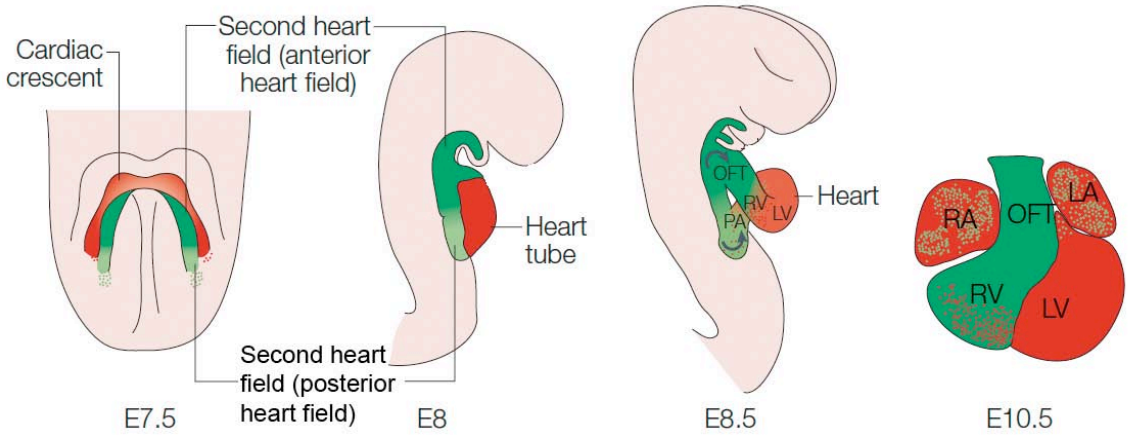

Figure 5. Two sources of mesodermal progenitor cells contribute to the developing heart from E7.5 to E10.5. The location and derivates of the first heart field (FHF) are shown in red, second heart field (SHF) derived structures are shown in green. Frontal views are depicted for E7.5 and E10.5, the elongation of the heart tube is displayed by lateral views at E8 and E8.5. LA, left atrium; LV, left ventricle; PA, primitive atria; OFT, outflow tract; RA, right atrium; RV, right ventricle. Modified from (12).

The anterior subpopulation of the SHF contributes to the arterial pole of the heart that consists of the outflow tract with the pulmonary trunk and the aortic arches. The anterior SHF is marked by an expression of the *fibroblast growth factor* genes *Fgf8* and *Fgf10*, and the T-box transcription factor *Tbx1*. Lately, the anterior heart field has been studied intensively, therefore a molecular network controlling its contribution to the arterial pole of the heart is emerging. *Tbx1* supports proliferation of SHF progenitor cells and inhibits their differentiation into cardiomyocytes possibly by induction of *Fgf8* expression.[16] The FGF and the bone morphogenetic protein (BMP) signaling pathways have opposing roles during SHF development. In the anterior heart field, FGF signaling pathway components (*Fgf8* and *Fgf10*) induce progenitor cell proliferation and smooth muscle differentiation, whereas BMP signaling pathway components (*Bmp2* and *Bmp4*) lead to the differentiation of progenitor cells into cardiomyocytes.[17,18]

Cells of the posterior SHF contribute to the inflow region of the heart, and express the canonical Wnt signaling ligand *wingless-related MMTV integration site 2* (*Wnt2*), but not the anterior SHF marker genes (*Fgf8, Fgf10, Tbx1*). The development of the atria and the atrioventricular canal thereby depends on a feed-forward loop by *Wnt2* and *GATA binding protein 6 (Gata6)*.[19] The canonical Wnt signaling pathway maintains SHF cells in an undifferentiated, proliferative state, and needs to be downregulated for myocardial differentiation in the entire SHF.[20]

Canonical Wnt signaling requires the protein beta-catenin (Ctnnb1) as a signaling mediator. In the absence of Wnt signaling, the Ctnnb1 protein gets phosphorylated by a destruction complex and afterwards degraded by the proteasome. The binding of a Wnt ligand to a Frizzled (Fzd)

receptor results in the disassembly of the destruction complex, the Ctnnb1 protein is stabilized and translocates into the nucleus, where it activates transcription of target genes by interaction with TCF/LEF transcription factors. During heart development, Ctnnb1-mediated Wnt signaling has divergent effects, depending on the developmental context, and therefore needs to be tightly regulated in a spatiotemporal manner.[20]

The myocardial sinus horns, the intrapericardial part of the caval veins, are not derived from the first or second heart fields, but they are added to the growing heart tube after the formation of atrial myocardium starting from E9.5.[21] Their mesenchymal precursor cells represent a distinct domain with a transcriptional network that is characterized by the absence of *Nkx2-5* and specific *T-box 18* (*Tbx18*) expression. The loss of *Tbx18* results in a delayed myocardialization of the sinus horns, which are positioned abnormal laterally inside the pericardium.[21,22]
Tbx18 belongs to a family of transcription factors that are characterized by its highly conserved DNA-binding domain, the T-box. In mammals six of the 17 known *Tbx* genes are crucial for embryonic heart development.[23] *Tbx18* is also expressed in the proepicardial organ (PEO), a transitory mesothelial cell cluster at the posterior pole. Starting from E9.0, cells of the PEO adhere to the naked myocardium of the heart and form the epicardium. During the onset of development, some epicardial cells undergo epithelial mesenchymal transition and become epicardium-derived cells (EPDCs) that are crucial for the formation of cardiac fibroblasts, smooth muscle cells of the coronary vessels, and coronary endothelial cells.[24] Furthermore, *Tbx18* and *Tbx3* are expressed in the SAN. Absence of *Tbx18* or *Tbx3* results in a decreased SAN volume, but both *Tbx* genes act independently during SAN development. *Tbx18* is crucial for the formation of the SAN head, whereas *Tbx3* regulates differentiation into SAN myocytes.[25] *Tbx18* is also expressed in the interventricular septum and the left ventricular wall starting from E10.5,[26] but the importance of this *Tbx18* expression domain remains to be deciphered.
The molecular network regulating murine sinus horn development is poorly understood as only a few genes have been described therein additionally to *Tbx18*. *Podoplanin* (*Pdpn*) is specifically expressed in the *Nkx2-5*-negative mesenchyme and myocardium of the venous pole,[27] and in *Pdpn*-deficient mice the myocardium of the cardinal veins is hypoplastic and the cardinal veins are dilated.[28] Moreover, the homeodomain transcription factor *short stature homeobox 2* (*Shox2*) is expressed in the sinus horn myocardium, and required for the recruitment of this myocardium.[29]

In addition to *Tbx18,* the PEO and the epicardium express the zinc finger transcription factor *Wilms tumor 1* (*Wt1*).[30] *Wt1* was first described as a tumor suppressor gene in the etiology of a pediatric kidney cancer (named Wilms tumor) that resulted from mutations inside the human *WT1* gene. However, further studies in mice revealed the importance of *Wt1* during embryonic organ formation, especially development of the genitourinary system and mesothelial tissues.

Wt1-deficient mice die around midgestation due to severe heart defects, and no kidneys are formed in these embryos.[31] *Wt1* is expressed in all mesothelial tissues like the epicardium, pericardium, and the lining of the body cavities (pericardial, pleural, and peritoneal).[32] In general, mesothelial tissues can be distinguished in a visceral mesothelium, the lining of the internal organs (e.g. heart and lung), and a parietal mesothelium, which covers the body wall. Therefore, the epicardium can also be considered as visceral pericardium. It is separated from the (parietal) pericardium by the pericardial cavity that is filled with the serous pericardial fluid. This pericardial fluid is crucial for the smooth movement of the heart inside the pericardial cavity.[33]

Aim of this thesis

The development of the heart mainly depends on the elongation of the early heart tube by addition of undifferentiated precursor cells, as most of the mature adult heart derives from the progenitor cells of the second heart field (see above). After the addition of the atria onto the growing heart tube, a third population of progenitor cells elongates the heart at the venous pole and forms the myocardial sleeves of the caval veins. At the beginning of my thesis, Christoffels *et al*. identified that these cells do not belong to the first or second heart field, but express the T-box transcription factor *Tbx18*.[21] This finding implicated a distinct character of the sinus horn progenitor population. To obtain additional knowledge about the development of the sinus venosus region of the heart, the aim of my thesis was to further analyze the development of the venous pole and its mesothelial lining.

Canonical Wnt/beta-catenin signaling is necessary for the maintenance of second heart field derived cells in a proliferative, undifferentiated state.[20] A similar mechanism may be crucial for the addition of sinus venosus precursor cells to the growing heart. For this reason, I wished to analyze conditional beta-catenin gain- and loss-of-function mutant mice for alterations in the formation of the sinus horns. Additional work was to focus on the morphological and molecular analysis of mutant mice as well as on lineage tracing experiments to define the contribution of both *Wt1* and *Tbx18* expressing cells to the developing sinus venosus region of the heart.

Sinus horn development is coupled with the formation of the murine pericardium, but the cellular and molecular programs underlying the formation of this tissue were completely unknown at the beginning of my work. To gain more insights into pericardial development, wildtype and different mutant mice with pericardial defects were to be analyzed by histological and molecular means.

Thus, this thesis focuses on the development of the posterior pole of the heart including the sinus horns and the pericardium. It reveals new insights into the cellular and molecular processes during the formation of this cardiac subregion.

Wt1 and Retinoic Acid Signaling in the Subcoelomic Mesenchyme Control the Development of the Pleuropericardial Membranes and the Sinus Horns

Julia Norden[1], Thomas Grieskamp[1], Ekkehart Lausch[2], Bram van Wijk[3], Maurice J. B. van den Hoff[3], Christoph Englert[4], Marianne Petry[1], Mathilda T.M. Mommersteeg[3], Vincent M. Christoffels[3], Karen Niederreither[5], and Andreas Kispert[1,*]

[1] Institut für Molekularbiologie, OE5250, Medizinische Hochschule Hannover, Carl-Neuberg-Str.1, D-30625 Hannover, Germany
[2] Centre for Pediatrics and Adolescent Medicine, University of Freiburg, Mathildenstraße 1, D-79106 Freiburg, Germany
[3] Department of Anatomy, Embryology and Physiology, Academic Medical Center, University of Amsterdam, Meibergdreef 15 L2-108, 1105 AZ Amsterdam, The Netherlands
[4] Molecular Genetics Group, Leibniz Institute for Age Research – Fritz Lipmann Institute, Beutenbergstr. 11, D-07745 Jena, Germany
[5] Departments of Medicine and Molecular and Cellular Biology, Center for Cardiovascular Development, Baylor College of Medicine, One Baylor Plaza, Houston, Texas 77030, USA

[*]Author for correspondence:

E-MAIL: kispert.andreas@mh-hannover.de
TEL.: +49 511 5324017
FAX.: +49 511 5324283

Running title: Wt1 and RA signaling in cardinal vein formation

Published in Circulation Research (Circ. Res. 2010;106;1212-1220).
Reprinted with permission.

WOLTERS KLUWER HEALTH LICENSE TERMS AND CONDITIONS

Mar 13, 2011

This is a License Agreement between Julia Norden ("You") and Wolters Kluwer Health ("Wolters Kluwer Health") provided by Copyright Clearance Center ("CCC"). The license consists of your order details, the terms and conditions provided by Wolters Kluwer Health, and the payment terms and conditions.

All payments must be made in full to CCC. For payment instructions, please see information listed at the bottom of this form.

License Number	2627180037463
License date	Mar 13, 2011
Licensed content publisher	Wolters Kluwer Health
Licensed content publication	Circulation Research
Licensed content title	Wt1 and Retinoic Acid Signaling in the Subcoelomic Mesenchyme Control the Development of the Pleuropericardial Membranes and the Sinus Horns
Licensed content author	Julia Norden
Licensed content date	Apr 16, 2010
Volume Number	106
Issue Number	7
Type of Use	Dissertation/Thesis
Requestor type	Individual
Title of your thesis / dissertation	Molecular programs in the venous pole of the developing murine heart
Expected completion date	May 2011
Estimated size(pages)	100
Billing Type	Invoice
Billing Address	Hohestieg 11 Braunschweig, other 38118 Germany
Customer reference info	
Total	0.00 EUR
Terms and Conditions	

Wt1 and Retinoic Acid Signaling in the Subcoelomic Mesenchyme Control the Development of the Pleuropericardial Membranes and the Sinus Horns

Julia Norden, Thomas Grieskamp, Ekkehart Lausch, Bram van Wijk, Maurice J.B. van den Hoff, Christoph Englert, Marianne Petry, Mathilda T.M. Mommersteeg, Vincent M. Christoffels, Karen Niederreither, Andreas Kispert

Rationale: The cardiac venous pole is a common focus of congenital malformations and atrial arrhythmias, yet little is known about the cellular and molecular mechanisms that regulate its development. The systemic venous return myocardium (sinus node and sinus horns) forms only late in cardiogenesis from a pool of pericardial mesenchymal precursor cells.

Objective: To analyze the cellular and molecular mechanisms directing the formation of the fetal sinus horns.

Methods and Results: We analyzed embryos deficient for the *Wt1* (Wilms tumor 1) gene and observed a failure to form myocardialized sinus horns. Instead, the cardinal veins become embedded laterally in the pleuropericardial membranes that remain tethered to the lateral body wall by the persisting subcoelomic mesenchyme, a finding that correlates with decreased apoptosis in this region. We show by expression analysis and lineage tracing studies that *Wt1* is expressed in the subcoelomic mesenchyme surrounding the cardinal veins, but that this *Wt1*-positive mesenchyme does not contribute cells to the sinus horn myocardium. Expression of the *Raldh2* (aldehyde dehydrogenase family 1, subfamily A2) gene was lost from this mesenchyme in $Wt1^{-/-}$ embryos. Phenotypic analysis of *Raldh2* mutant mice rescued from early cardiac defects by retinoic acid food supply revealed defects of the venous pole and pericardium highly similar to those of $Wt1^{-/-}$ mice.

Conclusions: Pericardium and sinus horn formation are coupled and depend on the expansion and correct temporal release of pleuropericardial membranes from the underlying subcoelomic mesenchyme. *Wt1* and downstream *Raldh2*/retinoic acid signaling are crucial regulators of this process. Thus, our results provide novel insight into the genetic and cellular pathways regulating the posterior extension of the mammalian heart and the formation of its coelomic lining. (*Circ Res*. 2010;106:1212-1220.)

Key Words: sinus horn ■ venous pole ■ sinoatrial node ■ Tbx18 ■ Raldh2

The systemic venous return of the mature mammalian heart, which terminates in the right atrium, consists of multiple anatomic components including the myocardial sleeves of the right superior and inferior caval veins, the sinoatrial node (SAN), the coronary sinus (persisting left caval vein in the mouse), and the sinus venarum.[1] The systemic venous return is a focus of congenital malformations and atrial arrhythmias,[2,3] necessitating insight into the cellular and molecular programs by which it arises during cardiac development. Most myocardial components of the heart are not represented in its initial anlage, but are continuously added by recruitment and differentiation of precursor cells.[4] The sinus horns, the myocardial parts of the common cardinal veins upstream of the venous valves that bulge into the pericardial cavity, form from pericardial precursors that differentiate into sinus venosus myocardium around the systemic venous connection to the atrium.[5] They form only after embryonic day (E)9.5, when outflow tract, left and right ventricle, and the common atrium have already been established. In adults, most of the right sinus horn myocardium is incorporated into the right atrium to form the sinus venarum. In humans, the left sinus horn will lose its connection to the body and form the coronary sinus, whereas in mouse it will persist as the left superior caval vein.

Few genes regulating venous pole development have been characterized, including the *Tbx18* (T-box transcription factor 18) that marks the sinus horn lineage.[5,6] *Wt1* (Wilms tumor 1) was initially identified as a tumor suppressor gene involved in the etiology of Wilms' tumor in humans. Genetic analyses in the

Original received June 26, 2009; resubmission received January 19, 2010; revised resubmission received February 10, 2010; accepted February 11, 2010.

From the Institut für Molekularbiologie (J.N., T.G., M.P., A.K.), OE5250, Medizinische Hochschule Hannover, Germany; Centre for Pediatrics and Adolescent Medicine (E.L.), University of Freiburg, Germany; Department of Anatomy, Embryology and Physiology (B.v.W., M.J.B.v.d.H., M.T.M.M., V.M.C.), Academic Medical Center, University of Amsterdam, Netherlands; Molecular Genetics Group (C.E.), Leibniz Institute for Age Research–Fritz Lipmann Institute, Jena, Germany; and Departments of Medicine and Molecular and Cellular Biology (K.N.), Center for Cardiovascular Development, Baylor College of Medicine, Houston, Tex.

Correspondence to Andreas Kispert, Institut für Molekularbiologie, OE5250, Medizinische Hochschule Hannover, Carl-Neuberg-Str.1, D-30625 Hannover, Germany. E-mail kispert.andreas@mh-hannover.de

Circulation Research **is available at http://circres.ahajournals.org** **DOI: 10.1161/CIRCRESAHA.110.217455**

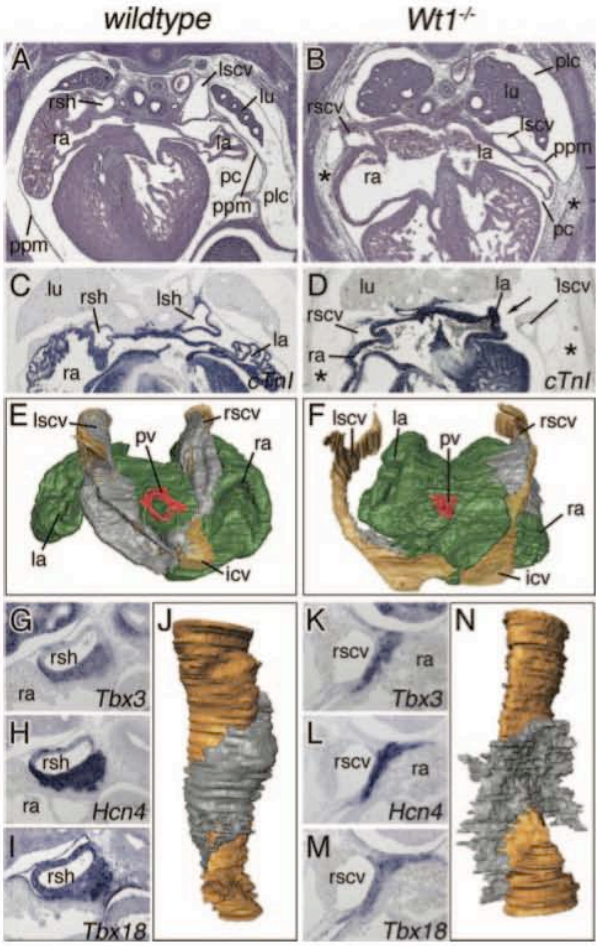

Figure 1. Sinus horn defects in *Wt1*-deficient hearts. Histological, molecular and morphological analyses of sinus horns **(A through F)** and the SAN **(G through N)** were carried out on transverse sections of the venous pole region of E14.5 wild-type and $Wt1^{-/-}$ hearts. **A through F,** Histological stainings with hematoxylin/eosin **(A and B)**, in situ hybridization analysis of *cTnI* expression **(C and D)**, and 3D reconstructions of serial sections stained for *cTnI* in a dorsal–posterior view. Atrial myocardium is shown in **green**, cardinal vein myocardium in **gray**, the lumen of the cardinal veins in **brown**, and the pulmonary vein myocardium in **red (E and F)**. **Asterisks (B and D)** mark persisting subcoelomic mesenchyme. **G through N,** In situ hybridization analyses of sections through the base of the cardinal veins for SAN marker genes with probes as indicated **(G through I and K through M)**, and 3D reconstructions of serial sections stained for *Tbx3* expression through the cardinal veins (in **brown**) to visualize the SAN (in **gray**) **(J and N)**. icv indicates inferior cardinal vein; la, left atrium; lu, lung; lscv, left superior cardinal vein; pc, pericardial cavity; plc, pleural cavity; ppm, pleuropericardial membrane; pv, pulmonary vein; ra, right atrium; rscv, right superior cardinal vein; rsh, right sinus horn.

mouse subsequently uncovered essential roles for the transcription factor Wt1 in the development of numerous organ systems.[7] In the heart, *Wt1* is required for the mesenchymal transition of epicardial cells. Failure to provide cellular constituents to the developing coronary vessels results in pericardial bleeding and midgestational lethality.[8,9] Here, we present data demonstrating an additional function of *Wt1* in the formation of the common cardinal veins and the pleuropericardial membranes (PPMs). We implicate retinoic acid (RA) signaling in the etiology of these defects and show a primary requirement of *Wt1* and *Raldh2* (aldehyde dehydrogenase family 1, subfamily A2) in the subcoelomic mesenchyme from which the PPMs are released.

Non-standard Abbreviations and Acronyms

E	embryonic day
EGFP	enhanced green fluorescent protein
GFP	green fluorescent protein
PPM	pleuropericardial membrane
RA	retinoic acid
RARE	retinoic acid response element
Raldh2	aldehyde dehydrogenase family 1, subfamily A2
SAN	sinoatrial node
Tbx18	T-box transcription factor 18
Wt1	Wilms tumor 1

Methods

Animal care was in accordance with national and institutional guidelines. Mice carrying a null allele of *Wt1* ($Wt1^{tm1Jae}$),[10] $Tbx18^{GFP}$ ($Tbx18^{tm2Akis}$)[5] and *Raldh2* ($Aldh1a2^{tm1Ipc}$),[11] $R26^{lacZ}$ and $tetO_{bi}LacZ$-*GFP* reporter mice,[12,13] and the *RARE-Hsp68LacZ* [synonym: *Tg(RARE-Hspa1b/lacZ)12Jrt/J*] reporter transgenic line,[14] which harbors a tetrameric repeat of the *RARβ2 RARE* linked to the *Hsp68* minimal promoter used to determine RA signaling, were all described before. For the $Wt1^{BAC\text{-}IRES\text{-}EGFPCre}$ transgenic line, the BAC clone RP23–266M16 was modified by inserting an IRES/EGFP-Cre cassette 17bp downstream of the translation stop site of the *Wt1* gene. (The generation and evaluation of this line will be described elsewhere.) In $Wt1^{rTA}$ mice, the coding sequence of an improved tetracycline-dependent transactivator *rTA2S*[15] was introduced into the *Wt1* locus by gene targeting (E Lausch, S Fees, C Steinwender, C Spangenberg, L Eshkind, E Bockamp, B Zabel, manuscript in preparation). All mouse lines were maintained on an outbred (NMRI or FvB) background.

An expanded Materials and Methods section is available in the Online Data Supplement at http://circres.ahajournals.org.

Results

Defects in the Systemic Venous Return of Wt1-Deficient Hearts

$Wt1^{-/-}$ mice maintained on an NMRI outbred background died during midgestation presenting defects reported on earlier, including lack of kidneys, diaphragmatic hernia, and defects in coronary vessel formation the latter of which may underlie embryonic lethality. Yet, histological inspection of surviving embryos at E14.5 revealed an undescribed variation in the systemic venous return that prompted us to analyze the cardiac venous pole more carefully (Figure 1). In wild-type embryos of this stage, the sinus horns bulged into the pericardial cavity (Figure 1A). These sinus horns were completely myocardialized (cardiac troponin I–positive; Figure 1C). Pericardial and pleural cavities were separated by the PPMs that were stretched out as thin tissue layers between their roots in the lung bud and their distal attachment points in the ventrolateral body wall (Figure 1A and 1C). In contrast, *Wt1* mutant hearts featured thinner, nonmyocardialized cardinal veins (Figure 1B and 1D). These occupied an abnormal lateral position within the PPMs that also tethered the atrial roofs to the body wall. The pleural cavity was not fully expanded, leaving the pericardium ventrally attached to the body wall by a mesh of loose

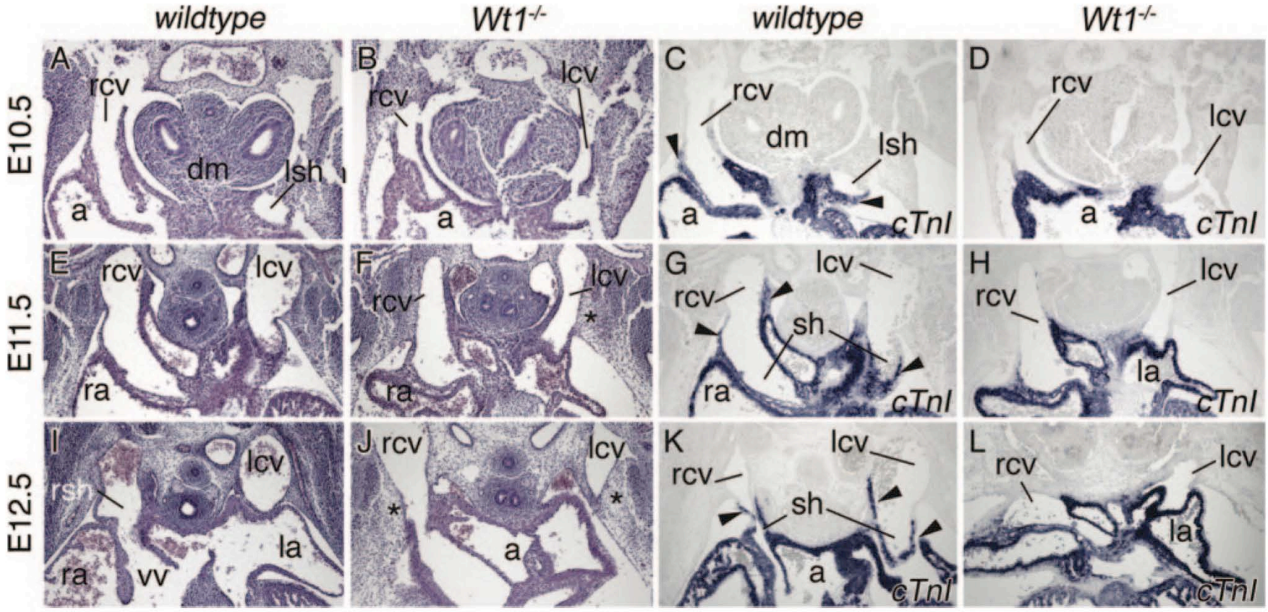

Figure 2. Developmental onset of sinus horn defects in *Wt1*$^{-/-}$ hearts. Histological and molecular analyses of sinus horn development were carried out on transverse sections of the venous pole region of E10.5 to E12.5 wild-type and *Wt1*$^{-/-}$ hearts as indicated. **A through L,** Hematoxylin/eosin stainings **(A, B, E, F, I, and J)** and in situ hybridization analysis of *cTnI* expression on adjacent sections **(C, D, G, H, K, and L)**. **Arrowheads** point to myocardialized sinus horns. **Asterisks** mark subcoelomic mesenchyme in the mutant. a indicates common atrium; dm, dorsal mesocardium; la, left atrium; lcv, left common cardinal vein; lsh, left sinus horn; ra, right atrium; rcv, right common cardinal vein; rsh, right sinus horn; sh, sinus horn; vv, venous valves.

mesenchymal cells (Figure 1B). More anteriorly on the left side, pleural and pericardial cavities communicated by a thin canal leaving space for the atria to touch the lung (arrow in Figure 1D). Because sections planes between different embryos were sometimes difficult to match, we performed serial sections and subsequent 3D reconstruction analysis. This confirmed our histological findings and showed that in *Wt1*$^{-/-}$ hearts, the nonmyocardialized superior cardinal veins were thin and lying lateral to the atria near the body wall. The defects were restricted to the sinus horns, as the myocardium of pulmonary vein and the dorsal atrial wall myocardium appeared unchanged (Figure 1F).

The SAN is an elongated "comma-shaped" structure at the junction of the right venous entrance and the atrium expressing *Tbx3*, the *Hcn4* gene (hyperpolarization-activated, cyclic nucleotide-gated K^+ 4), and *Tbx18* (Figure 1G through 1I).[6] In *Wt1*$^{-/-}$ hearts, these markers were detected at E14.5 but the domain of expression protruded away from the right superior cardinal vein (Figure 1K through 1M). Three-dimensional reconstruction of the SAN from serial sections stained for *Tbx3* expression confirmed that the SAN myocardium was not wrapped around the sinus horn as in the wild type (Figure 1J) but had an open "wing"-like structure (Figure 1N). Volume measurements revealed that the SAN cell mass was not significantly reduced in *Wt1*-deficient embryos (data not shown), arguing that SAN morphology rather than myocardial differentiation and growth are affected by loss of *Wt1*.

Sinus Horn Defects of *Wt1*$^{-/-}$ Embryos Arise Early in Development

To determine the onset of venous pole defects in *Wt1*-deficient hearts, we analyzed embryos at earlier developmen-

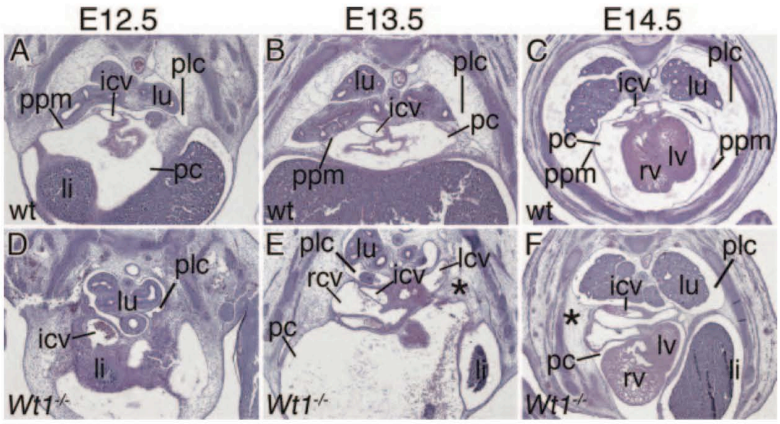

Figure 3. Developmental onset of mesothelial defects in *Wt1* hearts. Histological analysis by hematoxylin and eosin staining of PPM development was carried out on transverse sections of the posterior venous pole region of E12.5 to E14.5 wild-type and *Wt1*$^{-/-}$ hearts as indicated. li indicates liver; other abbreviations are as in Figures 1 and 2.

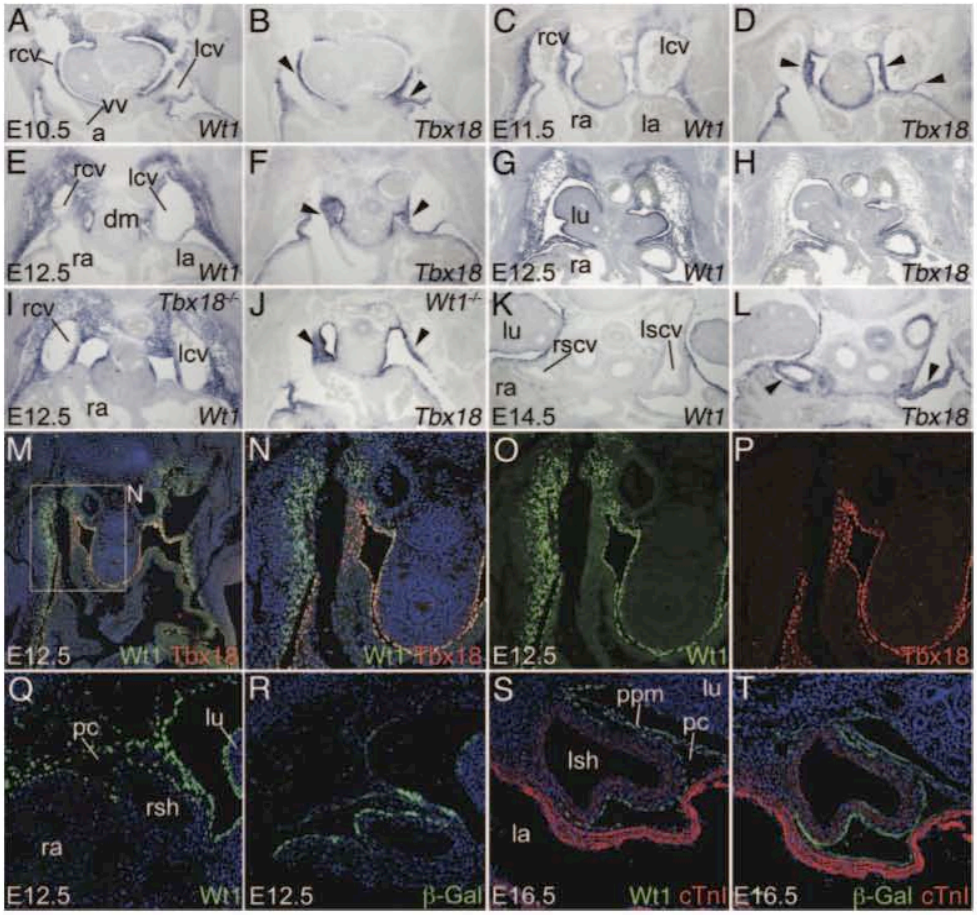

Figure 4. *Wt1* expression in the subcoelomic mesenchyme. A through L, Comparative in situ hybridization analysis of *Wt1* and *Tbx18* expression on transverse sections of the venous pole region of E10.5 to E14.5 hearts of wild-type **(A through H, K, and L)**, $Tbx18^{-/-}$ **(I)** and $Wt1^{-/-}$ **(J)** embryos. **Black arrowheads** point to *Tbx18* expression in the mesenchyme and myocardium of the sinus horns. **M through P,** Immunofluorescence analysis of Wt1 and Tbx18 protein at the cardiac venous pole. **Q through T,** Comparative immunofluorescence analysis of Wt1 and β-galactosidase protein expression in the venous pole region in $Wt1^{BAC\text{-}IRES\text{-}EGFPCre}/+$; $Rosa26^{LacZ}/+$ embryos. cTnI immunofluorescence **(red)** marks sinus horn and atrial myocardium. Stages, genotypes, and probes are as indicated. Abbreviations are as in the legends of Figures 1 and 2.

tal time points (Figures 2 and 3). In $Wt1^{-/-}$ embryos, the venous pole region appeared unchanged at E9.5 (data not shown). At E10.5, protrusions of the cardinal veins into the pericardial cavity generated short sinus horns that, however, failed to expand and myocardialize at subsequent stages (Figure 2A through 2L). Analysis of *Hcn4* expression indicated presence of dispersed pacemaker tissue at E12.5 (Online Figure I). The subcoelomic mesenchyme around the common cardinal veins was present but loosely organized at E11.5 and 12.5 (asterisks in Figure 2F and 2J). At E12.5, a mesothelial lining separated the posterior pleural and pericardial cavities in the wild type (Figure 3). These PPMs originated laterally in the body wall at the height of the developing ribs, and projected medially to connect to the hilus of the lung bud at more anterior levels (Figure 3A). In subsequent stages, the lateral insertion points moved ventrally following the distal extension of the ribs to become loosely connected to the sternum at E14.5. During this growth phase, the PPMs were stretched out to thin epithelial sheets. The pleural cavity dramatically gained in volume. Loose mesenchymal tissue initially filling the pleural cavity at the onset of its expansion was completely cleared by E14.5 (Figure 1A; Figure 3B and 3C). In $Wt1^{-/-}$ embryos, PPMs were not apparent as distinct mesothelial linings separating the 2 cavities at E12.5 and E13.5. Instead, the pericardium was tethered to the atrial roof and cardinal veins on one side and to a mesenchymal mesh that was continuous with the lateral body wall on the other side (Figure 3D and 3E). Inflation of this subcoelomic mesenchyme was delayed and clearance not achieved by E14.5 (Figures 1B and 3F). Thus, defects in sinus horn formation and PPM/subcoelomic mesenchyme organization arise early in sinus horn/caval vein development and may be linked.

Wt1 Is Not Expressed in Sinus Horns but in Mesothelia and the Underlying Mesenchyme

To determine the temporal and spatial requirement for Wt1 in sinus horn development more carefully, we analyzed expression of Wt1 from E10.5 to E14.5 in the venous pole region (Figure 4). We compared Wt1 expression to that of Tbx18, which is restricted to the mesenchyme and myocardium of developing sinus horns.[5]

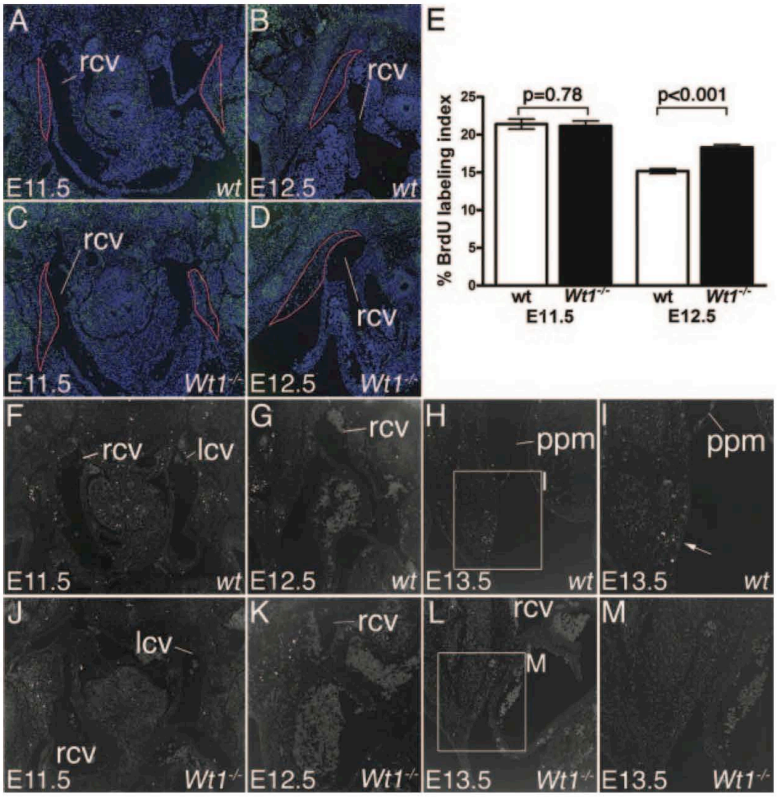

Figure 5. Analysis of cellular changes in the *Wt1*$^{-/-}$ lateral body wall. A through D, Analysis of cell proliferation in the *Wt1*-positive mesenchyme of the lateral body wall surrounding the common cardinal veins performed on transverse sections through the venous pole by 5-bromodeoxyuridine (BrdU) immunohistochemistry. Dorsal is oriented up. E, Proliferation rates (% 5-bromodeoxyuridine–labeling index) of **red-encircled regions** in genotypes, as shown in **A through D**. **F through M,** TUNEL staining for apoptosis in Wt1-expressing subcoelomic mesenchyme on transverse embryo sections. The **white arrow** in **I** points to a cluster of apoptotic cells in E13.5 wild-type embryos. Stages and genotypes are as indicated. Abbreviations are as in the legends of Figures 1 and 2.

From E10.5 to E12.5, *Wt1* was expressed in the developing mesothelia, including the epicardium, pericardium and pleura, and in the subcoelomic mesenchyme of the lateral body wall including the one surrounding the common cardinal veins, but surprisingly, not in the sinus horns and the SAN where *Tbx18* was strongly expressed (Figure 4A through 4H). Coimmunofluorescence analysis of Wt1 and Tbx18 in the venous pole region at E12.5 revealed patterns of protein expression identical to mRNA domains, confirming mutual exclusion of the 2 expression domains (Figure 4M through 4P). Complementary expression of *Wt1* in the mesenchyme surrounding the common cardinal veins and *Tbx18* in the sinus horn myocardium, prompted us to examine the possibility of negative cross-regulation of these transcription factors. However, *Tbx18* was not derepressed in the *Wt1* mutant and vice versa (Figure 4I and 4J). At E14.5, *Wt1* was maintained in the mesothelia whereas *Tbx18* expression persisted in the sinus horn myocardium (Figure 4K and 4L).

The sinus horn defect in *Wt1* mutants suggests that the *Wt1*-positive mesenchyme surrounding the common cardinal veins may provide precursor cells for the *Wt1*-negative sinus horn myocardium. To test this hypothesis, we used genetic lineage tracing systems to determine the fate of *Wt1*-expressing cells. First, we used a binary system with mice carrying a knock-in of the *tTA* gene in the *Wt1* locus and a reporter line with a *tetO*$_{bi}$*LacZ-GFP* transgene.[13] Expression of *tTA* under *Wt1* control elements leads to transcription of the *LacZ* gene and production of the β-galactosidase protein whose longevity provides a tool to trace cells initially expressing *Wt1*. We did not find β-galactosidase positive cells in the sinus horn myocardium at E12.5 and E14.5 using this system (Online Figure II). We next crossed a *Wt1*$^{BAC\text{-}IRES\text{-}EGFPCre}$ line, in which the expression of the *Cre* recombinase gene mimics that of the *Wt1* gene, with *R26*^{LacZ} reporter mice.[12] This system irreversibly labels *Wt1*-expressing cells and their daughters by *LacZ* expression (β-galactosidase activity). Again, we did not find β-galactosidase positive cells in the sinus horn myocardium at E12.5 and E16.5 (Figure 4Q through 4T), providing further evidence that the *Wt1*-positive mesenchyme of the lateral body wall does not represent a cellular source for the sinus horn myocardium.

Collectively, these analyses suggest Wt1 is not required within the sinus horn mesenchyme like Tbx18 is, but that Wt1 expression in the mesothelia and/or subcoelomic mesenchyme controls sinus horn formation by an indirect process.

Cellular Changes of the Lateral Body Wall Mesenchyme in *Wt1*$^{-/-}$ Mice

We next analyzed whether changes of proliferation and apoptosis may underlie the failure of sinus horn formation and the persistence of the subcoelomic body wall mesenchyme. Cell proliferation appeared unaffected in *Wt1*$^{-/-}$ embryos at E11.5 (wild type 0.214±0.0064 versus mutant 0.211±0.0067; P=0.78). At E12.5, we detected a significant but small increase of cell proliferation in the *Wt1*$^{-/-}$ lateral body wall mesenchyme (wild type 0.151±0.0031 versus mutant 0.183±0.0035; P<0.0001) (Figure 5A through 5E). Using TUNEL assays, we did not detect changes of the low levels of apoptosis in the subcoelomic mesenchyme at the venous pole region at E11.5 (we analyzed 3 wild-type and 3 *Wt1* mutant embryos) and E12.5 (4 embryos of each genotype were analyzed) in *Wt1*$^{-/-}$ hearts (Figure 5F, 5G, 5J, and 5K). At E13.5, we observed clusters of

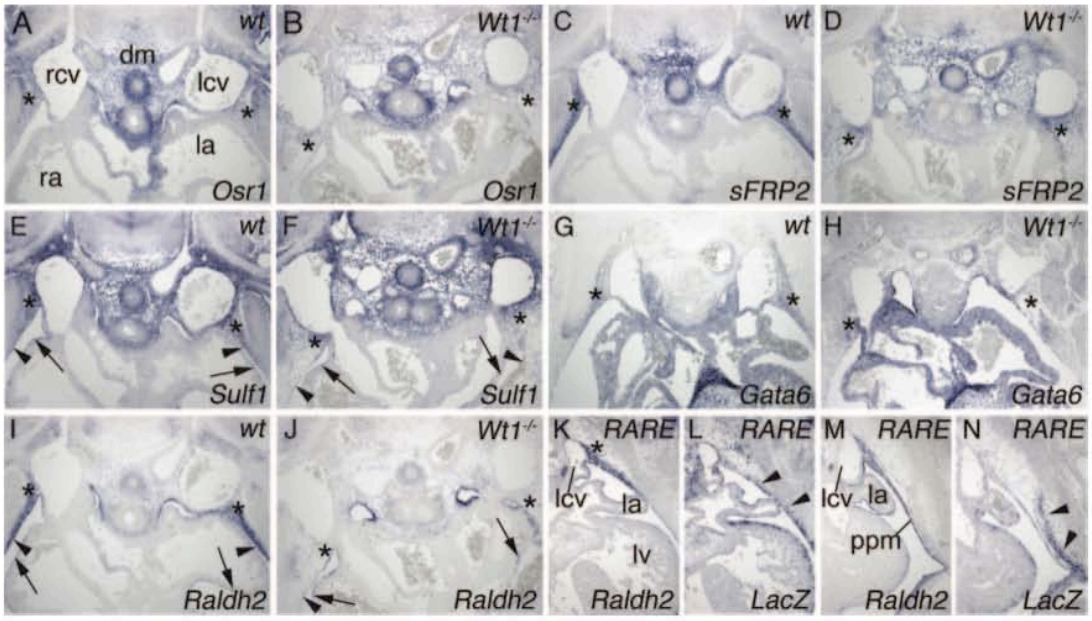

Figure 6. Absence of *Raldh2* expression in the *Wt1*$^{-/-}$ lateral body wall mesenchyme. A through J, In situ hybridization analysis of marker expression carried out on transverse sections of the venous pole region of E12.5 wild-type and *Wt1*$^{-/-}$ hearts. Genotypes and probes are as indicated. **Asterisks (A through K)** mark the subcoelomic lateral body wall mesenchyme. **Black arrows and arrowheads (E, F, I, and J)** mark epicardium and pericardium, respectively. **J,** Loss of *Raldh2* expression in the subcoelomic mesenchyme of *Wt1*$^{-/-}$ embryos. **K through N,** In situ hybridization analysis of *Raldh2* and *LacZ* expression carried out on transverse sections of the venous pole region of E12.5 **(K and L)** and E13.0 **(M and N)** hearts of *RARE-Hsp68LacZ*/+ transgenic embryos (RARE). **Arrowheads in L and N** mark RA signaling. Abbreviations are as in Figures 1 and 2.

apoptotic cells in the mesenchyme underlying the PPM insertion point in the body wall in 8 of 11 tested wild-type embryos (Figure 5H and 5I). These clusters of apoptotic cells were not detected in *Wt1*$^{-/-}$ embryos (n=5) at this stage (Figure 5L and 5M). Thus, loss of apoptosis in this region may contribute to the nonrelease of the PPMs from the lateral body wall and the persistence of the underlying mesenchyme.

Loss of *Raldh2* Expression in the Lateral Body Wall Mesenchyme

To identify molecular changes that may underlie and explain the defects of the venous pole in *Wt1* mutant hearts, we analyzed expression of genes that represent markers for the myocardium of the atria, the SAN and the sinus horns. Expression of these markers was unchanged in the *Wt1*$^{-/-}$ cardiac venous pole region arguing that regionalization and cellular contributions to SAN and atrial myocardium occurred normally (Online Figure III). *Tbx18* expression was found in the small region of SAN myocardium present (Figures 1M and 4J), arguing that *Wt1* controls formation of sinus horn but not of SAN myocardium.

Our analysis uncovered a number of novel markers for the subcoelomic mesenchyme of the lateral body wall that were coexpressed with *Wt1* in this region (Figure 6). The *Osr1* (odd-skipped related 1), the gene encoding *sFRP2* (secreted frizzled-related protein 2), and sulfatase 1 (*Sulf1*) were additionally expressed in the dorsal mesocardium (Figure 6A, 6C, and 6E), whereas *Sulf1* showed additional expression in epicardium (black arrow Figure 6E) and pericardium (black arrowhead in Figure 6E). Expression of *Osr1*, *sFRP2*, *Sulf1*, and *Gata6* (GATA binding protein 6) was maintained (albeit at seemingly lower levels) in the loose *Wt1*$^{-/-}$ lateral body wall mesenchyme, independently confirming the persistence of cells formerly expressing *Wt1* in this region (asterisks in Figure 6A through 6H). *Raldh2* was coexpressed with *Wt1* in the epicardium, pericardium and subcoelomic mesenchyme from E11.5 to E14.5 in the entire pericardial cavity (Online Figure IV). Intriguingly, expression of *Raldh2* was specifically lost in the lateral body wall mesenchyme (asterisks in Figure 6J) but persisted in the epicardium (black arrow in Figure 6J) and pericardium (black arrowhead in Figure 6J). Raldh2 is an enzyme that converts retinaldehyde to RA. To study which tissues respond to this compound in this region, we analyzed *LacZ* expression of a transgenic reporter line for RA signaling (*RARE-Hsp68LacZ*).[14] *LacZ* expression was detected in a dorsal to latero-ventral wave in the subcoelomic mesenchyme of the lateral body wall at E12.5 and E13.0 strongly arguing that RA signaling does not act onto the developing sinus horns (Figure 6K through 6N).

Because of the similarity of the cardinal vein phenotypes in *Wt1*$^{-/-}$ and *Tbx18*$^{-/-}$ mice, we tested whether loss of *Tbx18* affects expression of marker genes in the adjacent subcoelomic mesenchyme. However, unchanged expression of these genes (including *Raldh2*) in *Tbx18*$^{-/-}$ embryos excluded a paracrine Tbx18-dependent signal from the sinus horn myocardium/mesenchyme onto the subcoelomic mesenchyme (Online Figure V) and implied that sinus horn defects in *Wt1*- and *Tbx18* mutants are of different etiology.

Loss of *Raldh2* Results in Defects in Sinus Horn Formation

Loss of *Raldh2* expression in *Wt1* mutants suggested that Raldh2 is a downstream effector of *Wt1* in sinus horn

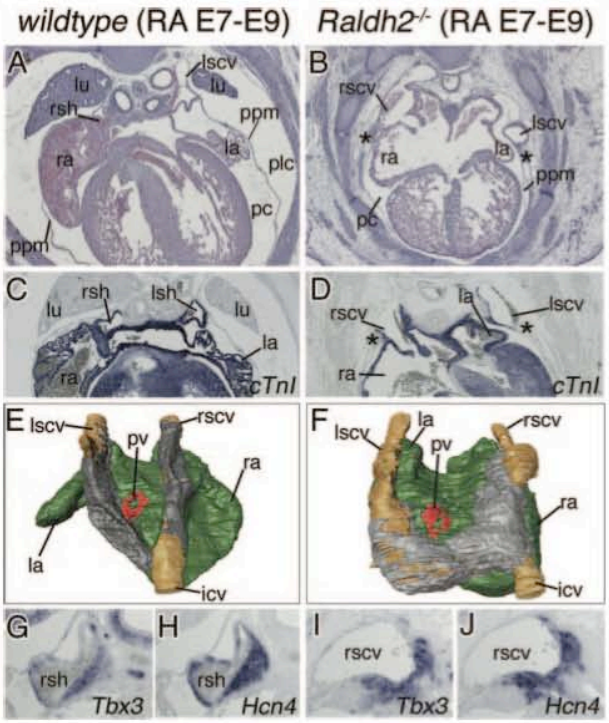

Figure 7. RA signaling is required for cardinal vein formation after E9.5 in the mouse heart. Histological, molecular, and morphological analyses of sinus horns **(A through F)** and the SAN **(G through J)** were carried out on transverse sections of the venous pole region of E14.5 wild-type **(left column)** and *Raldh2*-deficient embryos food supplied with RA between E7 and E9 (RA E7-E9) **(right column)**. **A through F,** Histological stainings with hematoxylin/eosin **(A and B)**, in situ hybridization analysis of *cTnI* expression **(C and D)**, and 3D reconstructions of serial sections stained for *cTnI* in a dorsal–posterior view. Atrial myocardium is shown in **green**, cardinal vein myocardium in **gray**, the lumen of the cardinal veins in **brown**, and the pulmonary vein myocardium in **red (E and F)**. **Asterisks (B and D)** mark persisting subcoelomic mesenchyme. **G through J,** In situ hybridization analysis of sections through the base of the cardinal veins for expression of SAN marker genes with probes as indicated. Abbreviations are as in Figures 1 and 2.

formation. We analyzed *Raldh2* mutant mice[11] at E14.5 (after sinus horn formation) that were rescued from early sinoatrial defects by RA food supply between E7.5 and E9.5 (Figure 7). *Raldh2*(RA E7–9)-deficient hearts featured thin ventricular walls and enlarged atria in accordance with the known role of RA in epicardial development and posteriorizing the chambers.[8,16] Compared to wild-type embryos similarly supplied with exogenous RA, the *Raldh2*$^{-/-}$ cardinal veins were thinner, less myocardialized, and buried in an abnormal position within the lateralized PPMs (Figure 7A through 7F). Pleural and pericardial cavities communicated on the left side, and the pleural cavity was not expanded leaving the pericardium ventrally attached to the body wall with a mesh of persisting mesenchymal cells (Figure 7B and 7D). Analysis of *Tbx3* and *Hcn4* expression indicated presence of myocardium of the SAN, whose atrial border, however, appeared rather diffuse (Figure 7G through 7J). Expression of *Wt1* and other markers for the lateral body wall mesenchyme was not changed in *Raldh2*$^{-/-}$(RA E7–9) embryos at E12.5 (Online Figure VI). Similar to *Wt1*-deficient embryos and in contrast to the wild-type situation, apoptotic cell clusters were absent from the subcoelomic mesenchyme underlying the PPMs at E12.5 and E13.5 in *Raldh2*-deficient embryos supplied with RA from E7.5 to E9.5 (Online Figure VII). Thus, embryos with a lack of RA signaling in the time interval critical for sinus horn formation (E9.5 to E14.5) exhibit pericardial and cardinal vein defects highly reminiscent of those of *Wt1*$^{-/-}$ embryos, suggesting that *Raldh2* and RA signaling mediate Wt1 function in the subcoelomic mesenchyme of the lateral body wall.

Discussion

Our study has established that the transcription factor Wt1 is required for the correct formation of the cardiac venous pole. We suggest that Wt1 functions primarily in the subcoelomic mesenchyme of the lateral body wall to mediate the release of the PPMs by apoptosis. This, in turn, mediates the correct repositioning of the cardinal veins medially to the lungs and the dorsal mesocardium. Wt1 function in the subcoelomic mesenchyme may be mediated by RA signaling. *Tbx18* acts independently in the sinus horn mesenchyme to warrant its growth and myocardial differentiation.

Sinus Horn Defects Are Secondary to Changes in PPM Formation

Our analysis of *Wt1*$^{-/-}$ embryos revealed that sinus horn defects are tightly associated with pleuropericardial abnormalities suggesting that alterations in mesothelial development may accompany or cause cardinal vein malformations. These pericardial defects are similar to congenital defects in human that have been described as rare anomalies. They may or may not be symptomatic, with symptomatic patients often experiencing chest pain. In the more frequently occurring partial pericardial absence, surgical intervention may be required to prevent strangulation of the heart. The etiology of these human defects is not well understood, but descriptive studies of human embryos have pointed to an important role of the PPMs.[17,18] The proximal aspects of the common cardinal veins (the ducts of Cuvier) are embedded in the PPMs. Thus, failure of one or both PPMs to close will result in lateralization of cardinal veins. At this point, it remains unclear why myocardialization of these lateralized cardinal veins fails, but physical separation from sources of differentiation signals (eg, the sinoatrial region) may be involved. Different opinions for the causative factor for the nonclosure of PPMs have been put forward.[18] In 1909, Perna proposed that the premature atrophy of the left duct of Cuvier results from insufficient blood supply to the PPMs.[19] Alternatively, altered growth of the heart may inappropriately stretch and tear the PPMs.[20] To our knowledge, normal and abnormal pericardial development has not been described in any detail in the mouse. Our phenotypic characterization of *Wt1*- and *Raldh2*-deficient embryos pinpoint to the decisive role of the subcoelomic mesenchyme of the lateral body wall in the etiology of pericardial defects. The persisting subcoelomic mesenchyme in these mutants tethers the PPMs to the lateral body wall, thus, preventing appropriate expansion and cardinal vein relocalization. It also hampers the inflation of the pleural cavity that may rely on a dorsal to ventral wave of PPM release by the swelling and subsequent disappearance of the underlying mesenchyme.

RA Signaling May Mediate Wt1 Function in the Subcoelomic Mesenchyme

RA has been identified as an important signaling factor in numerous developmental processes.[21] RA also controls heart morphogenesis and differentiation,[16] and acts as an epicardial factor for myocardial differentiation.[22] Our analysis of the expression and function of the main RA biosynthetic enzyme Raldh2 expands the role of RA signaling to pericardial development and sinus horn formation. *Raldh2* mutant embryos rescued from early cardiac defects by RA food supply exhibited a spectrum of phenotypic changes, including reduced PPMs, left-sided pericardial–pleural communication, persistence of the body wall mesenchyme, and lateralized cardinal veins, that are compatible with a primary requirement of RA for pericardial development. Using a RA reporter mouse, we detected RA signaling in the subcoelomic mesenchyme of the lateral body wall adjacent to the developing PPMs. RA signaling was spatially dynamic because it shifted ventrally preceding PPM detachment. Localized apoptosis of the RA signaling positive mesenchyme may mediate PPM release from the lateral body wall. This situation is somehow reminiscent of the role of RA signaling in vertebrate limb development where it mediates apoptosis of the interdigital mesenchyme to release the digits.[23] Noteworthy, administration of all-trans RA in patients with acute promyelocytic leukemia can lead to an RA syndrome that features pleural and pericardial effusion.[24] Loss of the RA-metabolizing enzyme Cyp26a1 in zebrafish results in defects in common cardinal vein formation.[25] Together, this suggests that RA is important for normal development and function of mesothelia and cardinal veins.

Colocalization of *Wt1* and *Raldh2* expression in the lateral body wall mesenchyme, loss of *Raldh2* expression in this domain in $Wt1^{-/-}$ embryos, and phenotypic similarities of the pericardial defects of either mutant strongly suggests that RA signaling acts downstream of *Wt1*. We tried to rescue pericardial defects of *Wt1*-deficient mice by feeding pregnant mice with RA starting from E8.5, ie, shortly before onset of sinus horn formation, until E14.5 when this process ends. A concentration of 0.25-g RA per gram of food, which was efficient to rescue sinoatrial defects of *Raldh2* mutant mice, did not rescue sinus horn and PPM defects in $Wt1^{-/-}$ mice. However, cardinal vein defects were not rescued in the $Raldh2^{-/-}$ embryos supplied with RA until E14.5 either, suggesting that exogenous RA does reach its target tissue after E9.5 in the embryo (Online Figure VIII). Hence, it remains open whether *Wt1* regulates additional genetic circuits that synergize with RA to mediate its downstream functions.

A link between *Wt1* and *Raldh* family members has already been described in other developmental contexts. *Raldh1* expression is downregulated in the urogenital ridge of $Wt1^{-/-}$ embryos.[26] *Wt1* and *Raldh2* are coexpressed in the epicardium and epicardially derived cells of the developing avian heart.[27] A direct regulation of *Raldh2* expression by Wt1 has also been proposed during liver development.[28] Here, *Wt1* and *Raldh2* expression coincide in the coelomic lining, and in $Wt1^{-/-}$ mice *Raldh2* expression is downregulated in these mesothelial cells, leading to defects in liver morphogenesis. Additionally, the left pleuroperitoneal membrane is not fully formed. The regulation of *Raldh2* expression by Wt1 may therefore represent a general mechanism during the development of murine mesothelia.

Cellular Contributions at the Cardiac Venous Pole

We have recently shown that the myocardialized proximal aspects of the superior and inferior caval veins form only after heart looping by recruitment and subsequent myocardial differentiation of *Tbx18*-positive pericardial precursors.[5] *Wt1* expression in the subcoelomic mesenchyme directly abuts the *Tbx18* expression domain at the venous pole, suggesting that *Wt1*-positive precursors feed into the pool of *Tbx18*-positive sinus horn cells. However, our lineage tracing experiments negate such a possibility, but instead stress that *Tbx18* exclusively marks the sinus horn myocardial lineage throughout heart development.[6] In $Tbx18^{-/-}$ mice, the cardinal veins are positioned inside the PPMs, but appear less lateralized compared to *Wt1*-deficient embryos. Delay but not failure of myocardialization of proximal cardinal veins in $Tbx18^{-/-}$ embryos[5] may relate to the different topological situation of the PPMs that are not tethered to the lateral body wall as in $Wt1^{-/-}$ embryos. Expression of *Wt1* and *Raldh2* is unchanged in $Tbx18^{-/-}$ mice, indicating that *Wt1* and *Tbx18* regulate different cellular and molecular programs during pericardial and caval vein development. Although the sinus horns fail to form in $Wt1^{-/-}$ embryos, the volume of the SAN is largely unchanged. This contrasts the complete lack of the large SAN head structure in $Tbx18^{-/-}$ embryos[6] and suggests that Wt1 controls the formation of myocardialized sinus horns but not of the region destined to form the SAN head that is regulated by Tbx18. Altered SAN morphology in $Wt1^{-/-}$ embryos, however, argues that positioning of the developing SAN next to the myocardialized sinus horns is critical for correct morphogenesis of this structure.

Acknowledgments

We thank Gregg Duester and Alexandre T. Soufan for technical help and John Burch and Janet Rossant for mice.

Sources of Funding

This work was supported by Netherlands Organization for Scientific Research Vidi grant 864.05.006 (to V.M.C.), German Research Foundation (Deutsche Forschungsgemeinschaft [DFG]) grant La 1381/3-1-3 (to E.L.), Wilhelm Sander-Stiftung (to E.L.), NIH grant R01 HL070733 (to K.N.), European Community's Sixth Framework Programme contract "HeartRepair" LSHM-CT-2005-018630 (to V.M.C., M.J.B.v.d.H., and A.K.), and DFG grant for the Cluster of Excellence REBIRTH (From Regenerative Biology to Reconstructive Therapy) and for the Clinical Research Group KFO136 at Hannover Medical School (to A.K.).

Disclosures

None.

References

1. Anderson RH, Brown NA, Moorman AF. Development and structures of the venous pole of the heart. *Dev Dyn*. 2006;235:2–9.
2. Stieber J, Hofmann F, Ludwig A. Pacemaker channels and sinus node arrhythmia. *Trends Cardiovasc Med*. 2004;14:23–28.
3. Moorman AF, Christoffels VM, Anderson RH. Anatomic substrates for cardiac conduction. *Heart Rhythm*. 2005;2:875–886.
4. Rochais F, Mesbah K, Kelly RG. Signaling pathways controlling second heart field development. *Circ Res*. 2009;104:933–942.

5. Christoffels VM, Mommersteeg MT, Trowe MO, Prall OW, de Gier-de Vries C, Soufan AT, Bussen M, Schuster-Gossler K, Harvey RP, Moorman AF, Kispert A. Formation of the venous pole of the heart from an Nkx2-5-negative precursor population requires Tbx18. *Circ Res*. 2006; 98:1555–1563.
6. Wiese C, Grieskamp T, Airik R, Mommersteeg MT, Gardiwal A, de Gier-de Vries C, Schuster-Gossler K, Moorman AF, Kispert A, Christoffels VM. Formation of the sinus node head and differentiation of sinus node myocardium are independently regulated by Tbx18 and Tbx3. *Circ Res*. 2009;104:388–397.
7. Lee SB, Haber DA. Wilms tumor and the WT1 gene. *Exp Cell Res*. 2001;264:74–99.
8. Moore AW, Schedl A, McInnes L, Doyle M, Hecksher-Sorensen J, Hastie ND. YAC transgenic analysis reveals Wilms' tumour 1 gene activity in the proliferating coelomic epithelium, developing diaphragm and limb. *Mech Dev*. 1998;79:169–184.
9. Martinez-Estrada OM, Lettice LA, Essafi A, Guadix JA, Slight J, Velecela V, Hall E, Reichmann J, Devenney PS, Hohenstein P, Hosen N, Hill RE, Munoz-Chapuli R, Hastie ND. Wt1 is required for cardiovascular progenitor cell formation through transcriptional control of Snail and E-cadherin. *Nat Gen*. 2010;42:89–93.
10. Kreidberg JA, Sariola H, Loring JM, Maeda M, Pelletier J, Housman D, Jaenisch R. WT-1 is required for early kidney development. *Cell*. 1993; 74:679–691.
11. Niederreither K, Subbarayan V, Dolle P, Chambon P. Embryonic retinoic acid synthesis is essential for early mouse post-implantation development. *Nat Gen*. 1999;21:444–448.
12. Soriano P. Generalized lacZ expression with the ROSA26 Cre reporter strain. *Nat Gen*. 1999;21:70–71.
13. Krestel HE, Mayford M, Seeburg PH, Sprengel R. A GFP-equipped bidirectional expression module well suited for monitoring tetracycline-regulated gene expression in mouse. *Nucleic Acids Res*. 2001;29:E39.
14. Rossant J, Zirngibl R, Cado D, Shago M, Giguere V. Expression of a retinoic acid response element-hsplacZ transgene defines specific domains of transcriptional activity during mouse embryogenesis. *Genes Dev*. 1991;5:1333–1344.
15. Urlinger S, Baron U, Thellmann M, Hasan MT, Bujard H, Hillen W. Exploring the sequence space for tetracycline-dependent transcriptional activators: novel mutations yield expanded range and sensitivity. *Proc Natl Acad Sci U S A*. 2000;97:7963–7968.
16. Niederreither K, Vermot J, Messaddeq N, Schuhbaur B, Chambon P, Dolle P. Embryonic retinoic acid synthesis is essential for heart morphogenesis in the mouse. *Development*. 2001;128:1019–1031.
17. Abbas AE, Appleton CP, Liu PT, Sweeney JP. Congenital absence of the pericardium: case presentation and review of literature. *Int J Cardiol*. 2005;98:21–25.
18. Faridah Y, Julsrud PR. Congenital absence of pericardium revisited. *Int J Cardiovasc Imaging*. 2002;18:67–73.
19. Perna G. Sopra un arresto di sviluppo della sierosa pericardica nell' uomo. *Anat Anz*. 1909;35:323.
20. Kaneko Y, Okabe H, Nagata N. Complete left pericardial defect with dual passage of the phrenic nerve: a challenge to the widely accepted embryogenic theory. *Pediatr Cardiol*. 1998;19:414–417.
21. Niederreither K, Dolle P. Retinoic acid in development: towards an integrated view. *Nat Rev Genet*. 2008;9:541–553.
22. Stuckmann I, Evans S, Lassar AB. Erythropoietin and retinoic acid, secreted from the epicardium, are required for cardiac myocyte proliferation. *Dev Biol*. 2003;255:334–349.
23. Zuzarte-Luis V, Hurle JM. Programmed cell death in the embryonic vertebrate limb. *Sem Cell Dev Biol*. 2005;16:261–269.
24. Leelasiri A, Numbenjapol T, Prayoonwiwat W, Mongkolsritrakul W, Srisawat C. Successful treatment of retinoic acid syndrome with dexamethasone: a case report. *J Med Assoc Thai*. 2005;88(Suppl 3):S302–S310.
25. Patatanian E, Thompson DF. Retinoic acid syndrome: a review. *J Clin Pharm Ther*. 2008;33:331–338.
26. Klattig J, Sierig R, Kruspe D, Makki MS, Englert C. WT1-mediated gene regulation in early urogenital ridge development. *Sex Dev*. 2007;1: 238–254.
27. Perez-Pomares JM, Phelps A, Sedmerova M, Carmona R, Gonzalez-Iriarte M, Munoz-Chapuli R, Wessels A. Experimental studies on the spatiotemporal expression of WT1 and RALDH2 in the embryonic avian heart: a model for the regulation of myocardial and valvuloseptal development by epicardially derived cells (EPDCs). *Dev Biol*. 2002;247: 307–326.
28. Ijpenberg A, Perez-Pomares JM, Guadix JA, Carmona R, Portillo-Sanchez V, Macias D, Hohenstein P, Miles CM, Hastie ND, Munoz-Chapuli R. Wt1 and retinoic acid signaling are essential for stellate cell development and liver morphogenesis. *Dev Biol*. 2007;312:157–170.

Novelty and Significance

What Is Known?

- The sinus horns, the myocardialized parts of the intrapericardial aspects of the common cardinal veins, form late in cardiac development, from a pool of pericardial cells that is distinguished from precursors of the other cardiac components by the presence of Tbx18 and absence of Nkx2-5 expression.
- The sinus horns contribute to the mature systemic venous return system but also to the pace maker tissue of the heart, the sinoatrial node (SAN), which is a common focus of congenital malformations and atrial arrhythmias.

What New Information Does This Article Contribute?

- The *Wt1* (Wilms tumor 1) gene is expressed in the subcoelomic mesenchyme of the lateral body wall surrounding the cardinal veins, but this *Wt1*-positive mesenchyme does not contribute cells to the sinus horn myocardium.
- *Wt1* expression in the subcoelomic mesenchyme is required for sinus horn formation, release and growth of the pleuropericardial membranes, and expansion of the pleural and pericardial cavities.
- Retinoic acid signaling may mediate Wt1 function in the subcoelomic mesenchyme for pleuropericardial membrane release, as well as relocalization and myocardialization of cardinal veins.

The cardiac venous pole is a common focus of congenital malformations and atrial arrhythmias, yet little is known about the cellular and molecular mechanisms that regulate its development. Here, we have identified expression of the *Wt1* gene and downstream retinoic acid signaling in the subcoelomic mesenchyme of the lateral body wall as a crucial requirement for the development of the myocardial components of the venous pole and of the pericardium. Our study uncovers the critical role of the subcoelomic mesenchyme in this program. Unexpectedly, this tissue does not represent a cellular source for sinus horn myocardium but controls sinus horn formation indirectly. We suggest that relocalization and myocardialization of cardinal veins depends on the correct temporal release of the pleuropericardial membranes in which the cardinal veins are embedded from the underlying body wall mesenchyme. Hydration and apoptotic removal of the mesenchyme may be cellular mediators in this process. Our results provide novel insight into the genetic and cellular pathways regulating the posterior extension of the mammalian heart, and the formation of its coelomic lining. Our study suggests that congenital malformations of the cardiac venous pole and pericardial defects present together and share a common etiology.

Supplemental Online Data

"Wt1 and retinoic acid signaling in the subcoelomic mesenchyme control the development of the pleuropericardial membranes and the sinus horns"

Julia Norden[1], Thomas Grieskamp[1], Ekkehart Lausch[2], Bram van Wijk[3], Maurice J.B. van den Hoff[3], Christoph Englert[4], Marianne Petry[1], Mathilda T.M. Mommersteeg[3], Vincent M. Christoffels[3], Karen Niederreither[5], and Andreas Kispert[1,*]

[1] Institut für Molekularbiologie, Medizinische Hochschule Hannover, Carl-Neuberg-Str.1, D-30625 Hannover, Germany

[2] Centre for Pediatrics and Adolescent Medicine, University of Freiburg, Mathildenstraße 1, D-79106 Freiburg, Germany

[3] Department of Anatomy, Embryology and Physiology, Academic Medical Center, University of Amsterdam, Meibergdreef 15 L2-108, 1105 AZ Amsterdam, The Netherlands

[4] Molecular Genetics Group, Leibniz Institute for Age Research – Fritz Lipmann Institute, Beutenbergstr. 11, D-07745 Jena, Germany

[5] Departments of Medicine and Molecular and Cellular Biology, Center for Cardiovascular Development, Baylor College of Medicine, One Baylor Plaza, Houston, Texas 77030, USA

[*]Author for correspondence:

E-MAIL: kispert.andreas@mh-hannover.de

TEL.: +49 511 5324017

FAX.: +49 511 5324283

Supplemental Online Materials and Methods

Mice and genotyping
In *Wt1*^{tTA} knock-in mice, the coding sequence of an improved tetracycline-dependent transactivator *tTA2S*[1] was introduced into the *Wt1* locus by gene targeting (Lausch *et al.*, manuscript in preparation). This exchanged exon 1 and 360 bp of 3' downstream sequence of *Wt1* for the coding sequence of *tTA2S,* substituting the *Wt1* translational start site with the ATG of *tTA2S*. Expression of *tTA2S* under endogenous *Wt1* control elements faithfully recapitulates the pattern of native *Wt1*, both in adult mice and during development. Heterozygous *Wt1*^{tTA} knock-in mice are phenotypically normal, showing no anatomical or histopathological abnormalities up to an age of fifteen months. *Wt1*$^{tTA/tTA}$ embryos, however, died prior to day E11.5 of gestation as described for *Wt1*$^{-/-}$ mice[2]. Administration of the tetracycline derivative doxycycline (which has a high affinity for tTA2S) to *Wt1*^{tTA} mice at a concentration of 0.1 mg per ml drinking water was sufficient to stringently suppress transcription of tetracycline-responsive transgenes in all *Wt1*-positive tissues *in vivo*, as analyzed by qPCR, histochemistry, immunohistochemistry, and chemiluminescence. For fate mapping of *Wt1*-positive cells *in situ,* *Wt1*^{tTA} knock-in mice were crossed with reporter strains carrying a *tetO*$_{bi}$*LacZ-GFP* transgene.[3] In double-transgenic animals maintained without doxycycline (-DOX), *Wt1*-controlled tTA2S drives expression of both the green fluorescence protein (GFP) and ß-galactosidase from a tTA-responsive bidirectional promoter, composed of seven *tet*-repressor binding sites (*TetO*$_7$) immediately upstream of an RNA polymerase II transcriptional start site of the cytomegalovirus immediate early promoter. For the generation of mutant embryos, heterozygous mice were intercrossed. For timed pregnancies, vaginal plugs were checked in the morning after mating, noon was taken as embryonic day (E) 0.5. Embryos were harvested in PBS, fixed in 4% paraformaldehyde overnight and stored in 100% methanol at –20°C before further use. Wildtype littermates were used as controls. Genomic DNA prepared from yolk sacs or tail biopsies was used for genotyping by PCR (protocols upon request). H. Hedrich, state head of the animal facility, approved the care of animals and experiments at Medizinische Hochschule Hannover.

Food supply of retinoic acid
Pregnant females were treated with retinoic acid (RA) to rescue venous pole development in *Raldh2*- and *Wt1*-deficient embryos similar to described protocols.[4,5] All-*trans*-RA (Sigma) from a 5 mg/ml ethanol stock suspension was diluted in 50 ml water and mixed with 50 g powdered food (irradiated PicoLab rodent diet 20) to a final concentration of 100 mg/g food. The RA-containing food mixture was left in the cage for *ad libitum* feeding and renewed twice a day until the day of sacrifice.

***Histological* analyses**
For histological stainings embryos were fixed in 4% paraformaldehyde, paraffin embedded, and sectioned to 5 or 10 μm. Sections were stained with haematoxylin and eosin, following standard procedures.

In situ hybridization analysis
In situ hybridization analysis with digoxigenin-labeled antisense riboprobes followed a published protocol.[6] Details of used probes upon request.

Immunohistochemistry
For immunohistochemistry rabbit polyclonal antibody against Wt1 (C-19, Santa Cruz Biotechnology, 1:200), goat polyclonal antibody against Tbx18 (C-20, Santa Cruz Biotechnology,

1:200), monoclonal antibody against cardiac Troponin I (1:500 MAB1691, Millipore),[7] and rabbit IgG fraction against β-Galactosidase (Cappel, 1:4000) were used as primary antibodies. Alexa488 goat-anti-rabbit (Invitrogen, 1:250) and biotinylated donkey-anti-goat (Dianova, 1:200) were used as secondary antibodies. Nuclei were stained with 4′,6-Diamidino-2-phenylindol (DAPI) (Roth) or Topro3 (Invitrogen). For staining with the Tbx18 antibody, paraffin sections were pressure cooked for 3 min in antigen unmasking solution (H-3300, Vector Laboratories Inc). The signal was amplified using the Tyramide Signal Amplification (TSA) system from Perkin-Elmer (NEL702001KT, Perkin Elmer LAS). For double staining with Wt1, Alexa488 goat-anti-rabbit secondary antibody was added during the streptavidine-HRP step of the TSA protocol. For β-Galactosidase, the primary antibody was amplified using the VECTASTAIN ABC Kit (Peroxidase rabbit IgG, Vector Laboratories, PK-4001). The detection of this antibody was performed with the DAB Peroxidase Substrate Kit from Vector Laboratories (SK-4100).

Documentation

Sections were photographed using a Leica DM5000 microscope with Leica DFC300FX digital camera. Immunofluorescence for *Wt1*$^{BAC\text{-}IRES\text{-}EGFPCre}$/+; *R26*^{lacZ}/+ lineage tracing was detected using a Leica SPE confocal microscope. All images were processed in Adobe Photoshop CS.

Three-dimensional reconstruction

Three-dimensional visualization and geometry reconstruction of patterns of gene expression determined by *in situ* hybridization was performed as described previously.[8] Shortly, serial sections were used for *in situ* hybridization and were documented as described. The remaining analysis was done with the help of the software “Amira” (Version 4.1.1, Mercury Computer Systems Inc). The pictures were aligned, and regions for reconstruction were labeled. After surface conversion a three-dimensional model was obtained.

Proliferation and apoptosis assays

Cell proliferation in the E11.5 and E12.5 embryos was investigated by detection of incorporated 5-bromo-2-deoxyuridine (BrdU) on 5-μm sections of paraffin-embedded specimens similar to previously published protocols.[9] Ten sections each of three embryos of each genotype at E11.5 and 15 sections each of four embryos of each genotype at E12.5 were used for quantification. The BrdU-labeling index was defined as the number of BrdU-positive nuclei relative to the total number of nuclei, as detected by DAPI counterstain, in the *Wt1* expressing region next to the cardinal veins. Statistical analyses were performed using the 2-tailed Student’s t-test. Data were expressed as mean ± SEM. Differences were considered significant when the P-value was below 0.05.

Detection of apoptotic cells in 10-μm paraffin sections of E10.5 to E13.5 embryos was based on modification of genomic DNA utilizing terminal deoxynucleotidyl transferase (TUNEL assay) and indirect detection of positive cells by fluorescein-conjugated anti-Digoxigenin antibody. The procedure followed exactly the recommendation of the manufacturer (Serologicals Corp.) of the ApopTag kit used. Three sections each of two embryos of each genotype at E10.5, of three embryos of each genotype at E11.5, of four embryos of each genotype at E12.5 and of six wildtype and five *Wt1*-mutant embryos at E13.5 were analyzed. Additionally three sections of two RARE-LacZ embryos of E12.5 and E13.0 each were used. The detection of apoptotic cells in the *Raldh2*-deficient mice was performed with three embryos of each stage. Wildtype and *Raldh2*-deficient embryos were littermates and fed with retinoic acid from embryonic day E7 to E9.

References

1. Urlinger S, Baron U, Thellmann M, Hasan MT, Bujard H, Hillen W. Exploring the sequence space for tetracycline-dependent transcriptional activators: novel mutations yield expanded range and sensitivity. *Proc of the Natl Acad Sci U S A.* 2000;97:7963-7968.
2. Kreidberg JA, Sariola H, Loring JM, Maeda M, Pelletier J, Housman D, Jaenisch R. WT-1 is required for early kidney development. *Cell.* 1993;74:679-691.
3. Krestel HE, Mayford M, Seeburg PH, Sprengel R. A GFP-equipped bidirectional expression module well suited for monitoring tetracycline-regulated gene expression in mouse. *Nucleic Acids Res.* 2001;29:E39.
4. Mic FA, Molotkov A, Benbrook DM, Duester G. Retinoid activation of retinoic acid receptor but not retinoid X receptor is sufficient to rescue lethal defect in retinoic acid synthesis. *Proc of the Natl Acad Sci U S A.* 2003;100:7135-7140.
5. Niederreither K, Vermot J, Schuhbaur B, Chambon P, Dolle P. Embryonic retinoic acid synthesis is required for forelimb growth and anteroposterior patterning in the mouse. *Development.* 2002;129:3563-3574.
6. Moorman AF, Houweling AC, de Boer PA, Christoffels VM. Sensitive nonradioactive detection of mRNA in tissue sections: novel application of the whole-mount in situ hybridization protocol. *J Histochem Cytochem.* 2001;49:1-8.
7. Snarr BS, O'Neal JL, Chintalapudi MR, Wirrig EE, Phelps AL, Kubalak SW, Wessels A. Isl1 expression at the venous pole identifies a novel role for the second heart field in cardiac development. Circ Res. 2007;101:971-974.
8. Soufan AT, Ruijter JM, van den Hoff MJ, de Boer PA, Hagoort J, Moorman AF. Three-dimensional reconstruction of gene expression patterns during cardiac development. *Physiol Genomics.* 2003;13:187-195.
9. Bussen M, Petry M, Schuster-Gossler K, Leitges M, Gossler A, Kispert A. The T-box transcription factor Tbx18 maintains the separation of anterior and posterior somite compartments. *Genes Dev.* 2004;18:1209-1221.

Supplemental Online Figures

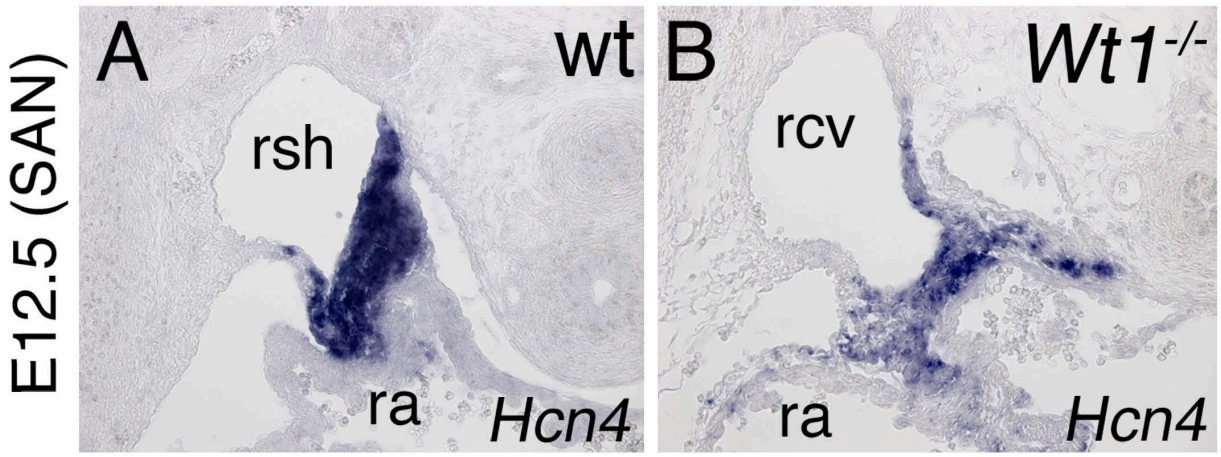

Online Figure I. SAN morphology is changed in *Wt1*-deficient hearts. *In situ* hybridization analysis for sinoatrial node (SAN) expression of *hyperpolarization-activated, cyclic nucleotide-gated K+ 4* gene (*Hcn4)* in E12.5 hearts of wildtype (wt) and *Wt1*-deficient (*Wt1*$^{-/-}$) embryos on transverse sections trough the base of the cardinal vein. rsh, right sinus horn; ra, right atrium; rcv, right common cardinal vein.

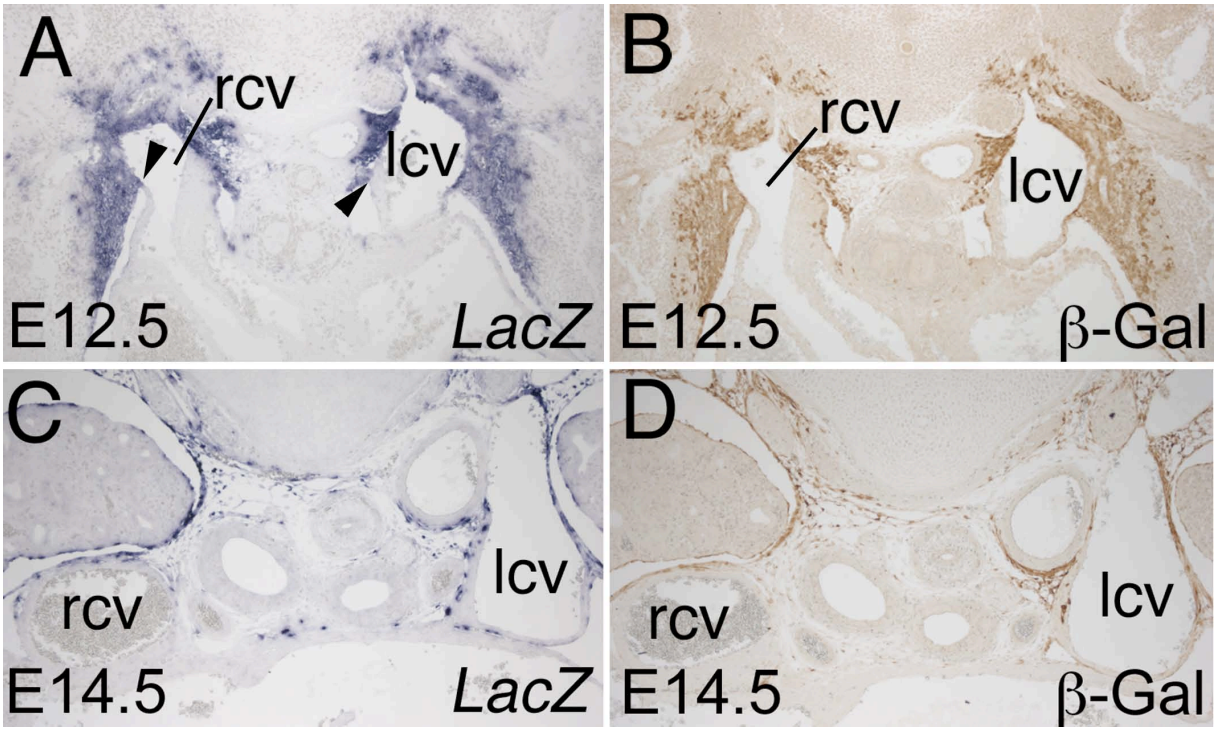

Online Figure II. Wt1-positive subcoelomic mesenchyme does not contribute to the sinus horns. Analysis of *LacZ* expression by *in situ* hybridization (A,C) and of ß-galactosidase protein (ß-Gal) by immunohistochemistry (B,D) in *Wt1*^{tTA} *x tetObiLacZ-GFP* embryos at E12.5 and E14.5 on transverse sections through the cardiac venous pole. Black arrowheads point to the border of the *LacZ* expression between the *Wt1*-positive subcoelomic mesenchyme of the lateral body wall and the absence of *LacZ* expression in the myocardium of the sinus horns. rcv, right common cardinal vein; lcv, left common cardinal vein.

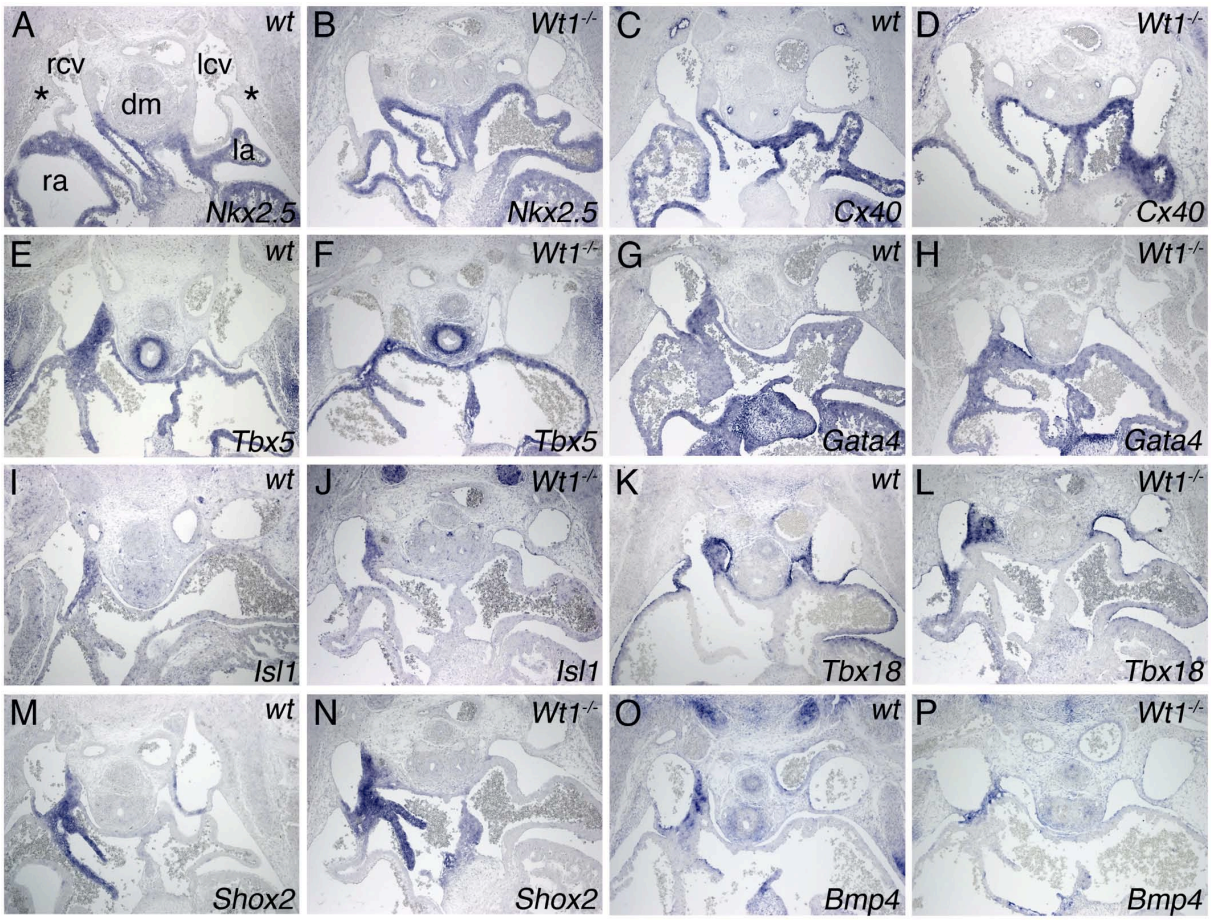

Online Figure III. No changes of marker gene expression for atrial, sinoatrial node (SAN) and sinus horn myocardium in *Wt1*-deficient hearts. *In situ* hybridization analysis was carried out on transverse sections of the venous pole region of E12.5 hearts of wildtype and *Wt1*-deficient embryos. Genotypes and probes are as indicated. *Nkx2.5* (A,B) and *Connexin40* (*Cx40)* (C,D) were confined to the atrial myocardium and were excluded from the myocardium of the sinus horns and the SAN. Expression of *Tbx5* (E,F) and *Gata4* (G,H) comprised the myocardium of the SAN in addition to that of the atria. *Isl1* expression (I,J) was confined to the SAN myocardium. The expression domain of *Tbx18* (K,L) comprised the epicardium and pericardium, the myocardium of the sinus horns and the SAN. *Shox2* (M,N) is found in the SAN myocardium and the venous valves, similar to *bone morphogenetic protein 4* (*Bmp4)* (O,P) that however appeared patchier in its expression. Asterisks in (A) mark the subcoelomic lateral body wall mesenchyme. dm, dorsal mesocardium; la, left atrium; lcv, left common cardinal vein; ra, right atrium; rcv, right common cardinal vein.

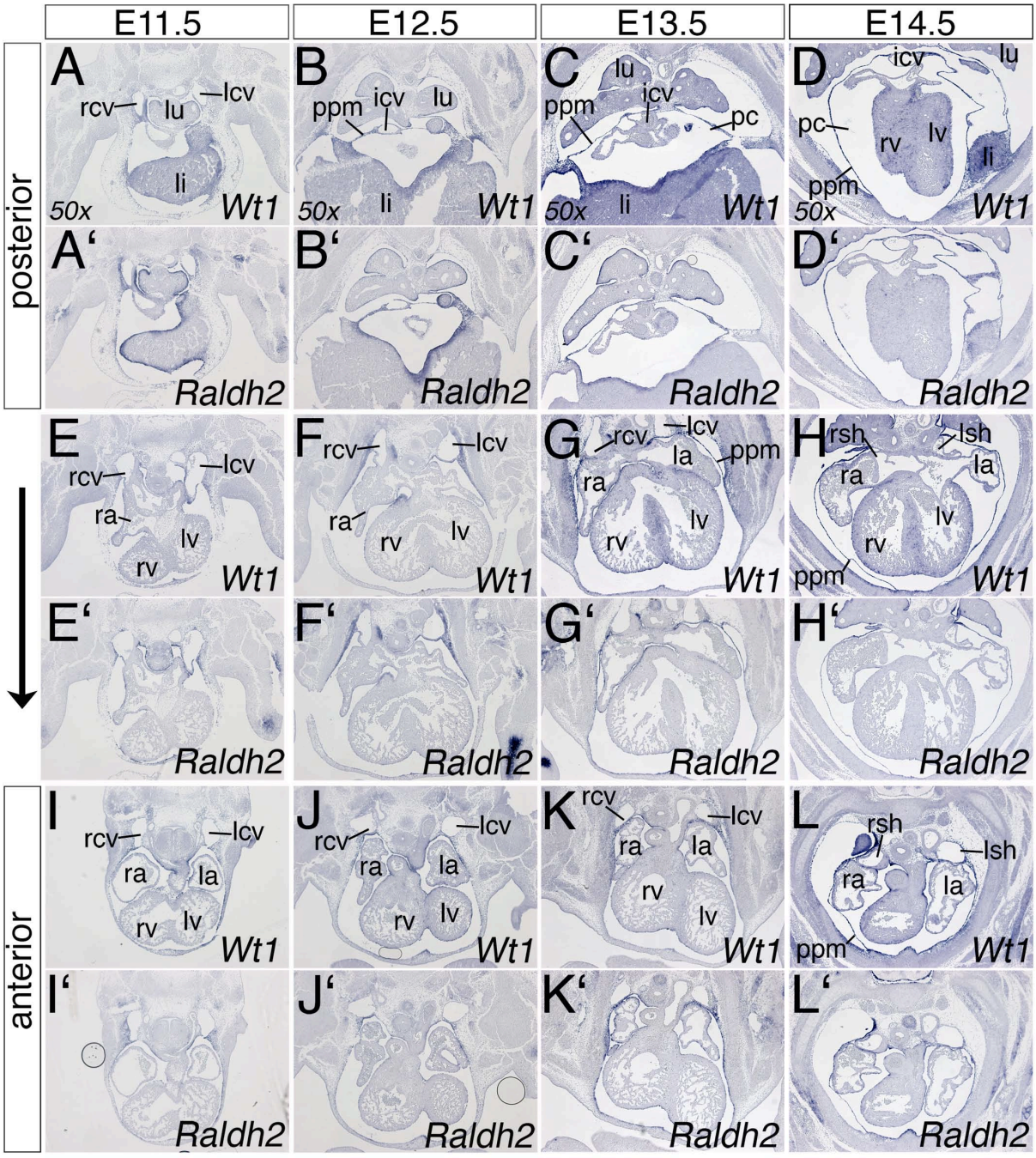

Online Figure IV. *Wt1* and *Raldh2* are coexpressed in epicardium, pericardium and subcoelomic mesenchyme of the lateral body wall during heart development. *In situ* hybridization analysis of *Wt1* and *Raldh2* gene expression carried out on transverse sections of wildtype embryos from E11.5 to E14.5 on different section planes. Probes and stages are as indicated. A-D', expression of *Wt1* and *Raldh2* at the posterior part of the pericardial cavity; E-H', expression of *Wt1* and *Raldh2* at the venous pole region; I-L', expression of *Wt1* and *Raldh2* at the anterior part of the pericardial cavity. icv, inferior cardinal vein; lu, lung; li, liver; la, left atrium; lv, left ventricle; lcv, left common cardinal vein; lsh, left sinus horn; pc, pericardial cavity; ppm, pleuropericardial membrane; ra, right atrium; rv, right ventricle; rcv, right common cardinal vein; rsh, right sinus horn.

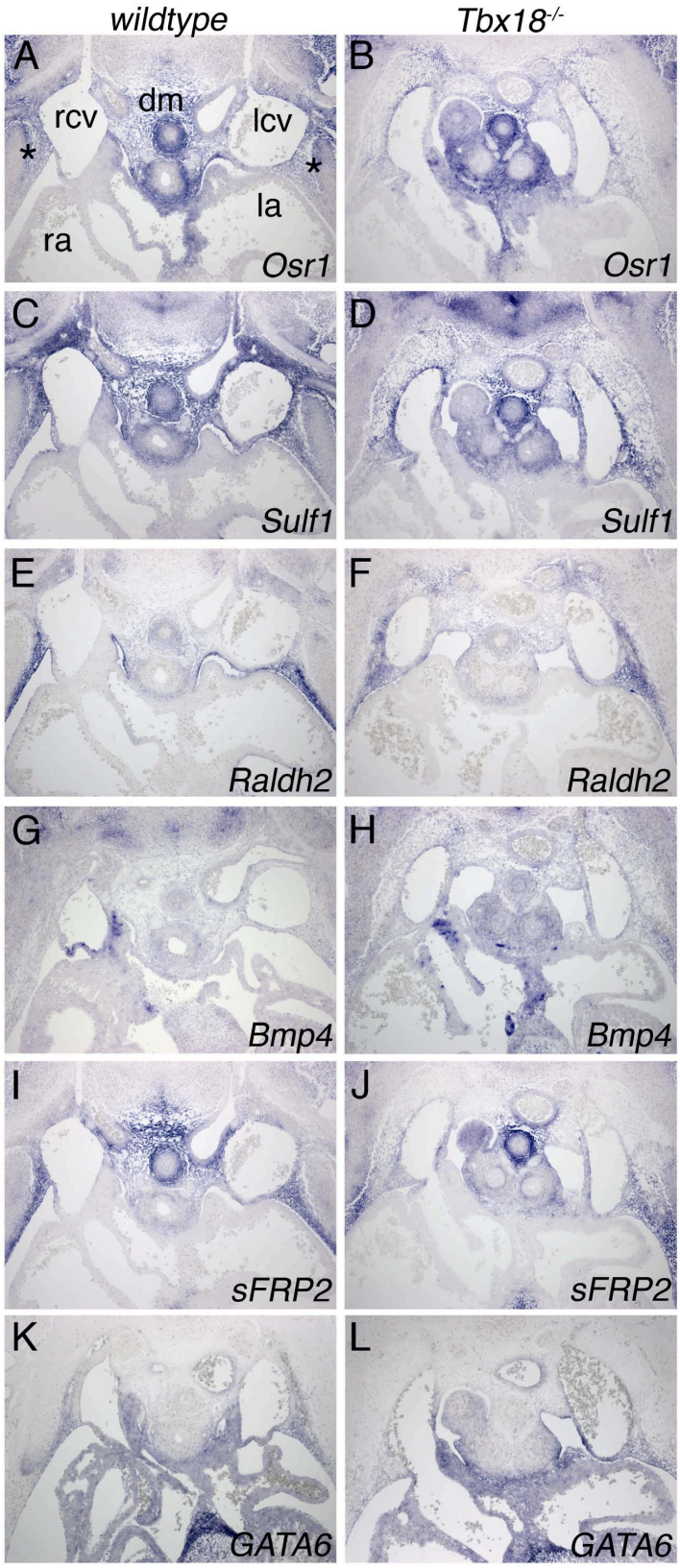

Online Figure V. Markers for the subcoelomic mesenchyme of the lateral body wall are unchanged in *Tbx18*-deficient embryos. *In situ* hybridization analysis of marker gene expression carried out on transverse sections of the venous pole region of E12.5 hearts of wildtype and *Tbx18*$^{-/-}$ embryos. Genotypes and probes are as indicated. Asterisks in (A) mark the subcoelomic lateral body wall mesenchyme. dm, dorsal mesocardium; la, left atrium; lcv, left common cardinal vein; ra, right atrium; rcv, right common cardinal vein.

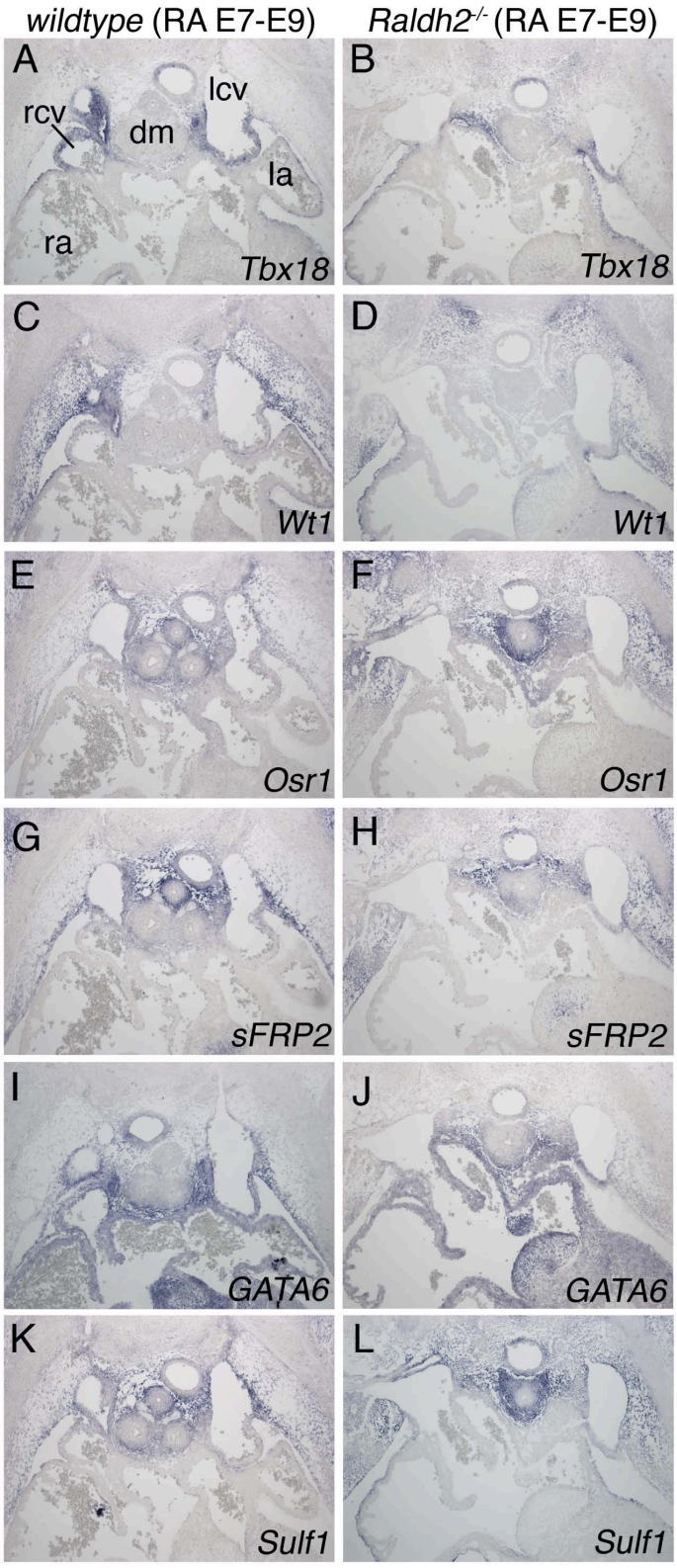

Online Figure VI. Markers for the subcoelomic mesenchyme of the lateral body wall are unchanged in *Raldh2*-deficient embryos. *In situ* hybridization analysis of marker gene expression carried out on transverse sections of the venous pole region of E12.5 hearts of wildtype and *Raldh2*$^{-/-}$ embryos food supplied with RA between E7 and E9 (RA E7-9). Genotypes and probes are as indicated. Asterisks in (A) mark the subcoelomic lateral body wall mesenchyme. dm, dorsal mesocardium; la, left atrium; lcv, left common cardinal vein; ra, right atrium; rcv, right common cardinal vein.

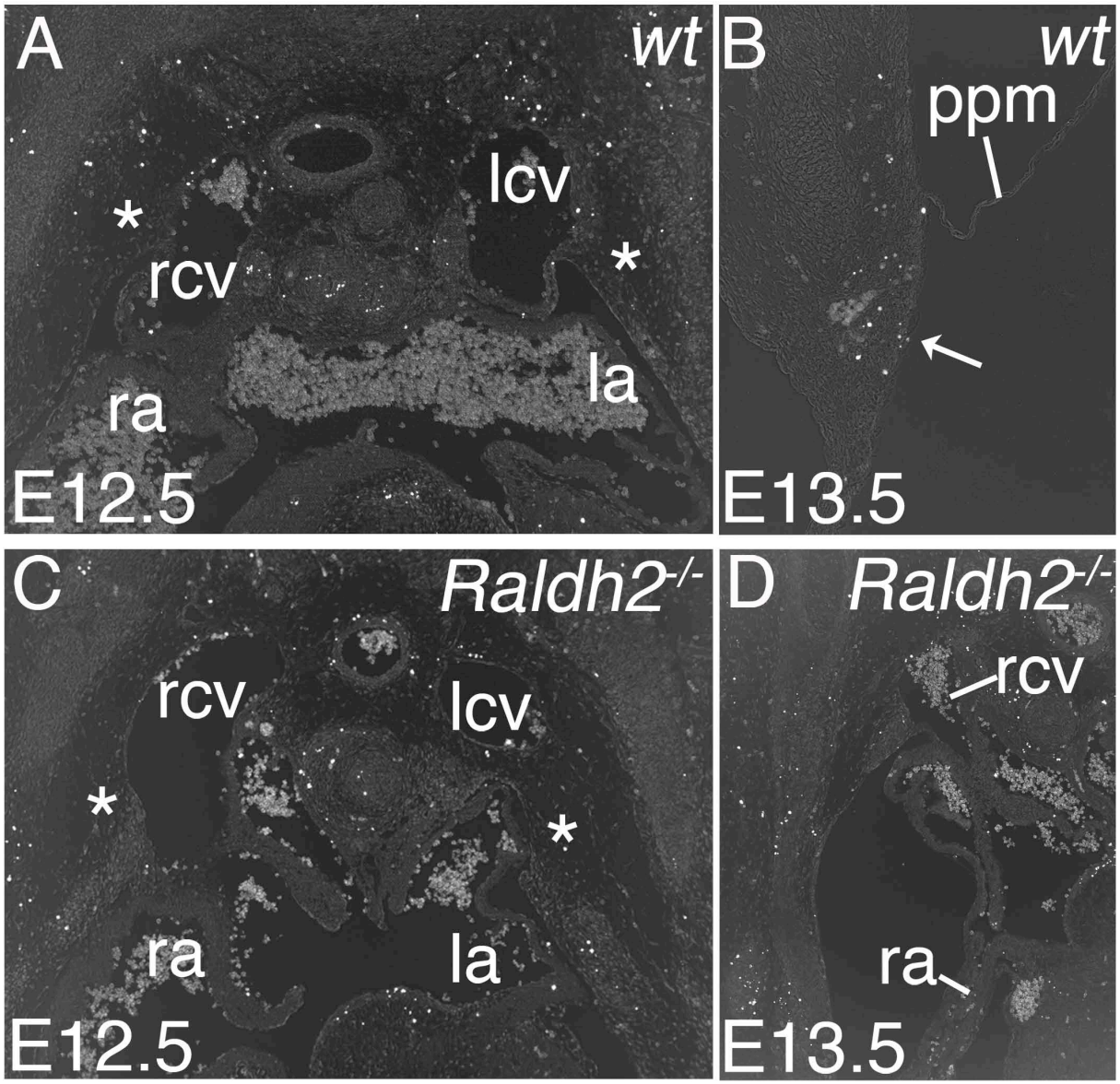

Online Figure VII. Absence of apoptotic cell clusters in the lateral body wall mesenchyme of *Raldh2*-deficient embryos. Analysis of apoptosis in the *Wt1*-positive subcoelomic mesenchyme on transverse sections trough the venous pole in wildtype and *Raldh2*-deficient embryos food supplied with RA between E7 and E9 (RA E7-E9) by TUNEL staining. Dorsal is oriented up. Stages and genotypes are as indicated. Asterisks in (A) mark the subcoelomic lateral body wall mesenchyme. The white arrow (B) points to the cluster of apoptotic cells in E13.5 wildtype embryos. rcv, right common cardinal vein; ra, right atrium; lcv, left common cardinal vein; la, left atrium; ppm, pleuropericardial membrane.

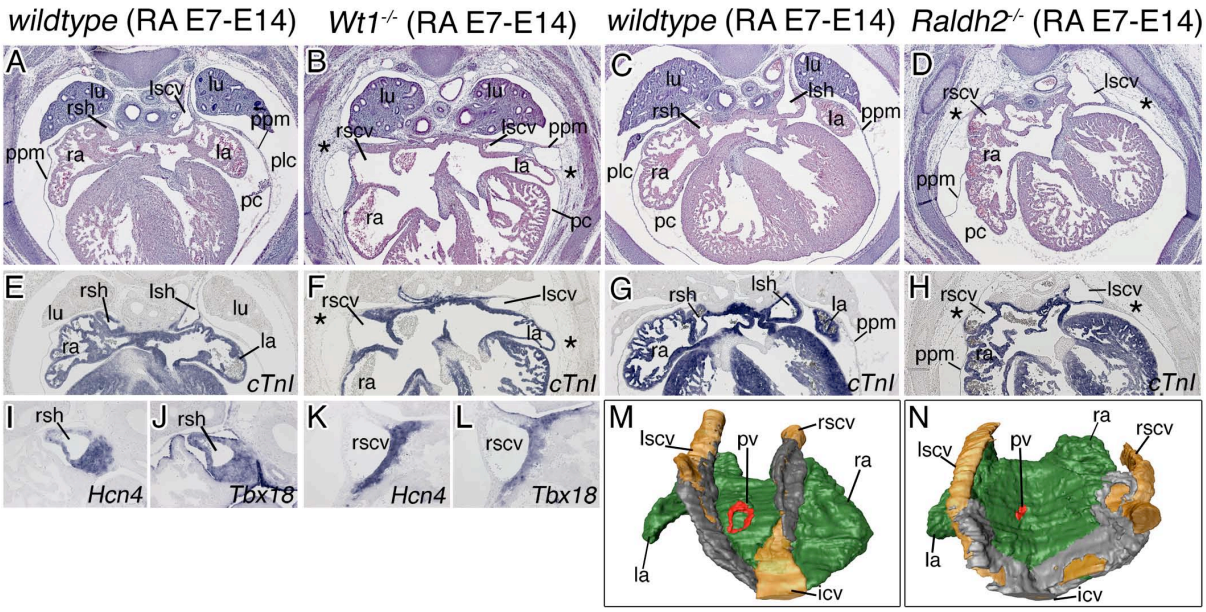

Online Figure VIII. Exogenous retinoic acid (RA) does not rescue *Raldh2*-deficiency in venous pole development after E9.5. Histological, molecular and morphological analyses of sinus horns (A-H,M,N) and the sinoatrial node (I-L) were carried out on transverse sections of the venous pole region of E14.5 wildtype, *Wt1*- and *Raldh2*-deficient embryos food supplied with RA between E7 and E14 (RA E7-14). A-H,M-N, Histological stainings with haematoxylin and eosin (A-D), *in situ* hybridization analysis of *cTnI* expression (E-H), and 3D-reconstructions of serial sections stained for *cTnI* in a dorsal-posterior view. Atrial myocardium is shown in green, cardinal vein myocardium in grey, the lumen of the cardinal veins in brown, and the pulmonary vein myocardium in red (M,N). Asterisks in B,D,F,H mark persisting subcoelomic mesenchyme. I-L, *in situ* hybridization analyses of sections through the base of the cardinal veins for expression of marker genes for the sinoatrial node with probes as indicated. icv, inferior cardinal vein; la, left atrium; lu, lung; lscv, left superior cardinal vein; pc, pericardial cavity; plc, pleural cavity; ppm, pleuropericardial membrane; pv, pulmonary vein; ra, right atrium; rscv, right superior cardinal vein; rsh, right sinus horn

Tbx18 is Necessary for the Closure of the Murine Pleuropericardial Ducts

Julia Norden, Thomas Grieskamp, and Andreas Kispert*

Institut für Molekularbiologie, OE5250, Medizinische Hochschule Hannover, Carl-Neuberg-Str.1, D-30625 Hannover, Germany

Author for correspondence:

E-MAIL: kispert.andreas@mh-hannover.de
TEL.: +49 511 5324017
FAX.: +49 511 5324283

Running title: Tbx18 in pericardial development

Manuscript in preparation.

Abstract

Aims: The pericardium is a mesothelial double-walled sac that completely surrounds the adult heart including the root of the great vessels, and protects and anchors the heart inside the body cavity. The development of the pericardium has been histological described in humans, but has escaped any detailed descriptive or molecular analysis in mice. The aim of this study was to examine the normal development of the pleuropericardial membranes (PPMs), which give rise to the mature pericardium of the adult heart, during murine embryogenesis, and define the role of the T-box transcription factor 18 (Tbx18) therein.

Methods and results: We describe murine pericardial development by histological analysis and examine gene expression during this process by *in situ* hybridization. *Tbx18* is expressed in the PPMs and in a newly identified mesenchymal tissue thickening protruding into the pleuropericardial ducts (PPDs). In *Tbx18*-deficient embryos this mesenchymal tissue thickening does not form. The closure of the PPDs fails, allowing pleural and pericardial cavities to communicate, and the lung to touch the atria. We also show that the detachment of the PPMs from the lateral body wall is affected by the loss of *Tbx18*.

Conclusion: Two distinct parallel processes are crucial for pericardial development. First, the PPMs are detached from the lateral body wall, and second, the PPDs are closed. These processes are coupled with the development and dorsocranial movement of the sinus venosus, and the positioning of the cardinal veins inside the pericardial cavity. During pericardial development *Tbx18* is mainly required for the closure of the PPDs by the attachment of the PPMs to the hilus of the lung.

Keywords: heart development, pericardium, sinus venosus, *Tbx18*

Non-standard abbreviations and acronyms

3D	three-dimensional
Aldh1a2	aldehyde dehydrogenase family 1, subfamily A2
E	embryonic day
GFP	green fluorescent protein
IFT	inflow tract
Osr1	odd-skipped related 1
PPD	pleuropericardial duct
PPM	pleuropericardial membrane
Tbx18	T-box 18
Wt1	Wilms tumor 1 homolog

Introduction

The pericardium is a mesothelial sac that completely surrounds the heart and the root of the great vessels. It separates the pleural and pericardial cavities and anchors and protects the heart. It also secretes a serous fluid into the pericardial cavity that is necessary for the movement of the heart along this membraneous tissue.[1] Furthermore, Limana *et al.* demonstrated that the pericardial fluid and therefore an intact pericardium are required for reactivation of embryonic gene programs in a regenerating adult heart after myocardial infarction.[2] The complete or partial absence of the pericardium is a rare congenital disease in humans. In most cases the defect is positioned on the left side, and males are more affected than females.[3] In general these defects are asymptomatic. Nevertheless, partial defects of the pericardium may lead to the strangulation of the heart in the foramen and thereby to death. Additionally, the absence of the pericardium is often associated with other congenital cardiac anomalies and with diaphragmatic hernia.[4] The etiology and the underlying cellular and molecular mechanisms of these defects are still unclear necessitating a more thorough analysis of normal and abnormal pericardial development.

In the human embryo, the pericardial cavity arises as a part of the intraembryonic cavity during gastrulation movements and the ventral closure of the embryo. First, the intraembryonic cavity is divided by the septum transversum, the precursor of the diaphragm, into a peritoneal and a thoracic cavity. This separation is initially incomplete leaving two pericardioperitoneal canals, which are positioned medially to the common cardinal veins, on each side of the foregut. The lung buds grow into these canals and expand dorsally, laterally and ventrally into the subcoelomic mesenchyme, leading to the degeneration of the laterodorsal mesenchyme and the formation of the pleural cavity. The disintegration of the surrounding mesenchyme is not complete, but two pleuropericardial folds persist between the growing lung and heart. These pleuropericardial folds contain the common cardinal veins and therefore are fixed to the posterior pole of the heart. The dorsocranial movements of the sinus venosus during the cardiac looping process shifts the common cardinal veins to a medial position, thereby stretching the pleuropericardial folds to become pleuropericardial membranes (PPMs).[5] In turn, the PPMs are released from the lateral body wall by several parallel processes including the degeneration of the subcoelomic mesenchyme, by the tensional force exerted by the growing rip cage, and the migration of the distal fixation points to a ventral position.[6] In the initial phase of these processes the pleuropericardial ducts (PPDs) between the lung and the heart are still needed for the movement of the lung, but will be closed during further development, possibly by fusion of the PPMs to the root of the lung. After this fusion event, pleural and pericardial cavities are completely separated. Further stretching and maturation of the PPMs form the parietal pericardium of human adults, which is attached posteriorly to the diaphragm, laterally to the mediastinal pleura, and ventrally to the sternum.[5,7,8]

The morphological, cellular and molecular processes regulating pericardial development in the mouse have been poorly defined. Only few relevant factors have been identified by the observation of pericardial defects in knockout mice. We recently published that the *Wilms tumor 1* gene (*Wt1*) and its interaction with retinoic acid signaling in the subcoelomic mesenchyme is necessary for pericardial development.[9] Moreover, the loss of *odd-skipped related 1* (*Osr1*, also known as *Odd1*) leads to similar pericardial defects. *Wt1* is downregulated in *Osr1*-deficient embryos, indicating that *Osr1* may act upstream of *Wt1* during pericardial development.[10]

T-box 18 (Tbx18) is a member of the conserved family of T-box transcription factors that is expressed in the proepicardium, the epicardium, and the sinus horns at the venous pole of the murine heart.[11] The *Tbx18*-positive cells of the venous pole define a specialized precursor cell population, which is needed for the myocardialization of the sinus horns and the formation of the sinoatrial node.[12,13] Christoffels *at al.* also described the abnormal lateral position of the sinus horns inside the PPMs in *Tbx18*-deficient embryos. Here, we further analyze this defect, and present data that link sinus horn and pericardial development. We conclude that the release of the PPMs from the subcoelomic mesenchyme and the closure of the PPDs, the latter of which requires expression of *Tbx18*, are crucial processes in pericardial development.

Material and Methods

Mice and genotyping

Transgenic mice harboring a knock-in of the GFP reporter in the *Tbx18* locus allele (*Tbx18*^{tm2Akis}, synonym: *Tbx18*^{GFP}) were described before.[13] Heterozygous embryos (*Tbx18*$^{GFP/+}$) were used as control embryos. All mice were maintained on an outbred (NMRI) background.

For the generation of mutant embryos, heterozygous mice were intercrossed. Vaginal plugs were checked in the morning after mating, for timed pregnancies noon was taken as embryonic day (E) 0.5. Embryos were harvested in PBS, fixed in 4% paraformaldehyde overnight and stored in 100% methanol at –20^{o}C before further use. Genomic DNA prepared from yolk sacs or tail biopsies was used for genotyping by PCR (protocols upon request). H. Hedrich, state head of the animal facility, approved the care of animals and experiments at Medizinische Hochschule Hannover.

Histological analysis

Embryos were fixed as mentioned above, paraffin embedded, and sectioned to 10 μm for histological stainings. Sections were stained with haematoxylin and eosin, following standard procedures. At least two embryos of each genotype were used for each analysis.

In situ hybridization analysis

Nonradioactive *in situ* hybridization analysis with digoxigenin-labeled antisense riboprobes was performed as described.[14] At least two embryos of each genotype were used for each analysis. Details of used probes upon request.

Proliferation assays and immunohistochemistry

Cell proliferation in 12.5 embryos was investigated by detection of incorporated 5-bromo-2-deoxyuridine (BrdU) on 5-μm sections of paraffin-embedded specimens similar to previously published protocols.[15] To define the *Tbx18*-positive region adjacent sections were stained for GFP by immunohistochemistry. For this GFP staining the primary antibody (rabbit polyclonal against GFP, 1:50, Santa Cruz Biotechnology) was detected using kits from Vector Laboratories (ABC Peroxidase Kit (Rabbit IgG), and DAB substrate kit). *Tbx18*-heterozygous littermates were used as controls.

Documentation

Sections were photographed using a Leica DM5000 microscope with Leica DFC300FX digital camera and afterwards processed in Adobe Photoshop CS3.

Three-dimensional reconstruction

For three-dimensional visualization and geometry reconstruction 10-μm serial sections of the whole heart of representative embryos of each genotype were used for haematoxylin and eosin stainings and documented as described. Further analysis was performed using the software "Amira" (Version 4.1.1, Mercury Computer Systems Inc) as described previously.[16] After documentation, the pictures were aligned, and regions for reconstruction were labeled. A three-dimensional model was obtained after surface conversion.

Results

The murine PPMs are released from the posterior dorsolateral body wall starting from E12.5

The closure of the PPDs and the detachment of the mesothelial PPMs from the lateral body wall occur in a complex series of morphogenetic processes. To visualize this program in mice, we prepared serial histological stainings of murine wildtype embryos starting from embryonic day (E) 9.5 to E14.5 (Figure 1, and data not shown) and generated schemes (Figure 2) of the thoracic cavity highlighting the key tissues.

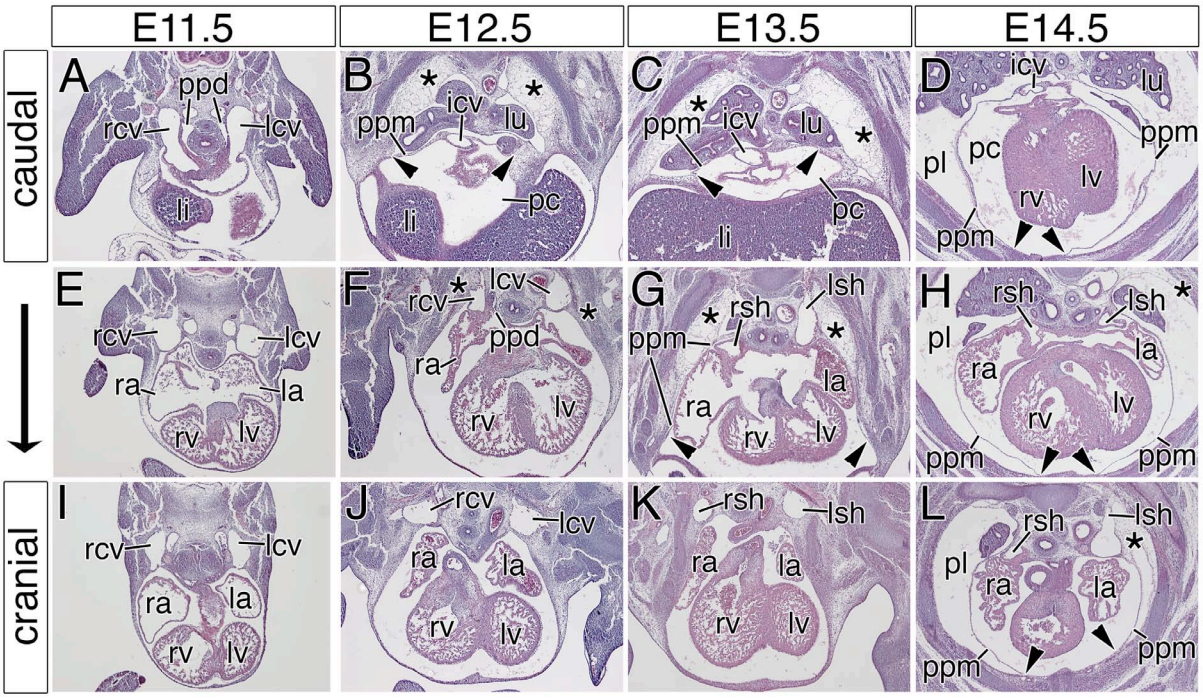

Figure 1. Pericardial development in wildtype hearts. A – L, Histological analysis by haematoxylin and eosin stainings of PPM development was performed on transverse sections of a caudal, a mid-transverse, and a cranial section plane of wildtype hearts from E11.5 to E14.5. Asterisks highlight the subcoelomic lateral body wall mesenchyme. Arrowheads mark the attachment point of the PPMs to the lateral body wall. icv, inferior cardinal vein; la, left atrium; lcv, left cardinal vein; li, liver; lu, lung; lsh, left sinus horn; lv, left ventricle; pc, pericardial cavity; ppd, pleuropericardial duct; pl, pleural cavity; ppm, pleuropericardial membrane; ra, right atrium; rcv, right cardinal vein; rsh, right sinus horn; rv, right ventricle.

The PPDs, which allowed the caudal movement of the lung at earlier developmental time points, were still open at E11.5. At this developmental stage, the inflow tract (IFT) of the heart including the right and left caval vein was positioned at a caudal position in the pericardial cavity (Figure 1A, 1E and 1I, Figure 2A and 2D). During further development the IFT shifted cranially and was positioned on a mid-transverse section plane at E12.5 (compare Figure 1A and 1F). Additionally the size of the body cavity enlarged. Both processes stretched the PPMs, which were attached to the sinus horns, and thereby formed free PPMs that were visible at caudal levels of the heart, next to the IFT, but not at more cranial section planes starting from E12.5 (Figure 1B, 1F and 1J). The PPMs were attached to the ventrolateral body wall distally, but were without contact to the dorsal mesocardium. Furthermore, the PPDs were not completely closed and a narrow duct was still detectable at E12.5 (Figure 1F, 2B, 2E, and 6C). Between E12.5 and E13.5, the lateral contact points of the PPMs moved ventrally following the distal extension of the ribs; mediodorsally the PPMs became attached to the hilus of the lung. Pleural and pericardial cavities were completely separated by the PPMs at E13.5 (Figure 1C, 1G, 2C, and 2F). Additionally, the subcoelomic mesenchyme in the pleural cavity and around the common cardinal veins became extremely loosely organized starting from E12.5, and was almost completely absent at E14.5. The PPMs were stretched into thin epithelial sheets during the

posteroanterior release from the dorsolateral mesenchyme and connected to the sternum by E14.5 (Figure 1D, 1H, 1L).

Thus, the development of the PPMs can be divided into two processes, which act in parallel and might be coupled with the dorsocranial movement of the sinus venosus during heart looping and the growth of the whole embryo. First, the PPDs, which are necessary for the growth and descent of the emerging lung during early embryonic development, are closed until E13.5. Second, the PPMs are released from the lateral body wall, which starts around E12.5 in a posterior, dorsal domain of the pericardial cavity and progresses anteroventrally until E14.5.

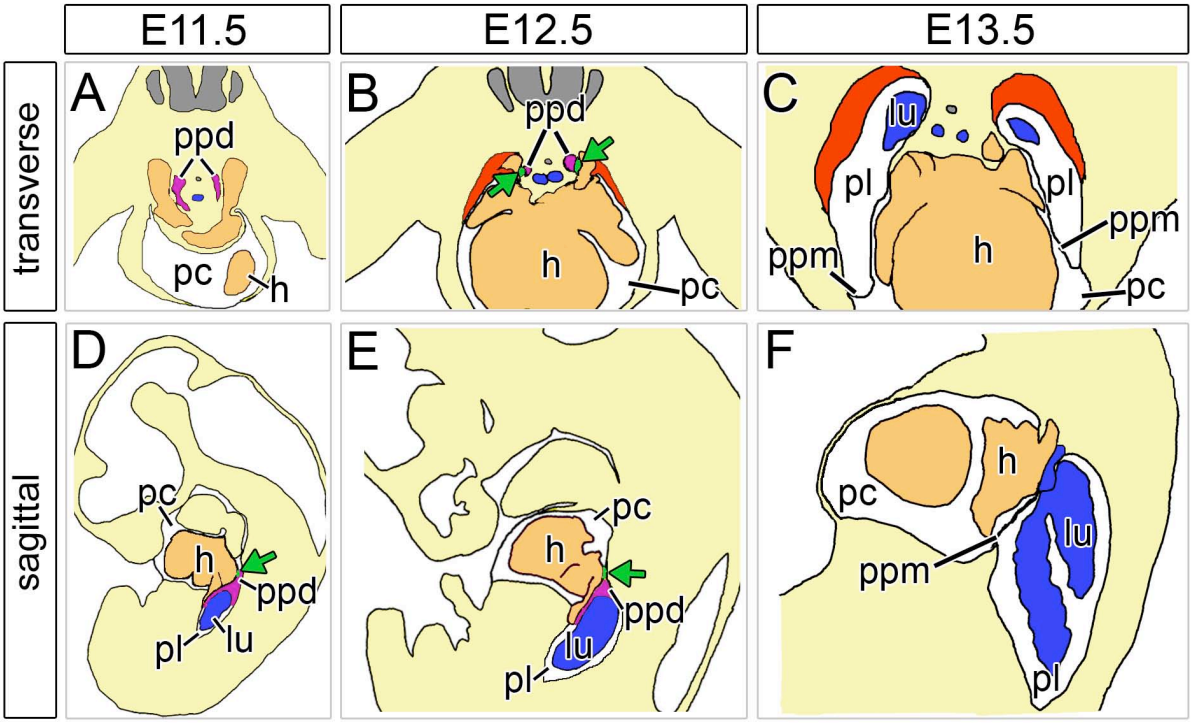

Figure 2. Schematic diagram of murine pericardial development. A – F, Scheme of pericardial development based on transverse and sagittal sections through the cardiac venous pole of wildtype embryos from E11.5 to E13.5. The lumen of the caval veins and the heart is marked in pale orange, the lung and trachea in blue, the PPDs in pink, a mesenchymal protrusion inside the PPDs in green (additionally marked by green arrows), and the degenerating subcoelomic mesenchyme in red. h, heart; lu, lung; pc, pericardial cavity; pl, pleural cavity; ppd, pleuropericardial duct; ppm, pleuropericardial membranes.

Gene expression during pericardial development

To define a molecular tool box and to get further insight into the mechanism regulating the development of the PPMs, we screened for genes that are expressed in the subcoelomic mesenchyme adjacent to the cardinal veins and/or in the developing PPMs by *in situ* hybridization (Figures 3 and 4). This search revealed new marker genes for the subcoelomic mesenchyme near the common cardinal veins at E12.5. They include *Wilms tumor 1* (*Wt1*) and its target gene *aldehyde dehydrogenase family 1, subfamily A2* (*Aldh1a2,* also known as

Raldh2) for which we previously reported a functional relevance in the subcoelomic mesenchyme for the release of the PPMs from the mediastinal pleura.[9] Furthermore, *Meis homeobox 1* (*Meis1*) and *Meis homeobox 2* (*Meis2*), target genes of retinoic acid signaling during forelimb development,[17] were detectable in the subcoelomic mesenchyme and confirmed the presence of active retinoic acid signaling in this domain (Figure 3A through 3D). We also detected expression of the transcription factor *GATA binding protein 6* (*Gata6*) in the subcoelomic mesenchyme as well as in cardiomyocytes and the atrioventricular canal (Figure 3E). Furthermore *secreted frizzled-related protein 2* (*Sfrp2*), a modulator of Wnt signaling, the notch receptor *Notch gene homolog 3 (Notch3*), and *sulfatase 1* (*Sulf1*) showed an expression in the laterodorsal mesenchyme and the dorsal mesocardium (Figure 3F through 3H). *Eph receptor A3* (*EphA3*) and *Eph receptor B2* (*EphB2*), two members of a large subfamily of Eph receptor tyrosine kinases, were specifically expressed in the subcoelomic mesenchyme, but not in other cardiac structures (Figure 3I and 3J). Furthermore, we detected the expression of *receptor tyrosine kinase-like orphan receptor 1* (*Ror1*) and *Osr1* in the laterodorsal mesenchyme (Figure 3K and 3L). Some of these genes (*Wt1*, *Aldh1a2*, *Gata6*, and *Sfrp2*) were additionally expressed in a mesenchymal thickening inside the remaining PPDs, implicating them in the closure of these ducts.

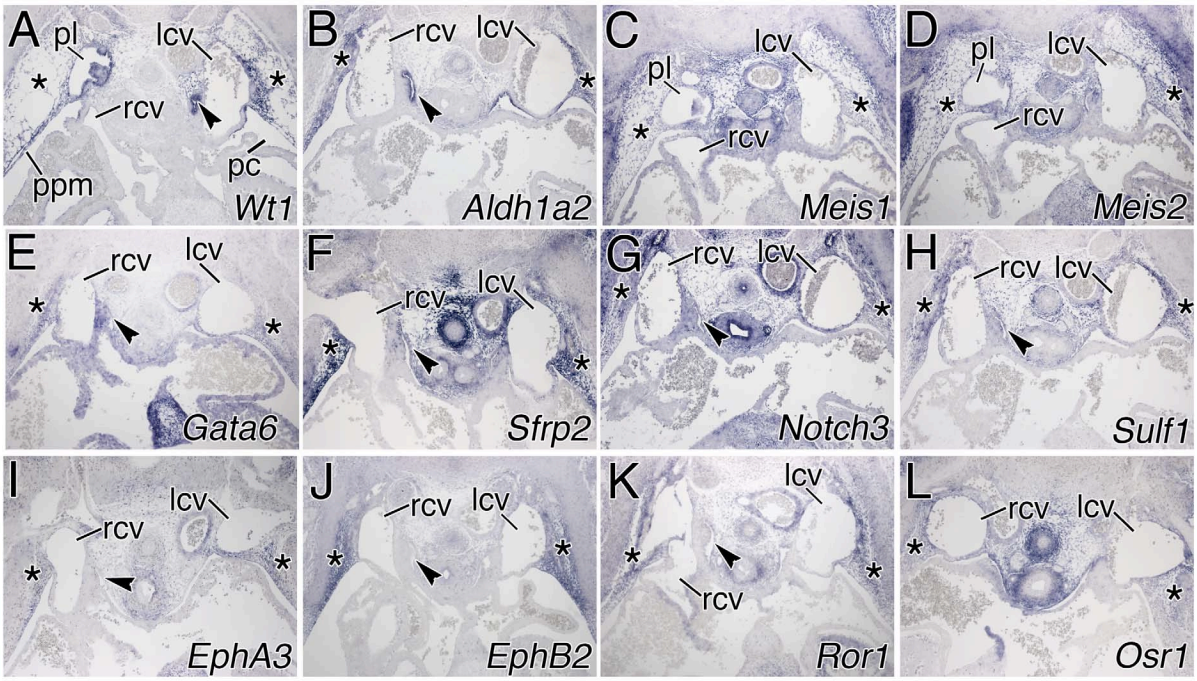

Figure 3. Gene expression in the subcoelomic mesenchyme. A – **L**, *In situ* hybridization analysis of genes encoding the mesothelial markers *Wt1* and *Aldh1a2* (**A**, **B**), the retinoic acid target gene *Meis1* and *Meis2* (**C**, **D***)*, the transcription factor *Gata6* (**E**), the modulator of canonical Wnt signaling, *Sfrp2* (**F***)*, the Notch receptor gene *Notch3* (**G**), the sulfatase *Sulf1* (**H**) and the kinases *EphA3*, *EphB2*, *Ror1* and *Osr1* (**I – L**) on transverse sections trough the venous pole region of wildtype hearts at E12.5. Asterisks highlight the subcoelomic lateral body wall mesenchyme. Arrowheads point to the remaining PPDs. lcv, left cardinal vein; pc, pericardial cavity; pl, pleural cavity; ppm, pleuropericardial membrane, rcv, right cardinal vein.

Since the PPMs were almost completely released from the subcoelomic mesenchyme at E14.5, we screened at this stage for genes that are specifically expressed in this tissue and may be involved in the release from the body wall. By *in situ* hybridization analysis we detected expression of the mesothelial markers *Wt1, Aldh1a2, Sulf1 and Upk3b* in the PPMs of wildtype embryos (Figure 4A through 4D). Additionally, the sinus venosus marker *Tbx18*, a target gene of the canonical Wnt/beta-catenin signaling (*Axin2*) and Wnt signaling pathway components (*Sfrp1*, *Sfrp2)* were expressed in the PPMs at E14.5 (Figure 4E through 4H). Therefore, the subcoelomic mesenchyme and the mesenchymal thickening inside the PPDs are distinct molecular entities.

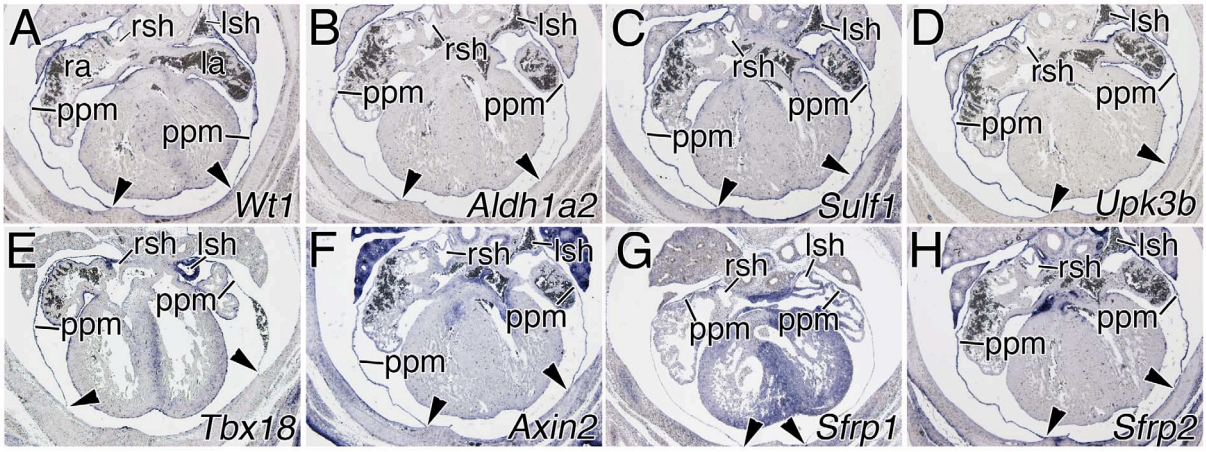

Figure 4. Gene expression in the PPMs. **A – H**, *In situ* hybridization analysis on mid-transverse sections of wildtype hearts for the mesothelial marker genes *Wt1*, *Aldh1a2*, *Sulf1* and *Upk3b*, the sinus horn marker gene *Tbx18*, and components of the Wnt signaling pathway *Axin2*, *Sfrp1* and *Sfrp2* at E14.5. Probes are as indicated, arrowheads mark the attachment point of the PPMs to the lateral body wall. la, left atrium; lsh, left sinus horns; ppm, pleuropericardial membranes; ra, right atrium; rsh, right sinus horn.

Tbx18 is required for PPD closure

We recently demonstrated the importance of *Tbx18* for the development of the venous pole of the heart including the positioning and myocardialization of the sinus horns, the myocardial parts of the right and left superior caval vein that are positioned within the pericardial cavity.[12] Additional to its expression in the developing sinus horns, we detected *Tbx18* in the PPMs (Figure 4E) prompting us to investigate the role of *Tbx18* in the development of this tissue. As *Tbx18*-null mice die shortly after birth due to severe malformations of the rib cage and respiratory insufficiency,[15] we were limited in our investigation of the pericardial phenotype to developmental stages up to E18.5 (Figure 5).

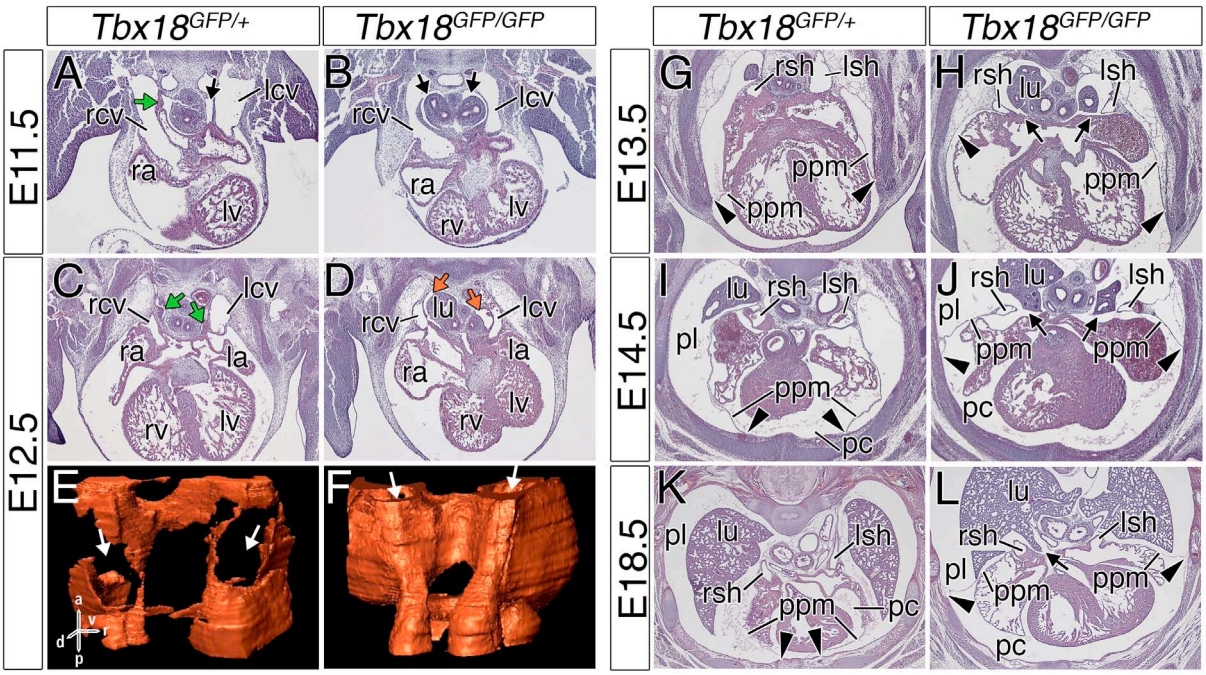

Figure 5. **Developmental onset of pericardial defects in *Tbx18*-mutant embryos. A – D, G - L**, Histological stainings with haematoxylin and eosin were performed on transverse sections through the venous pole of the heart. **E,F**, 3D-reconstruction of serial sections stained with haematoxylin and eosin to visualize the remaining lumen of the PPDs in control (**E**) and *Tbx18*-mutant (**F**) embryos at E12.5. Genotypes and stages are as indicated. Arrowheads mark the attachment point of the PPMs to the lateral body wall; black arrows point to the remaining PPDs; green arrows point to the mesenchymal thickening that is necessary for the closure of the PPDs; red arrows point to the PPDs in *Tbx18*-mutant embryos at E12.5 that was visualized by 3D reconstruction, and white arrows highlight the volume of the cardinal veins. la, left atrium; lcv, left cardinal vein; li, liver; lu, lung; lsh, left sinus horn; lv, left ventricle; pc, pericardial cavity; ppd, pleuropericardial duct; pl, pleural cavity; ppm, pleuropericardial membrane; ra, right atrium; rcv, right cardinal vein; rsh, right sinus horn; rv, right ventricle.

We started our analysis of *Tbx18*-deficient embryos by histological stainings. At E9.5 and E10.5, the positioning of the caval veins and the PPDs appeared unchanged in the *Tbx18*-mutant embryos (data not shown). At E11.5, the position of the caval veins was similar in both *Tbx18*-heterozygous (these were phenotypically indistinguishable from *Tbx18*-wildtype embryos and therefore used as control embryos) and *Tbx18*-deficient embryos. However, a mesenchymal thickening protruded into the PPDs of control embryos, but was absent from the mutant PPDs (Figure 5A and 5B, marked by a green arrow in control embryos). At E12.5, PPMs were not yet detectable in mid-transverse sections in either genotypes, but the sinus horns were positioned slightly more laterally in *Tbx18*-mutant embryos. Furthermore, the mesenchymal protrusions were again visible in the PPDs of control embryos (Figure 2B and 2E, marked by a green arrow). *Tbx18*-deficient embryos lacked this mesenchymal thickening and the PPDs appeared broader (Figure 5C and 5D). In order to visualize the closure of the PPDs, we performed a 3-dimensional (3D) reconstruction of the remaining volume of the PPDs at E12.5. This reconstruction confirmed that the PPDs were nearly completely absent in control embryos, but not in *Tbx18*-mutant embryos at this stage (Figure 5C through 5F). In control embryos the PPMs were partly released

from the disappearing subcoelomic mesenchyme and fixed to a lateral position next to the emerging ribs at E13.5. In *Tbx18*-mutant embryos the loose subcoelomic mesenchyme was still present next to the sinus horns, and the PPDs were not closed allowing the lung to contact the atria (arrows in Figure 5H). As a consequence, the sinus horns were positioned much more laterally on both sides of *Tbx18*-deficient hearts (Figure 5G and 5H). In E14.5 control embryos, the PPMs presented as thin epithelial sheets, which completely surrounded the heart; they were fixed dorsally to the hilus of the lung and ventrally to the sternum. The right and left sinus horns were positioned medial directly next to the hilus of the lung. In contrast, the PPMs of *Tbx18*-deficient embryos did not completely surround the heart, they were fixed at a lateral position and not to the sternum. Additionally the PPDs were still open, leaving a space for the lung to touch the atria. The right and left sinus horns were positioned abnormal laterally and within the PPMs at this stage (Figure 5I and 5J) and at E18.5 (Figure 5K and 5L).

To allow higher resolution imaging of PPD closure, we additionally performed histological analysis of E10.5 to E14.5 wildtype and mutant embryos on sagittal sections (Figure 6). No differences between control and mutant PPDs were detectable at E10.5 (Figure 6A and 6F). Starting from E11.5, the width of the PPDs decreased, mainly by the ingrowth of a dorsal mesenchymal tissue block located between the sinus horns and the atria (marked by a green arrow in Figure 2D, 2E, 6B and 6C), leaving only a small canal in control embryos at E12.5. In *Tbx18*-deficient embryos, this mesenchymal tissue protrusion was not established and the width of the PPDs failed to decrease (Figure 6G and 6H). In control embryos of E13.5 and E14.5, the PPDs were completely closed and the pleural and pericardial cavities fully separated (Figure 6D and 6E). In *Tbx18*-deficient embryos the PPDs remained open and the lung touched the atria at E13.5 and E14.5 (Figure 6I and 6J). Therefore, failure of formation of the mesenchymal tissue protrusion may underlie the observed defects in PPM and sinus horn development in *Tbx18*-deficient embryos.

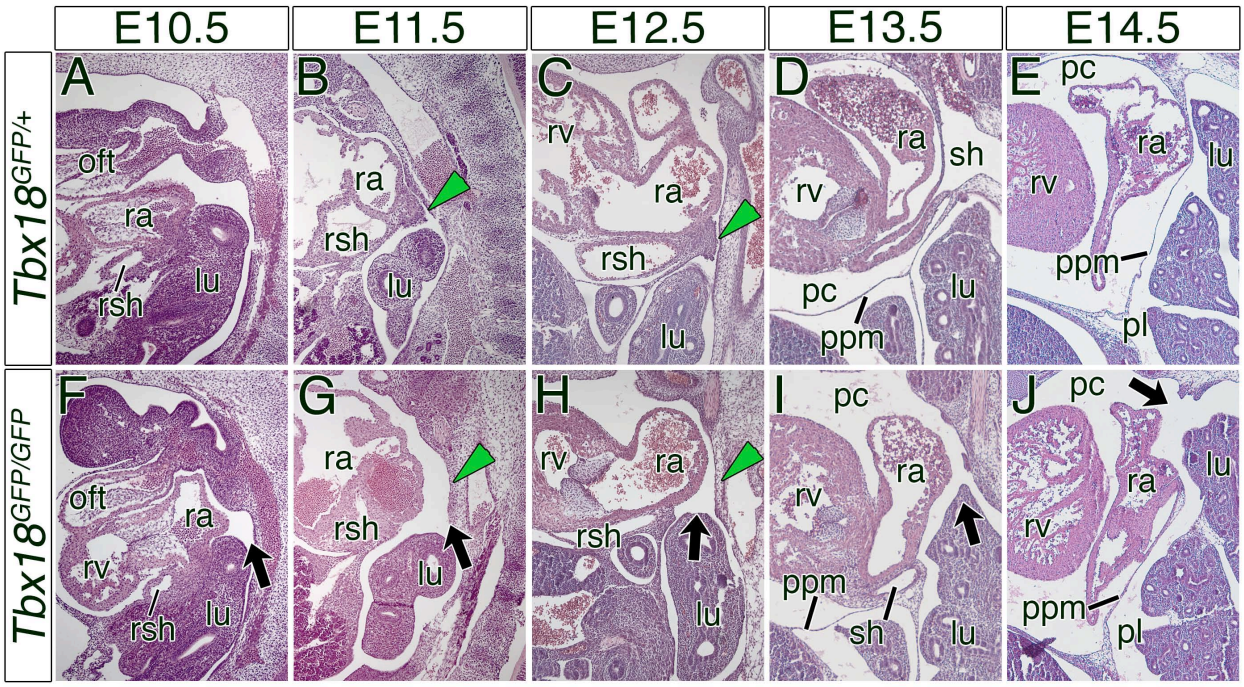

Figure 6. Insufficient closure of the PPD in *Tbx18*-mutant embryos. A – J, Histological analysis by haematoxylin and eosin staining was performed on sagittal sections of E10.5 to E14.5 control and *Tbx18*-deficient hearts as indicated. Arrows highlight the remaining PPDs in *Tbx18*-deficient embryos. Green arrowheads mark the mesenchymal thickening in control embryos and its loss, respectively, in *Tbx18*-deficient embryos. lu, lung; oft, outflow tract; pc, pericardial cavity; pl, pleural cavity; ppm, pleuropericardial membrane; ra, right atrium; rsh, right sinus horn; rv, right ventricle; sh, sinus horn.

Tbx18 is expressed and required in the developing sinus horns and an adjacent medial, highly proliferative mesenchymal tissue protrusion

The mesenchymal tissue protrusion that is positioned at the border between the sinus horns and the atria adjacent to the PPDs in the control embryos was not established in *Tbx18*-deficient embryos. Gene expression analysis in control embryos revealed that this mesenchymal protrusion was strongly positive for expression of *Tbx18* and *GFP* at E12.5 (Figure 7C and 7H). Obviously, lack of this tissue in the mutant situation did not permit to check for maintenance of expression of *Tbx18* and *GFP*, respectively. However, other expression domains of *Tbx18* including the sinus horns and the epicardium were reflected by the expression of *GFP* in *Tbx18*-heterozygous and *Tbx18*-deficient embryos at all analyzed stages (Figure 7A through 7O). This strongly indicates that *Tbx18* is cell-autonomously required for the formation of the mesenchymal tissue protrusion, which itself is necessary for PPD closure, but not for the precursor population of the sinus horns and the epicardium.

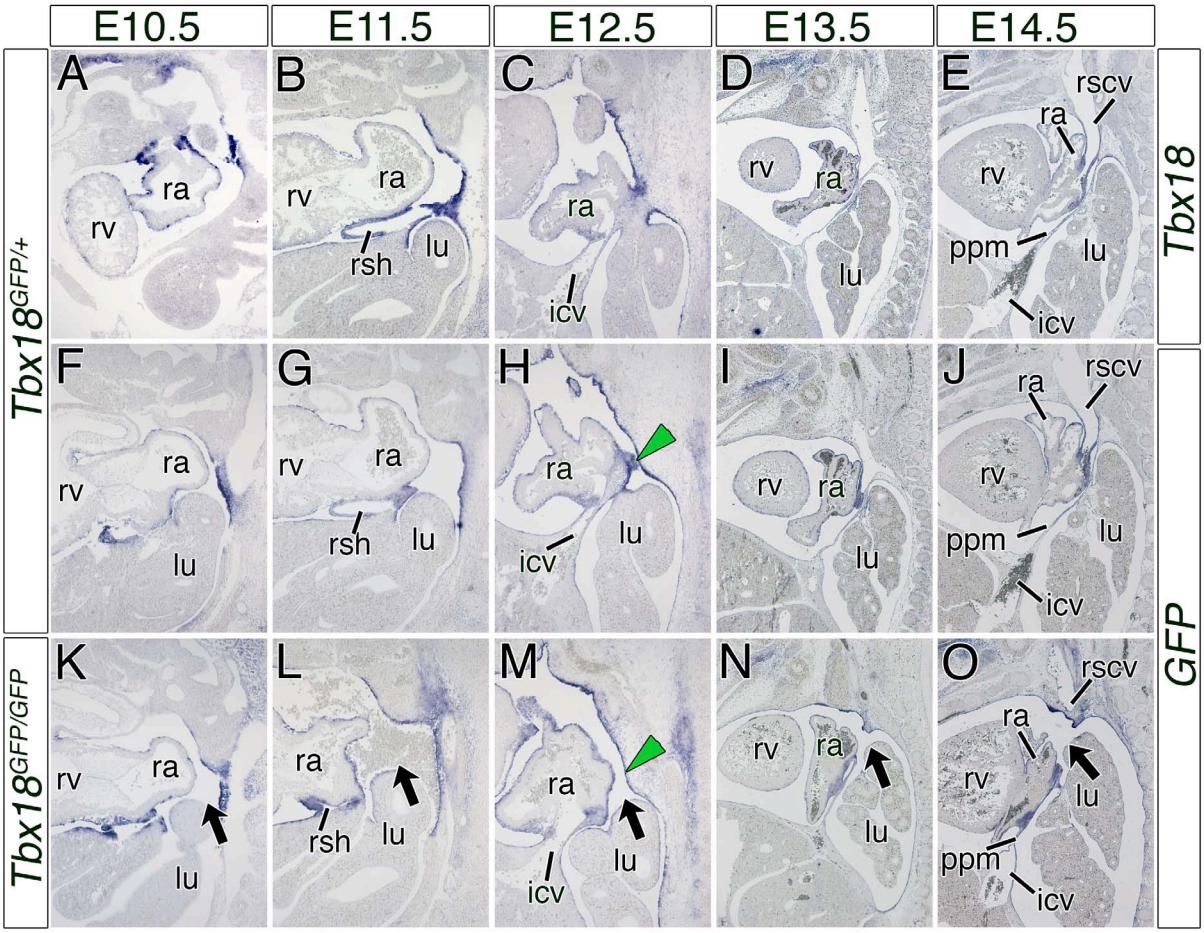

Figure 7. The PPDs in *Tbx18*-deficient embryos remains open due to the loss of a mesenchymal, *Tbx18*-positive thickening. A – O, *In situ* hybridization analysis on sagittal sections of wildtype hearts from E10.5 to E14.5. The expression of *GFP* reflects *Tbx18* expression in control embryos (**A – J)**. In *Tbx18*-deficient embryos the mesenchymal structure inside the right PPD is missing (**K – L**). Stages are as indicated on top, the genotype on the left side and the used RNA probe is indicated on the right side. Arrows point to the open right PPD. Green arrowheads mark the *GFP*-positive mesenchymal protrusion in control embryos and its loss, respectively, in *Tbx18*-deficient embryos at E12.5. icv, inferior caval vein; lu, lung; ppm, pleuropericardial membrane; ra, right atrium; rscv; right superior caval vein; rsh, right sinus horn; rv, right ventricle.

To define the molecular nature of the mesenchymal tissue protrusion that is likely to mediate PPD closure, we screened by *in situ* hybridization analysis for genes that are expressed in this thickening. First, we verified the expression of *Tbx18* on transverse sections of heterozygous embryos (Figure 8A). M*annan-binding lectin serine peptidase 1* (*Masp1*), the GATA binding proteins *Gata4* and *Gata6*, and *sulfatase 1* (*Sulf1*) were expressed in this mesenchymal aggregate in control embryos at E12.5 (Figure 8C, 8E, 8G, and 8I). Due to the lack of this structure in the PPDs of *Tbx18*-mutant embryos, expression of these genes was undetectable in mutant embryos. However, other expression domains of these genes were unchanged in control and *Tbx18*-deficient embryos. *Masp1* was expressed in parts of the left atrium, weakly in the mesothelial sheet of the pleural and pericardial cavities, and next to the trachea in both wildtype and *Tbx18*-deficient embryos (Figure 8C and 8D). *Gata4* and *Gata6* showed expression in the

myocardium of the atria and ventricles, *Gata6* was additionally expressed in the laterodorsal mesenchyme next to the sinus horns of both genotypes (Figure 8E through 8H). As the expression of the mesothelial marker genes *Sulf1*, *Aldh1a2, Wt1* and *Upk3b* were not altered in the mesothelial lining covering the pleural and pericardial cavities, the epicardium and/or the subcoelomic mesenchyme next to the sinus horns, these domains seemed unaffected in *Tbx18*-deficient embryos (Figure 8I through 8P).

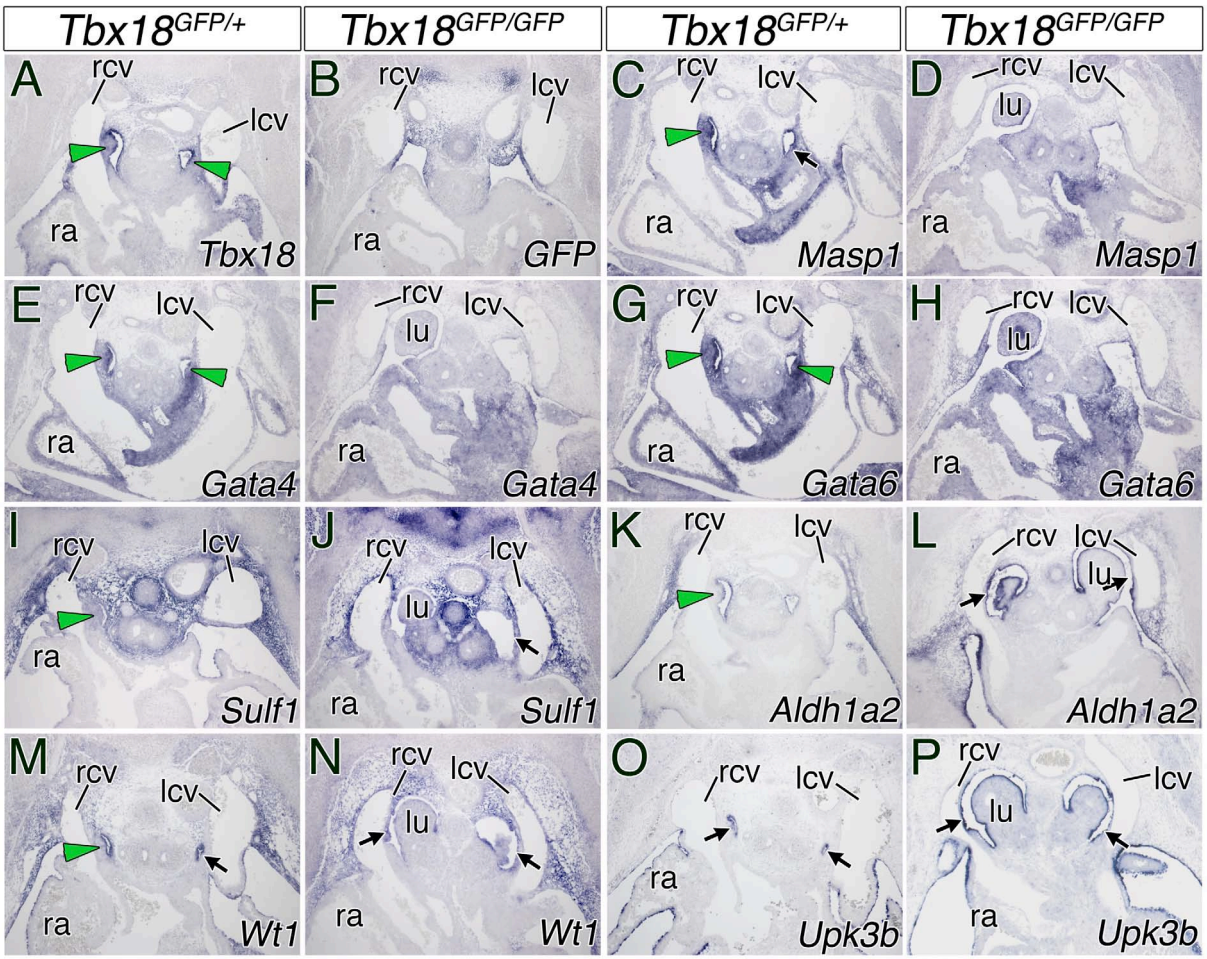

Figure 8. Analysis of cellular molecular changes in the lateral body wall and the PPDs of *Tbx18*-deficient mice. A – P, *In situ* hybridization analysis of marker expression carried out on transverse sections through the venous pole region of control and *Tbx18*-mutant mouse hearts at E12.5. Genotypes and probes are as indicated. Green arrowheads point to the *Tbx18*-positive mesenchymal protrusion that is important for the closure of the PPDs in control embryos. Black arrows highlight the mesothelial lining of the PPDs. Note the enlarged width of the PPDs in *Tbx18*-deficient embryos. lcv, left cardinal vein; lu, lung; ra, right atrium; rcv, right cardinal vein

We conclude that Tbx18 is required for establishment of a mesenchymal tissue thickening that protrudes into the PPDs to eventually seal them off. In contrast, Tbx18 seems dispensable in the subcoelomic mesenchyme and the PPMs.

To achieve further insides into the mechanism of the closure of the PPDs we analyzed proliferation by BrdU incorporation assay in both control and *Tbx18*-mutant embryos at E12.5

(Figure 9). GFP protein was detectable in the mesenchyme of the right sinus horn, the mesothelial lining of the PPDs, the PPMs and in the epicardium in either genotypes. This analysis depicted a high number of proliferating cells in the GFP-positive mesenchymal protrusion in control embryos at E12.5, the stage in which the closure of the PPDs occurred (marked by a green arrowhead in Figure 9A and 9C). This GFP-positive mesenchymal thickening, and therefore the proliferating cell, was absent in *Tbx18*-mutant embryos (Figure 9B and 9D). In summary, the high proliferation rate in the mesenchymal protrusion inside the PPDs in wildtype embryos suggests that an increase in cell number of this mesenchymal thickening leads to a constriction of the PPDs, resulting in a complete separation of the pleural and pericardial cavities.

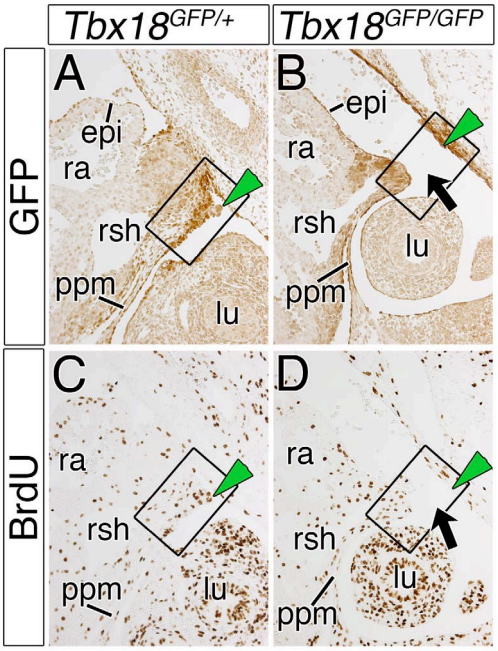

Figure 9. Cellular changes in the PPDs of *Tbx18*-deficient mice. A, B, Immunohistochemical analysis for GFP protein in control (genotype: *Tbx18*$^{GFP/+}$) and *Tbx18*-deficient embryos on sagittal sections through the PPDs at E12.5. **C, D**, Analysis of proliferation by BrdU immunohistochemistry in the boxed domain of the PPDs performed on sagittal sections through the PPDs at E12.5. BrdU positive cells are labeled in brown in C and D. Green arrowheads point to the mesenchymal protrusion inside the PPDs of control embryos. epi, epicardium; lu, lung; ppm, pleuropericardial membrane; ra, right atrium; rsh, right sinus horn.

Discussion

Partial absence of the pericardium is a rare congenital defect, which may lead to a strangulation of the heart and subsequent death.[18] The etiologies of this defect have remained unclear. Our analysis of murine pericardial development in wildtype and *Tbx18*-mutant embryos together with our recent analysis of *Wt1*-deficient[9] mice point to complex morphogenetic processes which are coupled with the development of the sinus horns at the cardiac venous pole.

Etiology of pericardial defects

During pericardial development two processes occur that are linked to the dorsocranial movement of the sinus venosus during heart looping and the growth of the whole embryo. On the one hand, the PPMs are detached from the underlying subcoelomic body wall mesenchyme. On the other hand, the PPDs, two canals in the septum transversum on both sides of the midline, are closed by the ingrowth of a mesenchymal thickening inside the PPDs. These processes act in parallel and, most likely, are independent from each other. Deficiencies in either of these two processes may cause pericardial hernia.

The subcoelomic mesenchyme next to the caval veins first becomes loosely organized and disappears completely between E12.5 and E14.5, a process that is coupled with the release of the PPMs. Molecular changes in the laterodorsal mesenchyme lead to severe pericardial phenotypes that are characterized by persisting subcoelomic mesenchyme and PPMs tethered to the lateral body wall. We recently showed that *Wt1* and its target gene *Aldh1a2* are required for the detachment of the PPMs from the laterodorsal mesenchyme. Retinoic acid induced apoptosis is absent in the *Wt1*-deficient embryos and therefore the subcoelomic mesenchyme persists. The PPMs are not released form the lateral body wall, the caval veins become abnormally positioned laterally, and the PPDs are not closed in *Wt1*-mutant embryos. However, the newly described *Tbx18*-positive mesenchymal thickening inside the PPDs, that is necessary for the closure of the PPDs, develops normally in the *Wt1*-deficient embryos. During further development, the growth of the pericardial cavity increases the tension of the laterally tethered caval veins resulting in PPM disruption and hernia in *Wt1*-deficient mice. [9] In our wildtype analysis we detected expression of *Meis1* and *Meis2*, which are direct target genes of retinoic acid signaling during limb development,[17] in the subcoelomic mesenchyme. This finding additionally points to a role of retinoic acid signaling during pericardial development. A similar pericardial defect including the persistence of the PPDs is described in *Osr1*-deficient embryos. Furthermore, the expression of *Wt1* is downregulated in the subcoelomic mesenchyme next to the caval vein in these *Osr1*-mutant embryos, pointing to a direct regulation of *Wt1* by *Osr1* during detachment of the PPMs.[10] Nevertheless, further analysis is required to fully understand the molecular mechanism regulating the detachment of the PPMs from the subcoelomic mesenchyme. The degeneration of the subcoelomic mesenchyme next to the sinus horns may

be similar to the enlargement of the middle ear cavities. Also the mesenchymal cells next to the developing tympanic cavity first become loosely packed and afterwards disappear through both apoptosis and redistribution of cells over the increasing surface area.[19] However, the molecular mechanisms regulating this process are also not understood by now.[20]

The second process of pericardial development is the closure of the PPDs. These ducts are necessary for the growth and descent of the emerging lung during early embryonic development, and they have to be closed for the complete separation of the pleural and pericardial cavities. A closed pericardium is essential to retain the low pressure in the pleural cavity during breathing,[21] and also for the formation of the pericardial fluid that may have a supportive role in regenerating heart cells after myocardial infarction.[2] Our analysis of *Tbx18*-deficient mouse embryos revealed the importance of *Tbx18* for the closure of the PPDs during murine embryonic development. In *Tbx18*-deficient embryos an undescribed pericardial defect was obvious, which was characterized by persisting PPDs and an incomplete detachment of the PPMs from the mediastinal pleura.

A *Tbx18*-positive medial mesenchymal protrusion inside the PPDs is necessary for its the closure

The *Tbx18*-positive mesenchymal protrusions, which are positioned at the lateral wall of the PPMs, had a key role during the closure of the PPDs. In wildtype embryos, this mesenchymal thickening first constricted the width of the PPDs, and later completely separated pleural and pericardial cavities by fusion to the hilus of the lung around E13.0. In both control and *Tbx18*-deficient mouse embryos a *Wt1*$^{+}$ and *Upk3b*$^{+}$ mesothelial layer was lining the complete PPDs, which was gone specifically at the attachment point after closure of the PPDs in control embryos. A similar process was proposed for the development of the human pericardium; therefore the fusion of two mesothelial surfaces might be the reason for the closure of the PPDs in humans[7] and, as our analysis revealed, also in mice. In humans, the ingrowth of the PPMs into the PPDs is sometimes described as an active movement of pleuropericardial folds that thereby get stretched and become thin PPMs.[4,22] We could not confirm this active ingrowth of pleuropericardial folds during murine pericardial development, as we were not able to detect the described pericardial folds in different mouse embryos and section planes from E9.5 to E18.5. Complete serial sections of murine embryos starting from E9.5 demonstrated that the interpretation of an active ingrowth of the PPMs might be the result of focusing to improper section planes instead of serial sections, maybe caused by the limited human material available.

After the PPMs were connected to the hilus of the lung, highly dynamic and complex morphogenetic changes occur. The whole embryo, and as a result the size of the thoracic cavity grew rapidly. In parallel the subcoelomic mesenchyme degenerated completely between E13.0 and E14.5, coupled with a dramatic increase in the size of the pleural cavity and the lung. During these growth processes the PPMs were fixed at the lateral body wall, the venous pole of the

heart and the hilus of the lung, therefore the PPMs were stretched out to thin epithelial layers. Maybe the tensile force onto the PPMs is, at least partially, necessary for the detachment from the lateral body wall, a mechanism that was already proposed for the development of the human pericardium.[6] In *Tbx18*-deficient embryos the attachment of the PPMs to the hilus of the lung and therefore the closure of the PPDs failed. As a consequence the PPMs were only fixed to the venous pole of the heart, but not to the lung hilus, and the caval veins were torn laterally due to the tension onto the PPMs during further embryonic development. To some extent the incomplete detachment from the lateral body wall in *Tbx18*-mutant embryos might be a secondary effect of the missing medial fixation of the caval veins to the lung hilus, and not a primary effect caused by cellular changes in the laterodorsal mesenchyme, since marker genes for the subcoelomic mesenchyme were not affected by the loss of *Tbx18*.

However, further analysis in mice is required to define the molecular mechanism regulating pericardial development. During our current analysis we were able to identify new marker genes for the subcoelomic mesenchyme and the PPMs in wildtype embryos. None of these genes (*Meis1, Meis2, Gata6, Sfrp1, Sfrp2, Axin2, Notch3, Sulf1, EphA3, EphB2, Ror1, Masp1*) was published to be involved in the development of the PPMs before. Therefore, our future work will focus on the role of these genes during pericardial development to obtain a molecular network for the underlying processes.

Acknowledgements

We thank Franziska Greulich for critically reading the manuscript.

Funding

This work was supported by grants from the European Community's Sixth Framework Programme contract ('HeartRepair' LSHM-CT-2005-018630), the German Research Foundation (DFG) for the Cluster of Excellence REBIRTH (From Regenerative Biology to Reconstructive Therapy) and for the Clinical Research Group KFO136 at Hannover Medical School to A.K.

References

1. Kirby ML, Waldo K. Cardiac development. Oxford University Press US; 2007.
2. Limana F, Bertolami C, Mangoni A, Di Carlo A, Avitabile D, Mocini D, Iannelli P, De Mori R, Marchetti C, Pozzoli O, Gentili C, Zacheo A, Germani A, Capogrossi M. Myocardial infarction induces embryonic reprogramming of epicardial c-kit(+) cells: role of the pericardial fluid. *Journal of Molecular and Cellular Cardiology*. 2009 Dez 4;
3. Vesely T, Julsrud P. Congenital absence of the pericardium and its relationship to the ligamentum arteriosum. *Surgical and radiologic anatomy : SRA*. 1989 Jan 1;11(2):171-5.
4. Faridah Y, Julsrud P. Congenital absence of pericardium revisited. *The international journal of cardiovascular imaging*. 2002 Feb 1;18(1):67-73.
5. Sadler TW, Langman J. Medizinische Embryologie. Die normale menschliche Entwicklung und ihre Fehlbildungen. 10. Aufl. Thieme, Stuttgart; 2003.
6. Salzer GM. Die Topogenese der Pleurahoehlen. *Z. Anat. Entwickl. Gesch.* 1960;122(3):232-240.
7. Salzer GM. Der Verschluss der pleuroperikardialen Verbindung bei menschlichen Embryonen. *Z Anat Entwickl Gesch*. 1959;121(2):54-70.
8. Frick H. Ueber den Abschluss der Verbindung zwischen Pleura und Perikard bei menschlichen Embryonen. *Z Anat Entwickl-Gesch*. 1949;114:230-241.
9. Norden J, Grieskamp T, Lausch E, Van Wijk B, van den Hoff M, Englert C, Petry M, Mommersteeg M, Christoffels V, Niederreither K, Kispert A. Wt1 and Retinoic Acid Signaling in the Subcoelomic Mesenchyme Control the Development of the Pleuropericardial Membranes and the Sinus Horns. *Circulation Research*. 2010 Feb 25;(106):1212 -1220.
10. Wang Q, Lan Y, Cho E, Maltby K, Jiang R. Odd-skipped related 1 (Odd 1) is an essential regulator of heart and urogenital development. *Developmental Biology*. 2005 Dez 15;288(2):582-94.
11. Kraus F, Haenig B, Kispert A. Cloning and expression analysis of the mouse T-box gene Tbx18. *Mechanisms of Development*. 2001 Jan 1;100(1):83-6.
12. Christoffels V, Mommersteeg M, Trowe M, Prall O, De Gier-De Vries C, Soufan A, Bussen M, Schuster-Gossler K, Harvey R, Moorman A, Kispert A. Formation of the venous pole of the heart from an Nkx2-5-negative precursor population requires Tbx18. *Circulation Research*. 2006 Juni 23;98(12):1555-63.
13. Wiese C, Grieskamp T, Airik R, Mommersteeg M, Gardiwal A, De Gier-De Vries C, Schuster-Gossler K, Moorman A, Kispert A, Christoffels V. Formation of the sinus node head and differentiation of sinus node myocardium are independently regulated by Tbx18 and Tbx3. *Circulation Research*. 2009 Feb 13;104(3):388-97.
14. Moorman A, Houweling A, de Boer P, Christoffels V. Sensitive nonradioactive detection of mRNA in tissue sections: novel application of the whole-mount in situ hybridization protocol. *J Histochem Cytochem*. 2001 Jan 1;49(1):1-8.
15. Bussen M, Petry M, Schuster-Gossler K, Leitges M, Gossler A, Kispert A. The T-box transcription factor Tbx18 maintains the separation of anterior and posterior somite compartments. *Genes & Development*. 2004 Mai 15;18(10):1209-21.
16. Soufan A, Ruijter J, van den Hoff M, de Boer P, Hagoort J, Moorman A. Three-dimensional reconstruction of gene expression patterns during cardiac development. *Physiological Genomics*. 2003 Mai 13;13(3):187-95.

17. Niederreither K, Vermot J, Schuhbaur B, Chambon P, Dolle P. Embryonic retinoic acid synthesis is required for forelimb growth and anteroposterior patterning in the mouse. *Development*. 2002;129(15):3563-74.

18. Abbas A, Appleton C, Liu P, Sweeney J. Congenital absence of the pericardium: case presentation and review of literature. *Int J Cardiol*. 2005 Jan 1;98(1):21-5.

19. Richter CA, Amin S, Linden J, Dixon J, Dixon MJ, Tucker AS. Defects in middle ear cavitation cause conductive hearing loss in the Tcof1 mutant mouse. *Human Molecular Genetics*. 2010 Apr 15;19(8):1551 -1560.

20. Chapman SC. Can you hear me now? Understanding vertebrate middle ear development. *Front Biosci*. 2011;16:1675-1692.

21. Drews U. Taschenatlas der Embryologie. 1. Aufl., Thieme Verlag; Stuttgart; 1993.

22. Brachet A. Die Entwicklung der grossen Koerperhoehlen und ihre Trennung voneinander. *Ergebn Anat Entwickl-Gesch*. 1897;7:886.

Canonical Wnt/beta-catenin Signaling is Required for Pericardial Development

Julia Norden and Andreas Kispert*

Institut für Molekularbiologie, OE5250, Medizinische Hochschule Hannover, Carl-Neuberg-Str.1, D-30625 Hannover, Germany

Author for correspondence:

E-MAIL: kispert.andreas@mh-hannover.de

TEL.: +49 511 5324017

FAX.: +49 511 5324283

Running title: canonical Wnt signaling in pericardial development

Manuscript in preparation.

Abstract

Aims: The pericardium is a mesothelial sac that entirely surrounds the heart and the roots of the great vessels; its complete or partial absence is a rare congenital human disease. Little is known about the molecular mechanism regulating its embryonic development both in mice and humans. Here, we wish to define a role of canonical (beta-catenin (Ctnnb1))-dependent Wnt signaling in murine pericardial development.

Methods and results: We analyzed the role of canonical Wnt signaling during early and late steps of pericardial development by histological stainings and *in situ* hybridization analysis of different pericardium specific *Ctnnb1* loss- and gain-of-function mutant embryos. Both genetic manipulations resulted in distinct pericardial malformations. Additionally, we examined defects in the formation of the sinus horns at the cardiac venous pole that are coupled with pericardial defects in *Ctnnb1*-deficient mice.

Conclusion: Canonical Wnt signaling regulates the detachment of the pleuropericardial membranes from the subcoelomic mesenchyme of the lateral body wall. Both, pericardial and venous pole development are coupled. However, myocardialization of the sinus horns is independent from their positioning inside the pericardial cavity.

Keywords: beta-catenin, pericardium, sinus venosus, heart development

Non-standard abbreviations and acronyms

Ctnnb1	beta-catenin
E	embryonic day
PPD	pleuropericardial duct
PPM	pleuropericardial membrane
SAN	sinoatrial node
Tbx	T-box
Wt1	Wilms tumor 1 homolog

Introduction

The adult pericardium is a thin mesothelial tissue that completely surrounds the heart and the roots of the great blood vessels. It is attached dorsally to the hilus of the lung, ventrally to the sternum, and caudally to the diaphragm. Its functions are the separation of the pleural and pericardial cavities and thereby the protection and fixation of the heart inside the thoracic cavity.[1] The complete or partial absence of the pericardium is a rare congenital human defect that is asymptomatic in most of the patients. However, the foramen formed by the partial absence of the pericardium may lead to heart strangulation, and therefore may cause death.[2] The molecular mechanism regulating pericardial development are only partially deciphered, and further analysis is required to understand the genetic background of congenital pericardial defects.

The mature pericardium derives from the embryonic pleuropericardial membranes (PPMs), which initially arise as two mesothelial tissue layers. At embryonic day (E) 9.5 and E10.5, the complete body wall of the thoracic cavity, a thin mesothelial tissue layer, is referred to as (embryonic) pericardium. This body wall thickens during the onset of development and the mesothelial lining of the pericardial cavity will give rise to the detached PPMs starting from E12.5. During the development of the PPMs two complex morphogenetic processes occur in parallel. First, the mesothelial lining of the pericardial cavity, which will form the PPMs, detaches from the subcoelomic mesenchyme of the lateral body wall. Recently, we demonstrated the importance of the transcription factor *Wilms tumor 1* (*Wt1*), which is expressed in the subcoelomic mesenchyme, for the degeneration of this tissue. In *Wt1*-deficient embryos the caval veins remain tethered to the persisting subcoelomic mesenchyme and were not myocardialized. In wildtype embryos *Wt1* induces the expression of the *aldehyde dehydrogenase family 1, subfamily A2* (*Aldh1a2*, also known as *Raldh2*), and the resulting retinoic acid signaling leads to apoptosis of the subcoelomic mesenchyme that is crucial for the release of the PPMs[3]. In a second morphogenetic process the pleuropericardial ducts (PPDs), which are essential for the movements of the lung during early embryonic development, are closed by an attachment of the PPMs to the hilus of the lung. This process requires expression of the T-box transcription factor *Tbx18* (Norden *et al*., manuscript in preparation).

Wnt signaling pathways are important for the regulation of gene transcription as well as cell proliferation, cell fate decisions, and cell polarity during embryonic development in both vertebrates and non-vertebrates.[4] Wnt proteins are secreted factors that act by binding to Frizzled (Fzd) receptors, thereby stabilizing the protein beta-catenin (Ctnnb1). Ctnnb1 is the central component of the canonical Wnt signaling pathway, and transmits Wnt signals to the TCF/LEF complex in the nucleus, thereby inducing transcription of target genes such as *Axin2*.[5] At E9.5 and E10.5, the canonical Wnt signaling ligand *wingless-related MMTV integration site 2* (*Wnt2,* also known as *m-irp*) is expressed in the embryonic pericardium, which is also the

thoracic body wall at this stage of development.[6] Additional, the BAT-gal reporter mouse line confirmed active Ctnnb1-signaling in the embryonic pericardium at E9.5.[7]

However, until now the role of canonical Wnt/β-catenin signaling in murine pericardial development has remained elusive. Here, we examine different conditional *Ctnnb1* loss- and gain-of-function mutant mice. We show that both pericardium-specific loss as well as ectopic activation of canonical Wnt signaling result in pericardial defects, which are associated with deficiencies in the sinus venosus region of the heart. Additionally, we show that myocardialization of the sinus horns, the intrapericardial parts of the caval veins, is independent from the position inside the pericardial cavity.

Material and Methods

Mice and genotyping

Mice with a knock in of the *cre*-recombinase into the *Tbx18* locus (*Tbx18*$^{tm4(cre)Akis}$, synonym: *Tbx18*^{cre})[8] and mice that express the cre-recombinase under the control of a *Prrx1* derived enhancer (*Tg(Prrx1-cre)1Cjt*, synonym: *Prrx1-cre*)[9] were described before. Additionally, we used two published reporter lines, the lacZ expressing reporter line *Gt(ROSA)26Sor* (synonym: *R26*^{LacZ})[10] and a fluorescent reporter line *(Gt(ROSA)26Sor*$^{tm4(ACTB-tdTomato,-EGFP)Luo}$/J, synonym: *R26*^{mTmG})[11]. For the conditional inactivation of *Ctnnb1* we used mice with two *loxP* sites flanking the *Ctnnb1* locus from exon 2 to exon 6 (*Ctnnb1*^{tm2Kem}, synonym: *Ctnnb1*^{fx})[12], the ectopic activation of beta-catenin was achieved by using mice with two *loxP* sites flanking exon 3 of the *Ctnnb1* locus (*Ctnnb1*^{tm1Mmt}, synonym: *Ctnnb1*$^{(Ex3)fl}$).[13]

All mice were maintained on an outbred (NMRI) background. The *Tbx18*^{cre} specific *Ctnnb1* loss-of-function mutants (*Tbx18*$^{cre/+}$*;Ctnnb1*$^{fx/fx}$) were obtained from matings of *Tbx18*$^{cre/+}$*;Ctnnb1*$^{fx/+}$ males with *Ctnnb1*$^{fx/fx}$ (*Ctnnb1*^{tm2Kem}*)*[12] females. *Tbx18*^{cre} specific *Ctnnb1* gain-of-function mice *(Tbx18*$^{cre/+}$*;Ctnnb1*$^{(Ex3)fl/+}$*)* were derived from matings of *Tbx18*$^{cre/+}$ males with *Ctnnb1*$^{(Ex3)fl/(Ex3)fl}$ (*Ctnnb1*^{tm1Mmt})[13] females. *Prrx1-cre* specific loss-of-function mutants (*Prrx1-cre;Ctnnb1*$^{fx/fx}$) derived from matings of heterozygous *Prrx1cre/+* (*Tg(Prrx1-cre)1Cjt*)[9] males with *Ctnnb1*$^{fx/fx}$ (*Ctnnb1*^{tm2Kem}*)*[12] females. The *Prrx1-cre* specific gain-of function mutants were obtained by intercrossing of *Prrx1-cre/+* (*Tg(Prrx1-cre)1Cjt*)[9] males with *Ctnnb1*$^{(Ex3)fl/(Ex3)fl}$ (*Ctnnb1*^{tm1Mmt})[13] females. For the analysis of the conditional *Ctnnb1* loss-of-function phenotype, heterozygous animals (*Tbx18*$^{cre/+}$*;Ctnnb1*$^{fx/+}$ or *Prrx1-cre/+; Ctnnb1*$^{fx/+}$) were used as control embryos. For the *Ctnnb1* gain-of-function analysis *Ctnnb1*$^{(Ex3)fl/+}$ heterozygous embryos without a *cre*-allele were used as control.

Mouse embryos were generated by timed matings; observation of vaginal plug was designated as embryonic day (E) 0.5. Embryos were harvested in PBS, fixed in 4% paraformaldehyde

overnight, and stored in 100% methanol at –20°C before further use. Genomic DNA prepared from yolk sacs or tail biopsies was used for genotyping by PCR (protocols upon request). H. Hedrich, state head of the animal facility, approved the care of animals and experiments at Medizinische Hochschule Hannover.

Histological analysis

Embryos were fixed as described above, paraffin embedded, and sectioned to 10-μm for histological stainings. Sections were stained with haematoxylin and eosin, following standard procedures. At least two embryos of each genotype were used for each analysis.

***In situ* hybridization analysis**

Nonradioactive *in situ* hybridization analysis with digoxigenin-labeled antisense riboprobes was performed as described.[14] At least two embryos of each genotype were used for each analysis. Details of used probes upon request.

Immunohistochemistry

For immunofluorescence analysis, mouse monoclonal antibody against GFP (1:250, 11814460001, Roche), and rabbit polyclonal antibody against Wt1 (1:400, C-19, Santa Cruz Biotechnology) were used as primary antibodies. Alexa488 donkey-anti-mouse (1:250, Invitrogen) and biotinylated goat-anti-rabbit (1:250, 111-065-003, Dianova) were used as secondary antibodies. Nuclei were stained with 4',6-diamidino-2-phenylindol (DAPI) (Roth). Paraffin embedded embryos were sectioned to 5-μm, and all used sections were pressure cooked for 3 min in antigen unmasking solution (H-3300, Vector Laboratories Inc). Endogenous peroxidase activity was blocked by 3% H_2O_2. The signal was amplified using either the Tyramide Signal Amplification (TSA) system from Perkin-Elmer (NEL702001KT, Perkin Elmer LAS) or the Mouse-on-mouse (M.O.M.) immunodetection kit from Vector Laboratories (PK-2200, Vector Labs). The anti-GFP staining was performed in a second experiment directly after the first immunodetection was finished and followed the published protocols.

Documentation

Sections were photographed using a Leica DM5000 microscope with Leica DFC300FX digital camera and afterwards processed in Adobe Photoshop CS3.

Results

Canonical Wnt signaling in the PPMs and the body wall mesenchyme is necessary for the release of the PPMs from the mediastinal pleura

Mice that express the *cre*-recombinase under the control of a *paired related homeobox 1 (Prrx1,* also known as *Prx1)* derived enhancer (*Tg(Prrx1-cre)1Cjt*, synonym: *Prrx1-cre*)[9] mediate recombination of loxP-flanked sequences in the early limb bud and craniofacial mesenchyme,[15] as well as in precursor cells of the outflow tract and right ventricle.[16] We detected an additional contribution of *Prrx1-cre* derived cells to the PPMs using $R26^{LacZ}$ reporter analysis[10] (Figure 1).

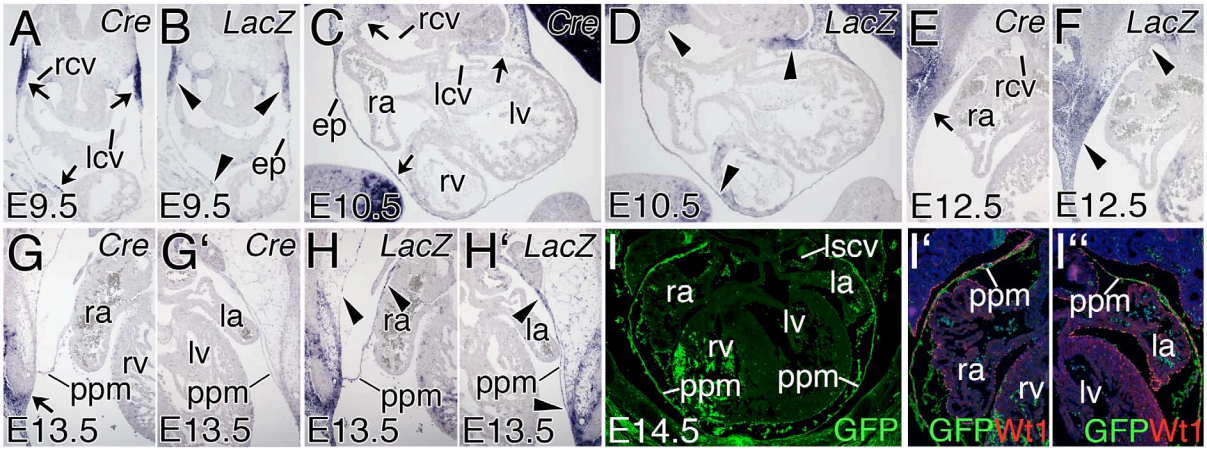

Figure 1. *Prrx1-cre* derived cells contribute to the PPMs. A – H, Lineage tracing experiments by *in situ* hybridization for *Cre* and *LacZ* on neighboring transverse sections trough the venous pole in *Prrx1-cre;*$R26^{LacZ/+}$ embryos from E9.5 to E13.5. **I thorough I''**, Immunofluorescence analysis of GFP (green) and Wt1 (red) on transverse section of a *Prrx1-cre;*$R26^{mTmG/+}$embryo at E14.5. **G** and **G'** as well as **H** and **H'** show the right and left PPM, respectively, of the same embryo. **I'** and **I''** are magnifications of the embryo seen in **I**. Stages and probes are as indicated. Arrows mark the *Cre* expression domains, arrowheads *LacZ*-positive regions in *Prrx1-cre;*$R26^{LacZ/+}$ embryos. ep, embryonic pericardium; la, left atrium; lcv, left cardinal vein; lscv, left superior caval vein; lv, left ventricle; ppm, pleuropericardial membrane; ra, right atrium; rcv, right cardinal vein; rv, right ventricle.

In *Prrx1-cre;*$R26^{LacZ/+}$ embryos *Cre* and *LacZ* expression were detectable in the lateral body wall mesenchyme next to the caval veins, the embryonic pericardium of the body wall, and the right ventricle at E9.5 and E10.5 (Figure 1A through 1D). The *cre* expression in the subcoelomic mesenchyme next to the caval veins was downregulated after E12.5, but these cells remained positive for *LacZ* at E12.5 and E13.5 (Figure 1E through 1H'). At E13.5, *cre* expression was absent from the free parts of the PPMs, but *LacZ* gene expression was detectable in the PPMs and in the body wall next to the attachment points of the PPMs at this stage (Figure 1G, 1G', 1H and 1H'). Because of the bright and distinct GFP expression after *cre*-recombination in the $R26^{mTmG}$ mice[11] we additionally performed lineage analysis using this reporter mouse line. The GFP protein was coexpressed with the mesothelial marker Wt1 in the PPMs at E14.5 (Figure 1I

through 1l''), which confirmed the derivation of the PPMs from *Prrx1-cre*-positive precursor cells, and the suitability of this mouse line for pericardium-specific gene manipulation.

Prrx1-cre and *Axin2,* a target gene of the canonical Wnt signaling pathway,[17] are coexpressed in the embryonic pericardium of wildtype embryos at E9.5 and E10.5 (Figure 1A, 1C, 5B, and 5I) suggesting that this pathway is active in pericardial precursor cells. To investigate the relevance of canonical Wnt signaling for pericardial development, we crossed *Prrx1-cre* males with females harboring a floxed allele of *Ctnnb1* (*Ctnnb1*^{fx})[12] to specifically delete *Ctnnb1* expression during early pericardial development starting from E9.5 (Figure 2)

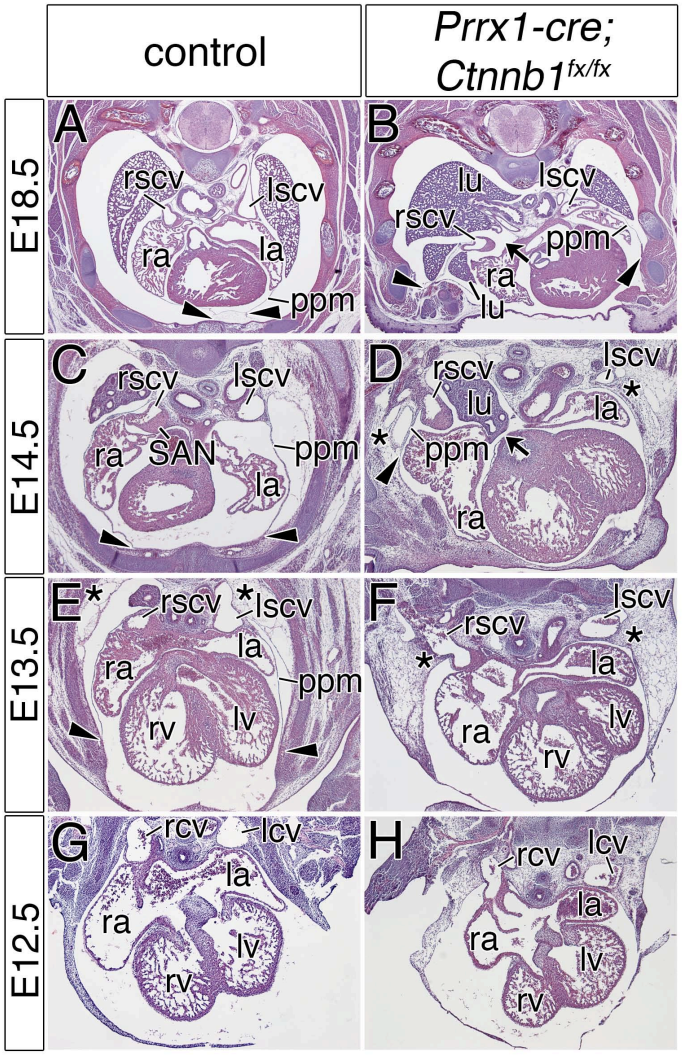

Figure 2. Developmental onset of pericardial defects in *Prrx1-cre;Ctnnb1*$^{fx/fx}$ mutant embryos. A through H, Histological analysis by haematoxylin and eosin stainings of transverse section of control (**left column**) and *Prrx1-cre;Ctnnb1*$^{fx/fx}$ mutant (**right column**) hearts from E18.5 to E12.5. Stages are as indicated. Asterisks mark the subcoelomic mesenchyme. Arrows point to the canal between lung and atrium in the mutant embryos, arrowheads indicate the attachment point of the PPMs to the lateral body wall. la, left atrium; lcv, left cardinal vein; lscv, left superior caval vein; lu, lung; lv, left ventricle; ppm, pleuropericardial membrane; ra, right atrium; rcv, right cardinal vein; rscv, right superior caval vein; rv, right ventricle; SAN, sinoatrial node.

As previously described, *Prrx1-cre;Ctnnb1$^{fx/fx}$* mutant embryos survived embryonic development and died shortly after birth.[18] In E18.5 control embryos (genotype: *Prrx1-cre;Ctnnb1$^{fx/+}$)* pleural and pericardial cavities were separated by the PPMs that were attached dorsally to the hilus of the lung and ventrally to the sternum. In *Prrx1-cre;Ctnnb1$^{fx/fx}$* mutant embryos, the PPMs were not connected to the hilus of the lung, leaving a space for a lobe of the lung to lie inside the pericardial cavity; the sinus horns were abnormally positioned laterally. The release of the PPMs from the lateral body wall was disturbed, resulting in the formation of short PPMs and indicating that *Ctnnb1* is indeed required for pericardial development. Additionally, the whole heart was tilted to the left within the pericardial cavity and the ribs were not fused ventrally (Figure 2A and 2B).

To define the developmental onset of this phenotype, we analyzed mutant embryos at earlier embryonic stages. At E14.5, the PPMs were almost completely released from the lateral body wall in control embryos. In *Prrx1-cre;Ctnnb1$^{fx/fx}$* mutant embryos the sinus horns occupied an abnormal lateral position within the very short PPMs that were also tethered by a persisting subcoelomic mesenchyme to the body wall. Thus, a wide canal on the right side allowed the lung to touch the atria at this stage (Figure 2C and 2D). At E13.5, the PPMs were partly released from the lateral body wall and only a small portion of the subcoelomic mesenchyme in the pleural cavity was detectable in control embryos. In contrast, the caval veins were tethered entirely to the persisting subcoelomic mesenchyme, PPMs were not apparent, and the heart was tilted to the left (Figure 2E and 2F). Furthermore, the whole body wall consisted of loose mesenchymal cells, and ribs were not developed. At E12.5, the PPMs were not detached from the lateral body wall and the venous pole region of the heart was similar developed in both control and *Ctnnb1*-mutant embryos (Figure 2G and 2H). We conclude from this histological analysis of *Prrx1-cre;Ctnnb1$^{fx/fx}$* mutant embryos that canonical Wnt/Ctnnb1 signaling is required for the release of the PPMs from the subcoelomic mesenchyme.

Myocardialization of the sinus horns is unaffected in *Prrx1-cre;Ctnnb1$^{fx/fx}$* mutant mice

To further clarify the observed defects in *Prrx1-cre;Ctnnb1$^{fx/fx}$* mutant mice we additionally examined these mutant mice for molecular marker expression by *in situ* hybridization (Figure 3). We recently reported on the pericardial defects in *Wt1*-deficient embryos,[3] that were highly similar to the ones observed here: the caval veins remained tethered in the subcoelomic mesenchyme, only short PPMs developed and a canal remained between the lung and the atria. Additionally, the sinus horns were not myocardialized in the *Wt1*-mutant embryos, which we attributed to their abnormal lateral position inside the PPMs.[3] In contrast and despite their abnormal lateral position, sinus horns were myocardialized in E18.5 *Prrx1-cre;Ctnnb1$^{fx/fx}$* mutant mice as revealed by normal expression of the cardiomyocyte specific *troponin I cardiac 3*, *(Tnni3,* also known as *cTnI)* (Figure 3A, 3A', 3C and 3C'). The transcription factor *T-box 18* (*Tbx18)* is important for myocardialization of the sinus horns[19] and pericardial development

(Norden *et al*., manuscript in preparation). *Tbx18* was expressed in the sinus horn myocardium, the SAN, and weakly in the PPMs of both genotypes at E18.5 (Figure 3B, 3B', 3D, and 3D'). The SAN marker gene *hyperpolarization-activated, cyclic nucleotide-gated K+ 4 (Hcn4)* and the mesothelial marker gene *Uroplakin 3b* (*Upk3b)*[20] were unchanged in *Prrx1-cre;Ctnnb1*$^{fx/fx}$ embryos at E18.5 (Figure 3E trough 3H'). Therefore, pericardium specific loss of *Ctnnb1* does not affect SAN formation, mesothelial identity of the PPMs, and sinus horn myocardialization.

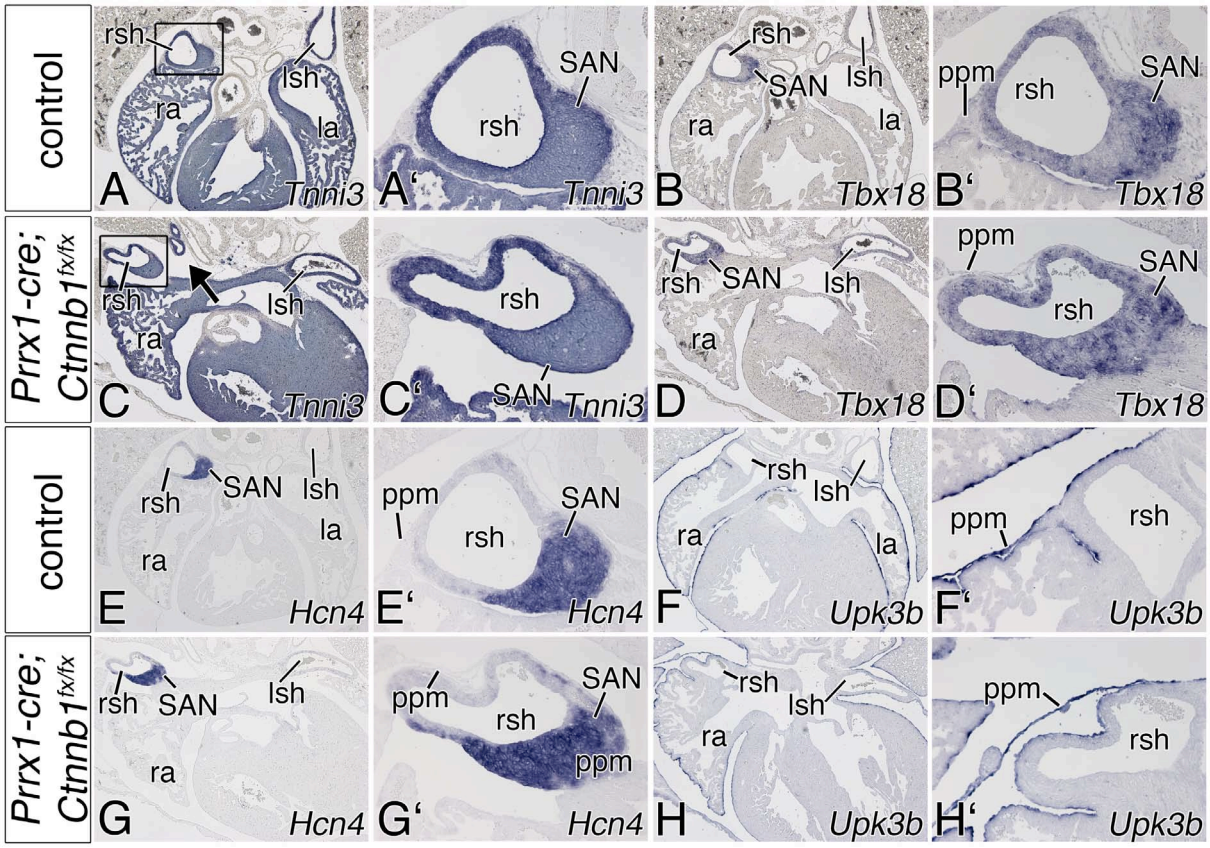

Figure 3. Myocardialization of the sinus horns is independent from its position next to the midline. A through H', *In situ* hybridization analysis of cardiomyocyte specific *Tnni3 (***A** and its magnification **A',C** and **C'***)*, the sinus horn marker gene *Tbx18* (**B** and **B', D** and **D'**) , the sinoatrial node marker gene *Hcn4* (**E** and **E', G** and **G'**), and the mesothelial marker gene *Upk3b* (**F** and **F', H** and **H'**) in transverse sections of whole hearts and detailed analysis of the sinus venosus in control and *Prrx1-cre;Ctnnb1*$^{fx/fx}$ mutant embryos at E18.5. Black boxes in A and C mark the magnified sections in A' or C', respectively. Genotypes are as indicated. Arrows indicate the connection between right atrium and lung in *Prrx1-cre,Ctnnb1*$^{fx/fx}$ mutant embryos. la, left atrium; lsh, left sinus horn; ppm, pleuropericardial membrane; ra, right atrium; rsh, right sinus horn; SAN, sinoatrial node.

At E14.5, the sinus horns as well as the SAN were positive for the cardiomyocyte specific gene *Tnni3* and the sinus horn marker *Tbx18* in control and in *Prrx1-cre;Ctnnb1*$^{fx/fx}$ embryos, excluding a delay of myocardialization in these mutant embryos (Figure 4A through 4D'). This analysis additionally revealed that the pericardial phenotype observed in *Prrx1-cre;Ctnnb1*$^{fx/fx}$ embryos is not secondary to a loss of *Wt1*. In control embryos *Wt1* was expressed in all mesothelial tissues including the PPMs at E14.5, and in the subcoelomic mesenchyme until its disintegration around this stage (Figure 4E and 4E'). In embryos with *Prrx1-cre* specific deletion of canonical

Wnt/Ctnnb1 signaling, the subcoelomic mesenchyme persisted and expressed *Wt1* at E14.5. The mesothelial character of the short PPMs was maintained in the *Ctnnb1*-deficient embryos (Figure 4G, and 4G'). The *Prrx1-cre* specific deletion of *Ctnnb1* was confirmed by the absence of *Axin2* expression in *Prrx1-cre;Ctnnb1*$^{fx/fx}$ mutant PPMs, in control embryos weak *Axin2* expression was detectable in the PPMs at E14,5 (Figure 4F, 4F', 4H, and 4H'). In conclusion, the *Prrx1-cre* specific loss of *Ctnnb1* affected early pericardial development. The subcoelomic mesenchyme was almost completely maintained, and the caval veins remained tethered inside this mesenchyme and positioned laterally next to the body wall.

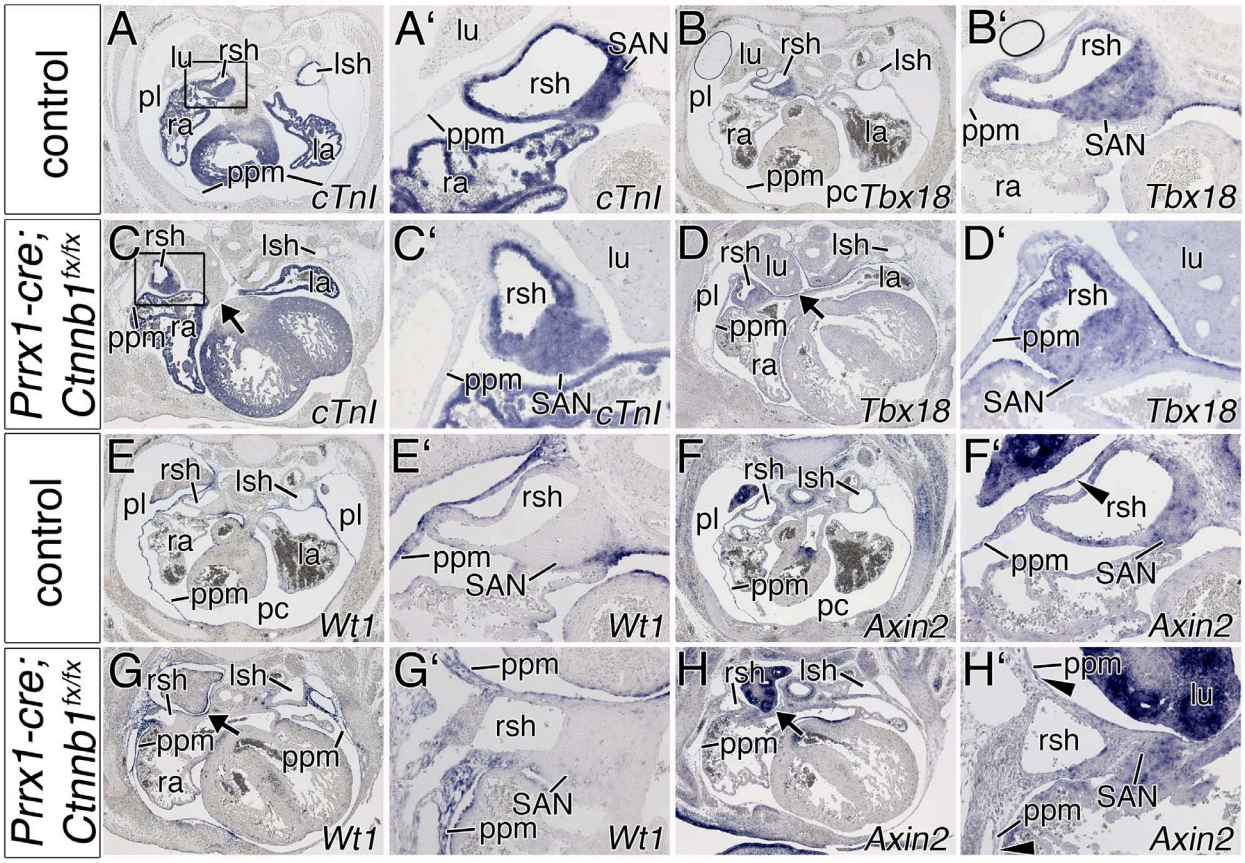

Figure 4. Myocardialization of the sinus horns is not affected in *Prrx1-cre;Ctnnb1*$^{fx/fx}$ mutant embryos. A through H', In situ hybridization analysis of cardiomyocyte specific *Tnni3* (**A** and its magnification **A'; C** and **C**'), the sinus horn marker gene *Tbx18* (**B** and **B', D** and **D'**), the mesothelial and subcoelomic mesenchyme marker gene *Wt1* (**E** and **E', G** and **G'**), and the Ctnnb1 target gene *Axin2* (**F** and **F', H** and **H'**) on transverse sections of the heart at E14.5. Genotypes are as indicated. Black boxes in A and C mark the magnified sections in A' or C', respectively. Arrows indicate the canal between right atrium and lung in *Prrx1-cre,Ctnnb1*$^{fx/fx}$ mutant embryos, arrowheads highlight the PPMs. la, left atrium; lsh, left sinus horn; lu, lung; pc, pericardial cavity; pl, pleural cavity; ppm, pleuropericardial membrane; ra, right atrium; rsh, right sinus horn; SAN, sinoatrial node.

Tbx18^{cre}-specific inactivation of canonical Wnt/Ctnnb1 signaling leads to pericardial defects

The T-box transcription factor *Tbx18* is expressed the proepicardium at E9.5, the epicardium until E16.5, and the myocardium of the left ventricle and the interventricular septum starting from E10.5. Additionally, *Tbx18* expression is found in the developing mesothelial lining of the pericardial cavity and the PPDs, which will give rise to the PPMs, starting from E10.5 (Figure 5).[21] At E9.5, we did not detect expression of *Tbx18* in the embryonic pericardium, whereas the pro-/epicardium already expressed *Tbx18*. *Tbx18* expression did not overlap with the weak expression of *Axin2* in the embryonic pericardium at this stage (Figure 5A and 5B). We verified the contribution of *Tbx18*-positive cells to the PPMs by lineage tracing experiments. In *Tbx18*$^{cre/+}$;*R26*$^{mTmG/+}$ embryos[11] the entire PPMs were positive for GFP that overlapped with the mesothelial marker Wt1[22] at E18.5 (Figure 5C and 5D). Additionally, the sinus horns, the epicardium, and part of the left ventricle were derived from *Tbx18*-positive progenitor cells. Therefore, the *Tbx18*$^{cre/+}$ mouse line provides an additional and independent tool to analyze Ctnnb1 function during pericardial development.

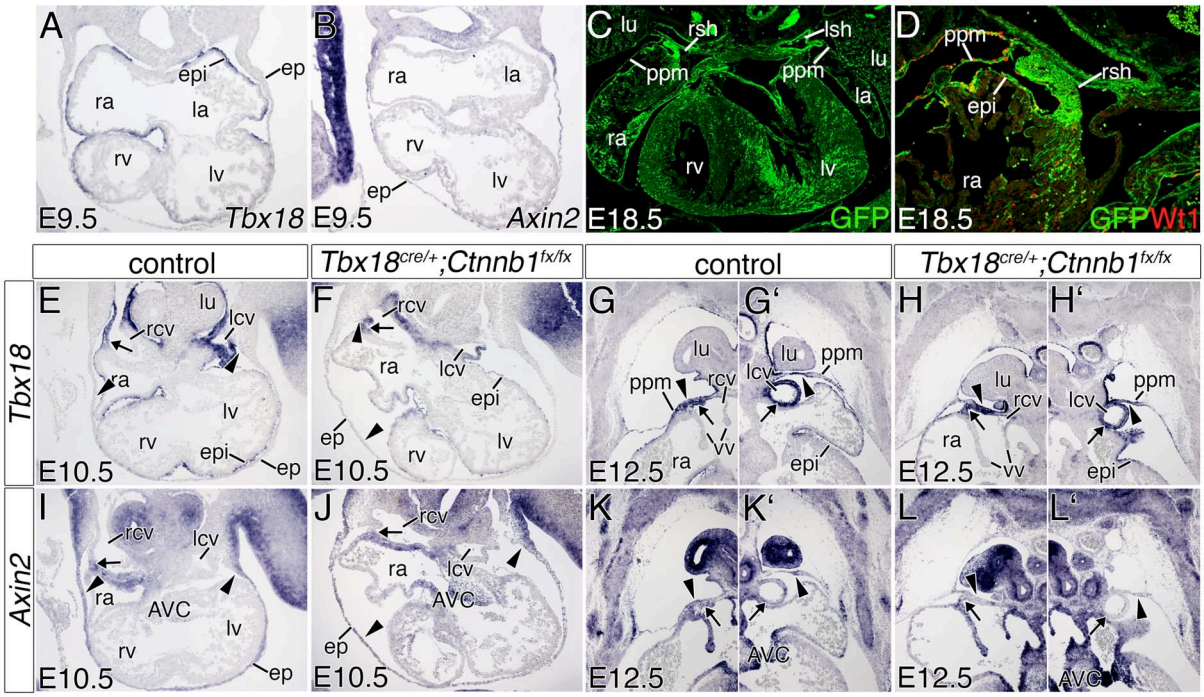

Figure 5. **The PPMs are derived from *Tbx18*-positive precursor cells. A, B**, *In situ* hybridization analysis on mid-transverse sections for expression of *Tbx18* and *Axin2* in wildtype embryos at E9.5. **C, D,** Immunofluorescence analysis of GFP, which marks *Tbx18*-derived cells, and the mesothelial marker Wt1 in *Tbx18*$^{cre/+}$;*R26*$^{mTmG/+}$ embryos at E18.5. **E through L'**, *In situ* hybridization analysis for *Tbx18* and the canonical Wnt target gene *Axin2* in control and *Tbx18*$^{cre/+}$;*Ctnnb1*$^{fx/fx}$ mutant embryos at E10.5 and E12.5. Genotypes and probes are as indicated. At E12.5, two pictures of each genotype and probe show the right and left PPM of one embryo seperately. Arrows point to the *Tbx18*-positive domain of the sinus horns, arrowheads mark the embryonic pericardium at E10.5 or the separated PPMs at E12.5. AVC, atrioventricular canal; ep, embryonic pericardium; epi, epicardium, la, left atrium; lcv, left cardinal vein; lsh, left sinus horn; lu, lung; lv, left ventricle; ppm, pleuropericardial membrane; ra, right atrium; rcv, right cardinal vein; rsh, right sinus horn; rv, right ventricle; vv, venous valves.

Heterozygous embryos (genotype: *Tbx18*$^{cre/+}$*;Ctnnb1*$^{fx/+}$*)* were undistinguishable from wildtype embryos and used as controls. *Tbx18* was expressed in the epicardium, the sinus horns and weakly in the mesothelial lining of the lung and the pleural cavity of both control and conditional *Ctnnb1* loss-of-function embryos (genotype: *Tbx18*$^{cre/+}$*;Ctnnb1*$^{fx/fx}$) at E10.5 and E12.5. Additionally, *Tbx18* was detected in the right and left PPM, mainly next to the hilus of the lung, in both genotypes at E12.5, excluding a regulation of the *cre*-driver *Tbx18* by the loss of *Ctnnb1* (Figure 5E through 5H'). *In situ* hybridization analysis for the *Ctnnb1* target gene *Axin2* verified the loss of canonical Wnt/Ctnnb1 signaling in the sinus horns at E10.5 and E12.5 as well as the PPMs at E12.5. Thus, the *Tbx18*^{cre}-mediated loss of *Ctnnb1* occurred specifically in the separated PPMs starting from E12.5, as *Tbx18* and *Axin2* were not coexpressed in the pericardium in earlier embryonic stages. In *Tbx18*-negative regions, e.g. the atrioventricular canal and the venous valves, *Axin2* expression was maintained in *Tbx18*$^{cre/+}$*;Ctnnb1*$^{fx/fx}$ embryos (Figure 5I through 5L').

The *Tbx18*$^{cre/+}$*;Ctnnb1*$^{fx/fx}$ embryos died shortly after birth due to skeletal malformations. Thus, we started our analysis of pericardial phenotypes by histological analysis at E18.5 (Figure 6). In control embryos, the PPMs were attached dorsally to the hilus of the lung and ventrally to the sternum and thereby completely surrounded the heart including the right and left sinus horns at this stage and at E14.5 (Figure 6A, 6C, 6E and 6G). In *Tbx18*^{cre} specific *Ctnnb1* knockout embryos, the release of the PPMs from the lateral body wall was disturbed. In mid-transverse section planes the PPMs were connected dorsally to the hilus of the lung, but the ventral attachment points were shifted laterally to a more dorsal position (Figure 6A through 6H). However, in more cranial section planes the caval veins were positioned laterally inside the PPMs at E14.5 and E18.5. Moreover, a thin mesothelial tissue bridge was fixing the right sinus horn to the hilus of the lung at E18.5 (marked by an arrow in Figure 6D, 7J and 7L). At E12.5, the PPMs were still attached to the lateral body wall in both genotypes and completely embedded in the subcoelomic mesenchyme at a more cranial level (Figure 6I through 6L). The subcoelomic mesenchyme, which was positioned next to the caval veins at E12.5, was completely vanished in both genotypes at E14.5 and E18.5. Additionally to the pericardial defects the dorsal domain of the sinus horns was thinner and the lung showed a bend at the position of the sinus horns in *Tbx18*^{cre} specific *Ctnnb1*-deficient embryos at E18.5 (Figure 6D). In conclusion, the conditional loss of *Ctnnb1* by *Tbx18*^{cre} recombination leads to an incomplete detachment of the lateral PPMs from the mediastinal pleura. At the medial attachment point a thin mesothelial tissue bridge fixed the sinus horn to the hilus of the lung at cranial levels and tethers the sinus horns in an abnormal lateral position within the PPMs.

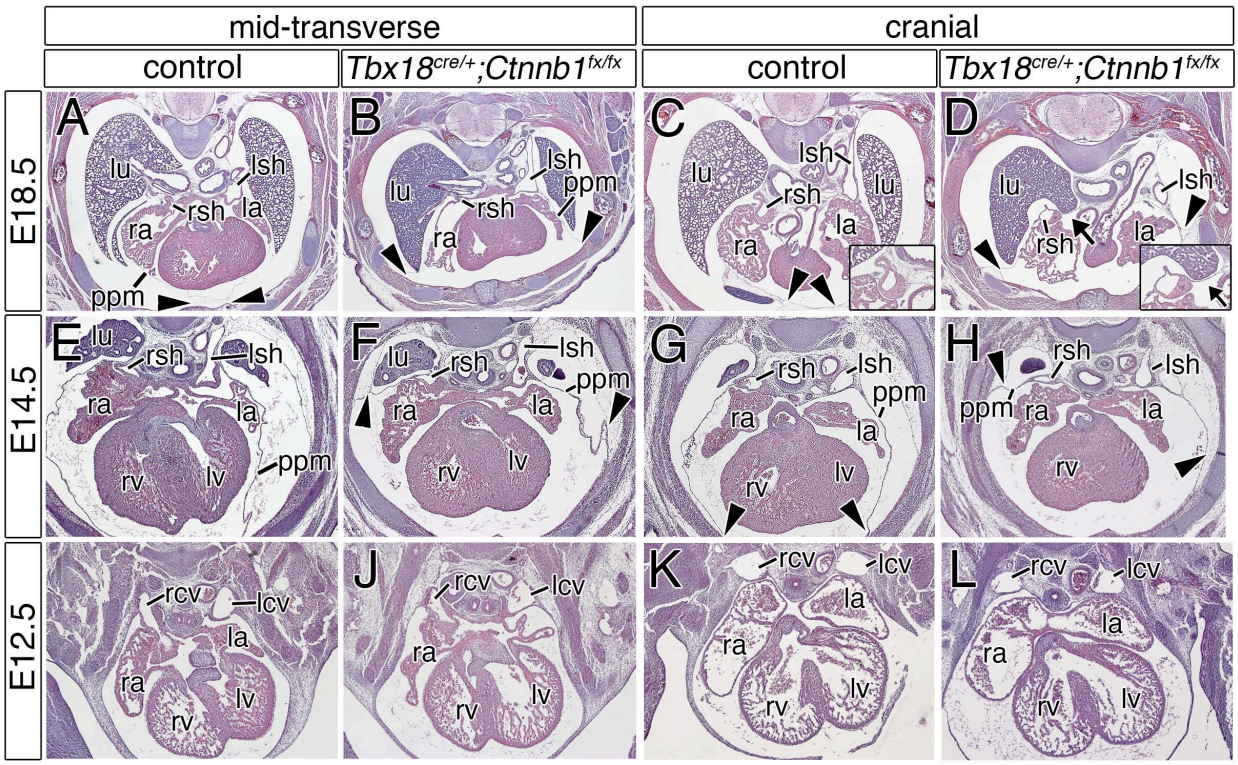

Figure 6. Developmental onset of pericardial defects in *Tbx18*$^{cre/+}$;*Ctnnb1*$^{fx/fx}$ mutant embryos. A through L, Histological analysis by haematoxylin and eosin staining of PPM development was performed on mid-transverse (**left columns**) and cranial (**right columns**) sections of E18.5 to E12.5 control and *Tbx18*^{cre} specific *Ctnnb1*-mutant hearts as indicated. **C,D**, Inserted clippings clarify the attachment of the PPM to the hilus of the lung on cranial transverse sections. The arrow highlights the thin mesothelial tissue bridge connecting the right sinus horn to the hilus of the lung. Arrowheads mark the attachment point of the PPMs to the body wall. la, left atrium; lcv, left cardinal vein; lsh, left sinus horn; lu, lung; lv, left ventricle; ppm, pleuropericardial membrane; ra, right atrium; rcv, right cardinal vein; rsh, right sinus horn; rv, right ventricle.

The mesothelial character of the PPMs is maintained in *Tbx18*$^{cre/+}$;*Ctnnb1*$^{fx/fx}$ embryos

The swelling and subsequent disintegration of the subcoelomic mesenchyme is required for the release of the PPMs from the lateral body wall.[3] In *Tbx18*$^{cre/+}$;*Ctnnb1*$^{fx/fx}$ embryos *Wt1* expression was maintained in the subcoelomic mesenchyme at E12.5 (Figure 7D), and this mesenchyme was completely vanished at E18.5 (Figure 6B). The mesothelial marker genes *Wt1* and *Upk3b* were detectable in the lining of the pericardial and pleural cavities, the epicardium and the lining of the lung in both control and mutant embryos at E12.5 and E18.5 (Figure 7A, 7B, 7D, 7E, 7G, 7H, 7J, and 7K). Therefore, the mesothelial character of the PPMs was preserved in *Tbx18*$^{cre/+}$;*Ctnnb1*$^{fx/fx}$ embryos. *Tbx18* is detectable in the mesothelial lining of the pleural and pericardial cavities, the epicardium and the sinus horns of both genotypes at E12.5 (Figure 7C and 7F). This expression of *Tbx18* in the mesothelial tissues was downregulated in control and *Tbx18*$^{cre/+}$;*Ctnnb1*$^{fx/fx}$ embryos at E18.5 (Figure 7I and 7L), excluding a regulation of *Tbx18* expression by canonical Wnt signaling. The expression of *Tbx18* in the dorsal domain of the sinus horns was reduced in *Tbx18*$^{cre/+}$;*Ctnnb1*$^{fx/fx}$ mutant embryos (Figure 7L). (Norden *et al.*, manuscript in preparation).

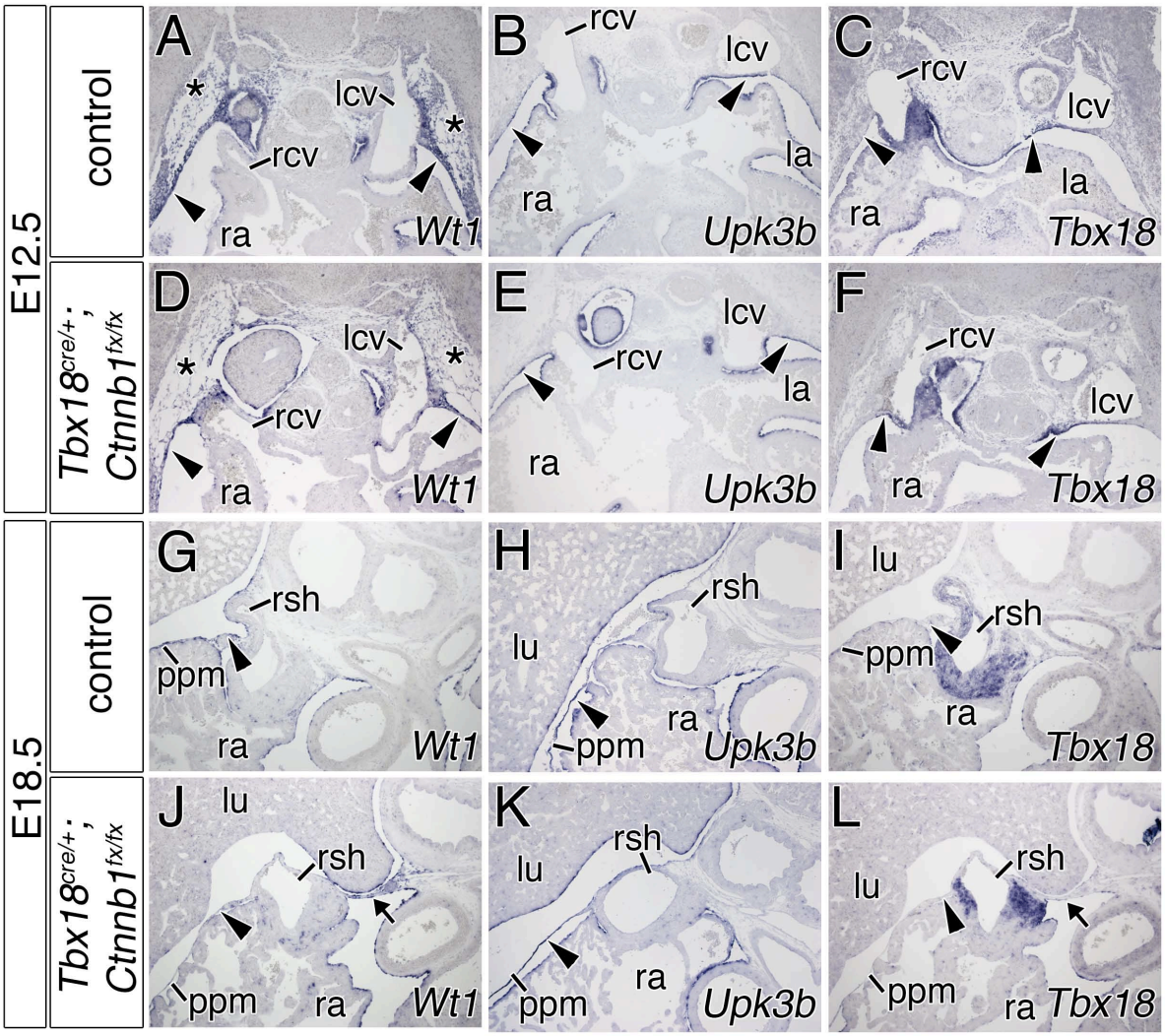

Figure 7. The mesothelial character of the PPMS is maintained. A through L, Expression of mesothelial marker genes *Wt1* and *Upk3b,* and the sinus horn marker *Tbx18* in control and *Tbx18*$^{cre/+}$;*Ctnnb1*$^{fx/fx}$ embryos analyzed by *in situ* hybridization at E12.5 (**A trough F**) and E18.5 (**G through L**). Genotypes and probes are as indicated. Asterisks highlight the subcoelomic mesenchyme next to the caval veins at E12.5, arrows mark the thin mesothelial tissue bridge connecting the right sinus horn to the hilus of the lung in mutant embryos, and arrowheads point to the PPM. la, left atrium; lcv, left cardinal vein; lu, lung; ppm, pleuropericardial membrane; ra, right atrium; rcv, right cardinal vein; rsh, right sinus horn.

Ectopic activation of canonical Wnt/beta-catenin signaling induces undifferentiated cell aggregates

To understand the role of *Ctnnb1*-dependent Wnt signaling during pericardial development in more detail, we used a gain-of-function approach with conditional (*Tbx18*^{cre}- or *Prrx1*^{cre}-mediated) expression of a stabilized form of *Ctnnb1* (*Ctnnb1*$^{(Ex3)fl}$).[13]

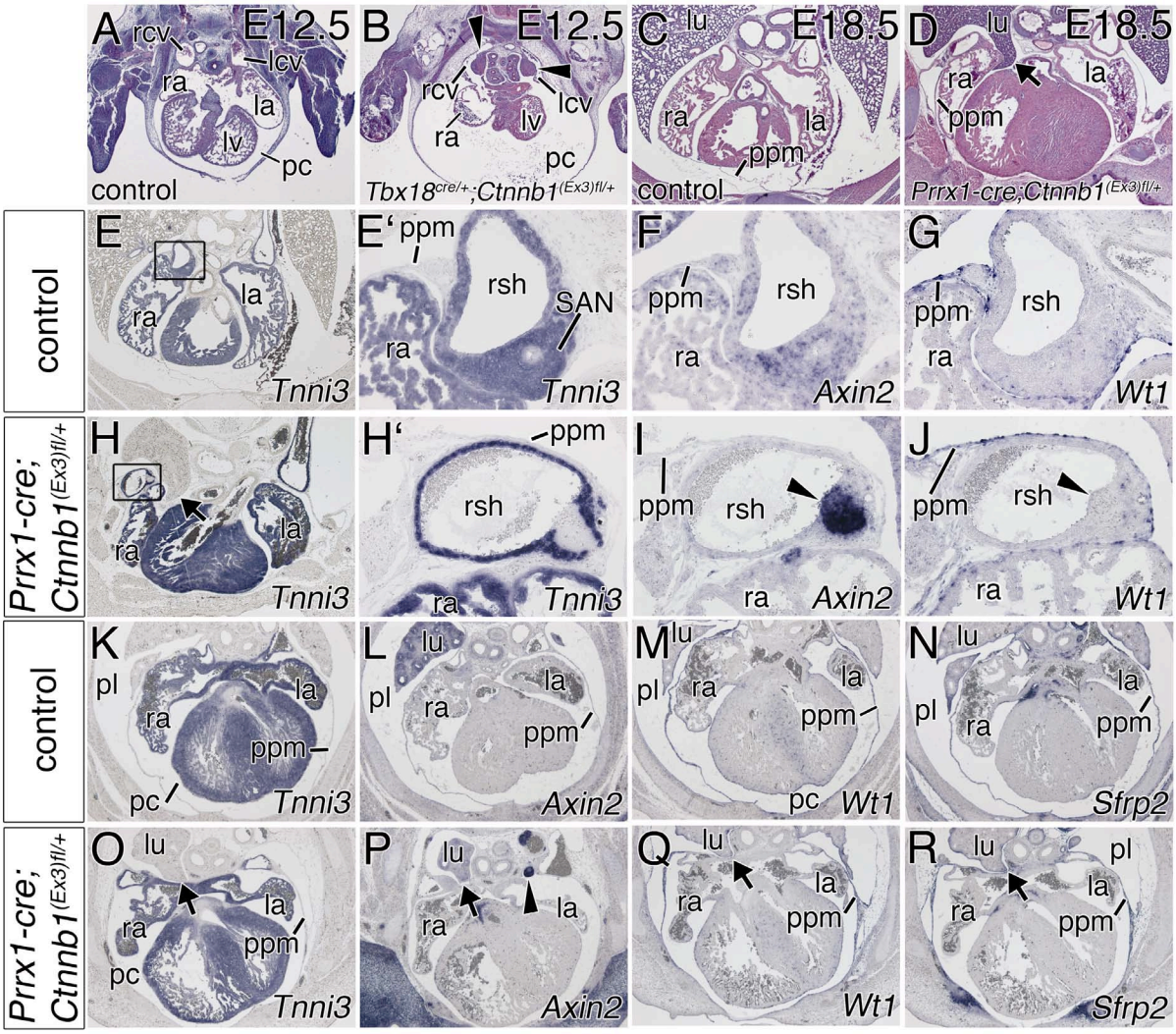

Figure 8. Ectopic activation of canonical Wnt signaling during pericardial development. A through D, Histological staining of control and *Tbx18^{cre};Ctnnb1$^{(Ex3)fl/+}$* mutant mice at E12.5 (**A and B**) or *Prrx1-cre;Ctnnb1$^{(Ex3)fl/+}$* embryos at E18.5 (**C and D**). **E through R**, *In situ* hybridization analysis on transverse sections of control and *Prrx1-cre;Ctnnb1$^{(Ex3)fl/+}$* mutant mice at E18.5 (**E through J**) or E14.5 (**K through R**). Genotypes and probes are as indicated. Black boxes in E and H mark the magnified sections in E' or H', respectively. Arrows point to the connection between lung and atria, arrowheads mark ectopic cell aggregates. la, left atrium; lcv, left cardinal vein; lsh, left sinus horn; lu, lung; lv, left ventricle; pc, pericardial cavity; pl, pleural cavity; ppm, pleuropericardial membrane; ra, right atrium; rcv, right cardinal vein; rsh, right sinus horn; SAN, sinoatrial node.

Tbx18$^{cre/+}$;Ctnnb1$^{(Ex3)fl/+}$ embryos died during midgestation before the release of the PPMs from the subcoelomic mesenchyme had started. Histological analysis of surviving embryos uncovered a highly enlarged pericardial cavity, the myocardium of the heart was thinned, the heart was tilted inside the pericardial cavity, and ectopic cell aggregates were detectable next to the sinus horns at E12.5 (Figure 8A and 8B). The effects of *Tbx18^{cre}*-mediated activation of Ctnnb1 for sinus horn and epicardial development will be described elsewhere (Norden *et al*., manuscript in preparation). Due to the early embryonic lethality, we abandoned the analysis of pericardial development in these mice.

Prrx1-cre;Ctnnb1$^{(Ex3)fl/+}$ gain-of-function embryos survived embryonic development and died shortly after birth.[18] By histological staining with haematoxylin and eosin we detected a pericardial phenotype that was reminiscent to the observed alterations in *Prrx1-cre;Ctnnb1*$^{fx/fx}$ loss-of-function embryos. The PPMs were not completely released from the lateral body wall and a wide canal allowed the lung to encircle the right atrium in *Prrx1-cre;Ctnnb1*$^{(Ex3)fl/+}$ gain-of-function embryos at E18.5 (Figure 8C and 8D). *In situ* hybridization analysis for cardiomyocyte specific *Tnni3* demonstrated that mutant sinus horns were myocardialized at E18.5 and E14.5; confirming that myocardialization of the sinus horns occurs independently from the normal location next to the hilus of the lung (Figure 8E', 8H', 8K, and 8O). In the *Prrx1-cre;Ctnnb1*$^{(Ex3)fl/+}$ embryos we detected *Tnni3*-negative cells, which were positive for a target gene of canonical Ctnnb1-mediated Wnt signaling, *Axin2,* at E18.5 (Figure 8F and 8I). Ectopic *Axin2*-positive cell aggregates were also detectable next to the PPMs at E14.5 (Figure 8L and 8P). The mesothelial, *Wt1*-positive character was preserved in the PPMs at both stages (Figure 8G, 8J, 8M, and 8Q). Furthermore, the persisting subcoelomic mesenchyme in *Prrx1-cre;Ctnnb1*$^{(Ex3)fl/+}$ gain-of-function embryos expressed *Wt1*. In control embryos this mesenchyme was completely resolved at E18.5 and E14.5, but expressed *Wt1* at earlier developmental stages (Figure 7A). The remaining subcoelomic mesenchyme and the PPMs in *Prrx1-cre;Ctnnb1*$^{(Ex3)fl/+}$ embryos additionally showed expression of the Wnt antagonist *secreted frizzled-related protein 2 (Sfrp2),* which was also detectable in the PPMs and the attachment point of the PPMs to the sternum in control embryos at E14.5 (Figure 8N and 8R) and in the subcoelomic mesenchyme next to the caval veins at E12.5 (data not shown).

Discussion

Myocardialization of the sinus horns is independent from a medial positioning

We have recently reported that *Wt1*-deficient mice feature laterally positioned, non-myocardialized sinus horns. We speculated at this time that the lack of sinus horn myocardialization was due to the physical separation from sources of differentiation signals.[3] However, in *Prrx1-cre;Ctnnb1* loss- and gain-of-function mutants the sinus horns were myocardialized despite their lateralization and tethering to the persisting subcoelomic mesenchyme. This excludes a function of canonical Wnt/Ctnnb1 signaling in the subcoelomic mesenchyme or the PPMs for the myocardialization of the sinus horns, and also excludes a role of the dorsal mesocardium/lung hilus tissue as a source of the respective signals. Nevertheless, our study shows the necessity of Ctnnb1-mediated Wnt signaling in the lateral body wall mesenchyme and/or the PPMs for the development of the pericardium, especially the release of the PPMs from the subcoelomic mesenchyme. Additionally, in the developing sinus horns

canonical Wnt/Ctnnb1 signaling is required for the proliferation of precursor cells and, as a result, for the myocardialization of the *Tbx18*-positive dorsal domain of the sinus horns (Norden *et al*., manuscript submitted).

Ctnnb1-mediated Wnt signaling is necessary for murine pericardial development

Our analysis revealed the requirement of canonical Wnt signaling for diverse steps during murine pericardial development. The conditional *Ctnnb1* loss- and gain-of-function approaches using two different *cre*-lines (*Tbx18*^{cre} and *Prrx1-cre*) caused pericardial deficiencies. We were able to distinguish between early (*Prrx1-cre*) and late (*Tbx18*^{cre}) effects of deletion and ectopic activation of *Ctnnb1*, respectively.

Prrx1-cre and *Axin2* (which marks active canonical Wnt signaling) were coexpressed in the embryonic pericardium at E9.5 and E10.5; coexpression was maintained in the lateral body wall next to the detachment point of the PPMs until at least E12.5. Thus, early canonical Wnt/Ctnnb1 signaling in the embryonic pericardium and/or the lateral body wall next to the detachment point of the PPMs is crucial for the release of the PPMs from the subcoelomic mesenchyme. During heart development, canonical Wnt signaling keeps progenitor cells of the second heart field in a proliferative, undifferentiated state, therefore these cells are able to elongate the growing heart.[1] Currently, the progenitor cells of the PPMs and the precise molecular role of Ctnnb1 during its development remain unidentified. However, the levels of active Ctnnb1 signaling in this domain have to be tightly regulated, as both the loss and the ectopic activation of Ctnnb1 resulted in severe pericardial defects.

We recently published that the release of the PPMs from the lateral body wall is a prerequisite for the correct repositioning of the cardinal veins medially to the hilus of the lung,[3] therefore the communication between the lung and the atria is most likely a secondary defect. The failure to release the PPMs from the lateral body wall may also cause the tilting of the heart within the pericardial cavity. In wildtype mouse embryos, the release of the PPMs from the subcoelomic mesenchyme and the stretching of the PPMs are coupled with the development and dorsocranial movement of the sinus venosus of the heart (Norden *et al*., manuscript in preparation). The fixation of the caval veins to the persisting subcoelomic mesenchyme may therefore hamper the dorsocranial movements of the sinus venosus and the positioning of the heart inside the pericardial cavity. Further analysis of the PPM release will focus on the examination of new Ctnnb1 target genes in the subcoelomic mesenchyme during pericardial development and molecular changes, e.g. proliferation and apoptosis, in this domain. The underlying mechanisms of the disappearance of the subcoelomic mesenchyme may be similar to the development of middle ear cavities. However, the molecular mechanisms regulating these processes have remained elusive until now.[23] In the middle ear apoptosis of the mesenchyme may act in parallel with a redistribution of the mesenchymal cells over the increasing area of the growing middle ear capsule.[24,25]

Our *Tbx18*^{cre} specific deletion of *Ctnnb1* addressed a later requirement for canonical Wnt signaling for pericardial development since *Tbx18* (and therefore *cre*) and *Axin2* are not coexpressed in the lateral body wall at E9.5 and E10.5. *Tbx18*^{cre} primarily affected *Ctnnb1* expression during PPM release starting from E12.5. Pericardial defects in *Tbx18*^{cre}*;Ctnnb1*$^{fx/fx}$ mutant embryos, therefore, argues that Wnt signaling is required for the progression of the detachment of the *Tbx18*-derived PPMs from the lateral body wall as well. Notably, canonical Wnt signaling is not required for the medial anchoring of the PPMs to the lung hilus as no canal between the lung and atria was detectable in the *Tbx18*^{cre}*;Ctnnb1*$^{fx/fx}$ mutant embryos. However, the caval veins were positioned laterally inside the PPMs in these embryos, especially at E18.5 when a thin mesothelial tissue bridge connected the right sinus horn to the hilus of the lung in *Tbx18*^{cre}*;Ctnnb1*$^{fx/fx}$ mutant embryos. The molecular and cellular mechanisms underlying these defects remain to be defined. Tension stress onto the PPMs during the growth of the embryo and the thoracic cavity might be a mechanical factor influencing the release of the PPMs from the lateral body wall, as proposed for the development of the human pericardium.[26]

In conclusion, this study uncovers the importance of the Wnt/Ctnnb1 signaling pathway for pericardial development The levels of active Wnt/Ctnnb1 signaling have to be tightly regulated during these processes, as both the loss and the ectopic activation of *Ctnnb1* resulted in pericardial abnormalities.

Acknowledgements

We thank Franziska Greulich for critically reading the manuscript.

References

1. Kirby ML, Waldo K. Cardiac development. Oxford University Press US; 2007.
2. Faridah Y, Julsrud P. Congenital absence of pericardium revisited. *The international journal of cardiovascular imaging*. 2002 Feb 1;18(1):67-73.
3. Norden J, Grieskamp T, Lausch E, Van Wijk B, van den Hoff M, Englert C, Petry M, Mommersteeg M, Christoffels V, Niederreither K, Kispert A. Wt1 and Retinoic Acid Signaling in the Subcoelomic Mesenchyme Control the Development of the Pleuropericardial Membranes and the Sinus Horns. *Circulation Research*. 2010 Feb 25;(106):1212 -1220.
4. Gessert S, Kühl M. The multiple phases and faces of wnt signaling during cardiac differentiation and development. *Circulation Research*. 2010 Juli 23;107(2):186-99.

5. Grigoryan T, Wend P, Klaus A, Birchmeier W. Deciphering the function of canonical Wnt signals in development and disease: conditional loss- and gain-of-function mutations of beta-catenin in mice. *Genes & Development*. 2008;22(17):2308-41.

6. McMahon J. Nucleotide sequence, chromosomal localization and developmental expression of the mouse int-1-related gene. *Development*. 1989 Nov 1;107(3):643-50.

7. Maretto S, Cordenonsi M, Dupont S, Braghetta P, Broccoli V, Hassan A, Volpin D, Bressan G, Piccolo S. Mapping Wnt/beta-catenin signaling during mouse development and in colorectal tumors. *Proc Natl Acad Sci USA*. 2003 März 18;100(6):3299-304.

8. Trowe M, Shah S, Petry M, Airik R, Schuster-Gossler K, Kist R, Kispert A. Loss of Sox9 in the periotic mesenchyme affects mesenchymal expansion and differentiation, and epithelial morphogenesis during cochlea development in the mouse. *Developmental Biology*. 2010 Juni 1;342(1):51-62.

9. Logan M, Martin J, Nagy A, Lobe C, Olson E, Tabin C. Expression of Cre Recombinase in the developing mouse limb bud driven by a Prxl enhancer. *genesis*. 2002 Juni 1;33(2):77-80.

10. Soriano P. Generalized lacZ expression with the ROSA26 Cre reporter strain. *Nat Genet*. 1999 Jan;21(1):70–1.

11. Muzumdar M, Tasic B, Miyamichi K, Li L, Luo L. A global double-fluorescent Cre reporter mouse. *genesis*. 2007;45(9):593-605.

12. Brault V, Moore R, Kutsch S, Ishibashi M, Rowitch D, McMahon J, Sommer L, Boussadia O, Kemler R. Inactivation of the beta-catenin gene by Wnt1-Cre-mediated deletion results in dramatic brain malformation and failure of craniofacial development. *Development*. 2001 Apr 1;128(8):1253-64.

13. Harada N, Tamai Y, Ishikawa T, Sauer B, Takaku K, Oshima M, Taketo M. Intestinal polyposis in mice with a dominant stable mutation of the beta-catenin gene. *EMBO J*. 1999 Nov 1;18(21):5931-42.

14. Moorman A, Houweling A, de Boer P, Christoffels V. Sensitive nonradioactive detection of mRNA in tissue sections: novel application of the whole-mount in situ hybridization protocol. *J Histochem Cytochem*. 2001 Jan 1;49(1):1-8.

15. ten Berge D, Brouwer A, Korving J, Martin JF, Meijlink F. Prx1 and Prx2 in skeletogenesis: roles in the craniofacial region, inner ear and limbs. *Development*. 1998 Okt 1;125(19):3831 -3842.

16. Liu W, Selever J, Wang D, Lu M, Moses K, Schwartz R, Martin J. Bmp4 signaling is required for outflow-tract septation and branchial-arch artery remodeling. *Proc Natl Acad Sci USA*. 2004 März 30;101(13):4489-94.

17. Jho E-hoon, Zhang T, Domon C, Joo C-K, Freund J-N, Costantini F. Wnt/beta-catenin/Tcf signaling induces the transcription of Axin2, a negative regulator of the signaling pathway. *Mol Cell Biol*. 2002 Feb;22(4):1172–83.

18. Hill T, Taketo M, Birchmeier W, Hartmann C. Multiple roles of mesenchymal beta-catenin during murine limb patterning. *Development*. 2006 Apr 1;133(7):1219-29.

19. Christoffels V, Mommersteeg M, Trowe M, Prall O, De Gier-De Vries C, Soufan A, Bussen M, Schuster-Gossler K, Harvey R, Moorman A, Kispert A. Formation of the venous pole of the heart from an Nkx2-5-negative precursor population requires Tbx18. *Circulation Research*. 2006 Juni 23;98(12):1555-63.

20. Bochmann L, Sarathchandra P, Mori F, Lara-Pezzi E, Lazzaro D, Rosenthal N. Revealing New Mouse Epicardial Cell Markers through Transcriptomics. *PLoS ONE*. 2010 Juni 28;5(6):e11429.

21. Kraus F, Haenig B, Kispert A. Cloning and expression analysis of the mouse T-box gene Tbx18. *Mech Dev*. 2001 Jan;100(1):83–6.

22. Armstrong J, Pritchard-Jones K, Bickmore W, Hastie N, Bard J. The expression of the Wilms' tumour gene, WT1, in the developing mammalian embryo. *Mechanisms of Development*. 1993 Jan 1;40(1-2):85-97.

23. Chapman SC. Can you hear me now? Understanding vertebrate middle ear development. *Front Biosci*. 2011;16:1675-1692.

24. Richter CA, Amin S, Linden J, Dixon J, Dixon MJ, Tucker AS. Defects in middle ear cavitation cause conductive hearing loss in the Tcof1 mutant mouse. *Human Molecular Genetics*. 2010 Apr 15;19(8):1551 -1560.

25. Piza J, Northrop C, Eavey RD. Embryonic middle ear mesenchyme disappears by redistribution. *The Laryngoscope*. 1998 Sep 1;108(9):1378-1381.

26. Salzer GM. Die Topogenese der Pleurahoehlen. *Z. Anat. Entwickl. Gesch.* 1960;122(3):232-240.

Wnt/beta-catenin Signaling Maintains the Mesenchymal Precursor Pool for Murine Sinus Horn Formation

Julia Norden[1], Franziska Greulich[1], Makoto Mark Taketo[2], and Andreas Kispert[1,*]

[1] Institut für Molekularbiologie, OE5250, Medizinische Hochschule Hannover, Carl-Neuberg-Str.1, D-30625 Hannover, Germany

[2] Department of Pharmacology, Graduate School of Medicine, Kyoto University, Sakyo, Kyoto 606-8501, Japan

[*]Author for correspondence:

E-MAIL: kispert.andreas@mh-hannover.de

TEL.: +49 511 5324017

FAX.: +49 511 5324283

Running title: Beta-catenin signaling in caval vein development

Edited version accepted in Circulation Research,

Circulation Research 2011, in press.

Abstract

Rationale: Canonical (beta-catenin (Ctnnb1))-dependent Wnt signaling plays an important role in the development of second heart field (SHF) derived structures of the heart by regulating precursor cell proliferation. The signaling pathways that regulate the most posterior elongation of the heart i.e. the addition of the systemic venous return from a *Tbx18*-positive precursor population, have remained elusive.

Objective: To define the role of Ctnnb1-dependent Wnt signaling in the development of the cardiac venous pole.

Methods and Results: We show by *in situ* hybridization analysis that Wnt pathway components are expressed and canonical Wnt signaling is active in the developing sinus horns. We analyzed sinus horn (*Tbx18*^{cre}) specific *Ctnnb1* loss- and gain-of-function mutant embryos. In *Ctnnb1*-deficient embryos, the dorsal part of the sinus horns is not myocardialized, but consists of myofibroblasts; the sinoatrial node (SAN) is unaffected. Stabilization of Ctnnb1 in this domain results in the formation of undifferentiated cell aggregates. Analysis of cellular changes revealed a role of canonical Wnt signaling in proliferation of the *Tbx18*$^{+}$ mesenchymal progenitor cell population.

Conclusions: Canonical Wnt signaling in the *Tbx18*$^{+}$*Nkx2-5*$^{-}$ mesenchymal cell population of the sinus horns is important for the balance between proliferation and differentiation of these precursors.

Keywords: Canonical Wnt signaling, beta-catenin, sinus horn, cardiac progenitor

Non-standard abbreviations and acronyms

3D	three-dimensional
AVC	atrio-ventricular canal
Bmp	bone morphogenetic protein
Ctnnb1	beta-catenin
DAPI	4',6-diamidino-2-phenylindol
E	embryonic day
Fgf	fibroblast growth factor
FHF	first heart field
Fzd	frizzled homolog
Gja	gap junction protein, alpha
GFP	green fluorescent protein
Nkx2-5	NK2 transcription factor related, locus 5
OFT	outflow tract
SAN	sinoatrial node
Sfrp	secreted frizzled-related protein
Shh	sonic hedgehog
SHF	second heart field
Tbx	T-box
Tnni	troponin I, cardiac
Wnt	wingless-related MMTV integration site

What is known?

- Canonical (beta-catenin (Ctnnb1))-dependent signaling is important for the balance between proliferation and terminal differentiation in the precursor cell population of the second heart field, which contributes to the formation of atria, right ventricle, and outflow tract.
- The sinus horns, the myocardialized parts of the intrapericardial aspects of the common cardinal veins, are added to the posterior pole of the already formed heart tube from a distinct mesenchymal *Tbx18*$^{+}$ cell population from E9.5 to E14.5.
- The sinoatrial node (SAN), the main pacemaker of the heart, also derives from a *Tbx18*$^{+}$ precursor cell population at the posterior pole of the heart.

What new information does this article contribute?

- Canonical Wnt signaling is active during sinus horn development.
- *Ctnnb1* is required for myocardialization of the dorsal part of the sinus horns.
- *Ctnnb1* is not required for SAN formation.
- Canonical Wnt signaling positively regulates proliferation of the *Tbx18*$^{+}$*Nkx2-5*$^{-}$ precursor cell population of the sinus horns, but prevents differentiation into cardiomyocytes when constitutively activated.

Novelty and significance

The cardiac venous pole consists of the sinus horns, the sinus venarum, the coronary sinus (persisting left superior caval vein in the mouse), and the sinoatrial node (SAN). Although it is a common focus of congenital malformations and arrhythmias, the signals and factors that regulate its formation are largely unknown. Here, we identify canonical Wnt signaling as a crucial pathway in the formation of fully myocardialized sinus horns. We show that canonical Wnt signaling is required and sufficient to maintain the proliferation of Tbx18^{+} mesenchymal precursor cells of the sinus horns. However, *Ctnnb1*-dependent Wnt signaling is dispensable for the development of the SAN, which also derives from Tbx18^{+} progenitors.

Introduction

The multi-chambered mammalian heart develops by a complex morphogenetic process from a linear tube, which is established shortly after gastrulation as a functional organ. Growth and elongation of this simple tube only partly relies on proliferation of cardiomyocytes within the tube itself but largely depend on recruitment and differentiation of mesenchymal precursor cells at the poles. In fact, myocardium of the linear heart tube, which is established at E8.25 in the mouse, will only contribute to the left ventricle. Myocardium of the outflow tract (OFT), right ventricle, and large portions of the atria of the mature heart derive from a population of splanchnic mesodermal precursor cells that is contiguous and dorsal to the heart tube. These pharyngeal mesodermal precursors, which are now termed the second heart field (SHF), express *ISL1 transcription factor, LIM/homeodomain* (*Isl1)*, *T-box 1* (*Tbx1)* and the *fibroblast growth factor* genes *Fgf8* and *Fgf10,* and therefore, are molecularly distinguished from the progenitors of the linear heart tube, the first heart field (FHF), which express *NK2 transcription factor related, locus 5 (Nkx2-5)*, *T-box 5* (*Tbx5)* and *heart and neural crest derivatives expressed transcript 1* (*Hand1)*.[1] Although molecularly distinct, both precursor populations can be envisaged as a continuum that allows the spatiotemporally regulated contribution of precursors to the growing heart tube.

The systemic venous return consists of the myocardial sleeves of the right superior and inferior caval veins, the sinus venarum, the coronary sinus (persisting left superior caval vein in the mouse), and the sinoatrial node (SAN).[2] This posterior part of the heart develops after the chambers have been established at E9.5, by recruitment and myocardialization of mesenchymal precursor cells to the common atrium until E14.5.[3,4] This precursor cell pool is distinguished from the FHF and SHF by presence of *T-box 18* (*Tbx18)* and absence of *Nkx2-5* expression. Loss of *Tbx18* in this "third heart field" leads to a delay in myocardialization of the sinus horns, and a marked reduction of the SAN.

Continuous elongation of the heart tube requires a tight control of proliferation and deployment of mesenchymal progenitor cells. A number of studies identified canonical Wnt signaling as a crucial upstream regulator of SHF proliferation. Conditional inactivation of *beta-catenin* (*Ctnnb1*) under control of the *myocyte enhancer factor 2C* (*Mef2c)* in the anterior aspect of the SHF resulted in reduced proliferation and subsequent truncation of the OFT and right ventricle.[5] More recently, Tian et al. showed that *wingless-related MMTV integration site 2 (Wnt2)* acts in the posterior portion of the SHF to stimulate proliferation of precursor cells and subsequent formation of a portion of the atrioventricular canal (AVC) and the atria.[6] Thus, canonical Wnt signaling maintains proliferation in the SHF to allow the polar elongation of the heart. Notably, Wnt signaling does not play such a role in the FHF. In fact, Ctnnb1 inhibits cardiac differentiation in this region.

The signaling pathways that regulate the most posterior elongation of the heart i.e. the addition of the systemic venous return, have remained elusive. Although the SHF and sinus horn

mesoderm bear different molecular signatures (*Nkx2-5*$^{+}$*Isl*$^{+}$ vs *Nkx2-5*$^{-}$*Tbx18*$^{+}$) we wondered whether canonical Wnt signaling exerts a similar function in the latter context. Here, we present data obtained from genetic loss- and gain-of function experiments in the mouse that demonstrate a function of canonical/Ctnnb1-dependent Wnt signaling in sinus horn development.

Material and Methods

Mice

Mice with a knock-in of the *cre* recombinase gene into the *Tbx18* locus (*Tbx18*$^{tm4(cre)Akis}$, synonym: *Tbx18*^{cre}),[7] mice with two *loxP* sites flanking the *Ctnnb1* locus from exon 2 to exon 6 (*Ctnnb1*^{tm2Kem}, synonym: *Ctnnb1*^{fx}),[8] mice with two *loxP* sites flanking exon 3 of the *Ctnnb1* locus (*Ctnnb1*^{tm1Mmt}, synonym: *Ctnnb1*$^{(Ex3)fl}$),[9] and the fluorescent reporter line *(Gt(ROSA)26Sor*$^{tm4(ACTB-tdTomato,-EGFP)Luo}$/J, synonym: *R26*^{mTmG})[10] were all described before. All lines were maintained on an outbred (NMRI) background. Animal care was in accordance with national and institutional guidelines.

An expanded Materials and Methods section is available in the online data supplement.

Results

(Canonical) Wnt signaling in sinus horn development

To determine the spatiotemporal involvement of Wnt signaling in sinus horn development, the expression of genes encoding Wnt ligands (*Wnt1, -2, -2b, -3, -3a, -4, -5a, -5b, -6, -7a, -7b, -8a, -8b, -9a, -9b, -10a, -10b, -11,* and *Wnt16*), Frizzled receptors (*Fzd1* to *Fzd10*), and Wnt antagonists of the family of Secreted frizzled-related proteins (*Sfrp1* to *Sfrp5),* was analyzed by *in situ* hybridization on sections of the cardiac venous pole. Since sinus horn development occurs from embryonic day (E) 9.5 to E14.5, we used E10.5, E12.5, and E14.5 embryos for this expression screen (Figure 1, Online Figure 1). Most of the tested components of the Wnt signaling pathway showed no caval vein specific gene expression. However, the Wnt ligand *Wnt2* was expressed in the walls of the left and right cardinal vein that bulged into the pericardial cavity at E10.5 (Online Figure 1A), E12.5 and E14.5 (Figure 1A and 1E). Expression of *Wnt10a* was detectable in both caval veins and in the atrial and ventricular myocardium at E14.5 (Figure 1B and 1F). *Fzd7* and *Sfrp1* were expressed in the intrapericardial component of the cardinal veins at all tested embryonic stages (Online Figure 1C and 1D; Figure 1C and 1D, 1G and 1H). *Sfrp1* was additionally expressed in the left ventricle at E12.5, and in both the atria and the left ventricle at E14.5. Therefore, genes encoding two Wnt ligands (*Wnt2, Wnt10a*), one Frizzled

receptor (*Fzd7*) as well as one Wnt antagonist (*Sfrp1*) were expressed in the developing sinus horns, pointing to a role of Wnt signaling in the development of this posterior portion of the murine heart. To verify that the presence of these ligands and receptors is associated with activation of the canonical Wnt signaling pathway, we investigated expression of *Axin2*, a *bona fide* target of Ctnnb1-dependent Wnt signaling. Weak *Axin2* expression was detectable in the sinus horns of wildtype embryos at all three stages. Furthermore, *Axin2* was found in the venous valves, the atrial septum, and the developing AVC at E12.5 and E14.5 (Figure 1I and 1M).

Defects of the systemic venous return from sinus horn specific inactivation of *Ctnnb1*

To investigate the role of canonical Wnt signaling in sinus horn development, we employed a tissue-specific inactivation approach using a *Tbx18*^{cre} line generated in our laboratory[7] and a floxed allele of *Ctnnb1 (Ctnnb1*^{fx}*)*,[8] the unique intracellular mediator of this signaling pathway. The T-box transcription factor gene *Tbx18* has multiple sites of expression in the developing heart including the proepicardial organ at E9.5, the epicardium until E16.5, and the myocardium of the left ventricle and the interventricular septum. Importantly, *Tbx18* expression marks the sinus horn lineage from E8.25 onwards,[11] allowing the specific genetic removal of *Ctnnb1* in mesenchymal precursors as well as in differentiated myocardium of this cardiac subregion. The specific inactivation of the canonical Wnt signaling pathway in the *Tbx18*^{cre}-expressing sinus horns was confirmed by absence of *Axin2* expression in the sinus horns but its maintenance at other sites of cardiac expression at E12.5 and E14.5 (Figure 1J and 1N). Expression of *Tbx18* was unaffected, excluding that the cre driver activity depends on *Ctnnb1* function (Figure 1K and 1L, 1O and 1P).

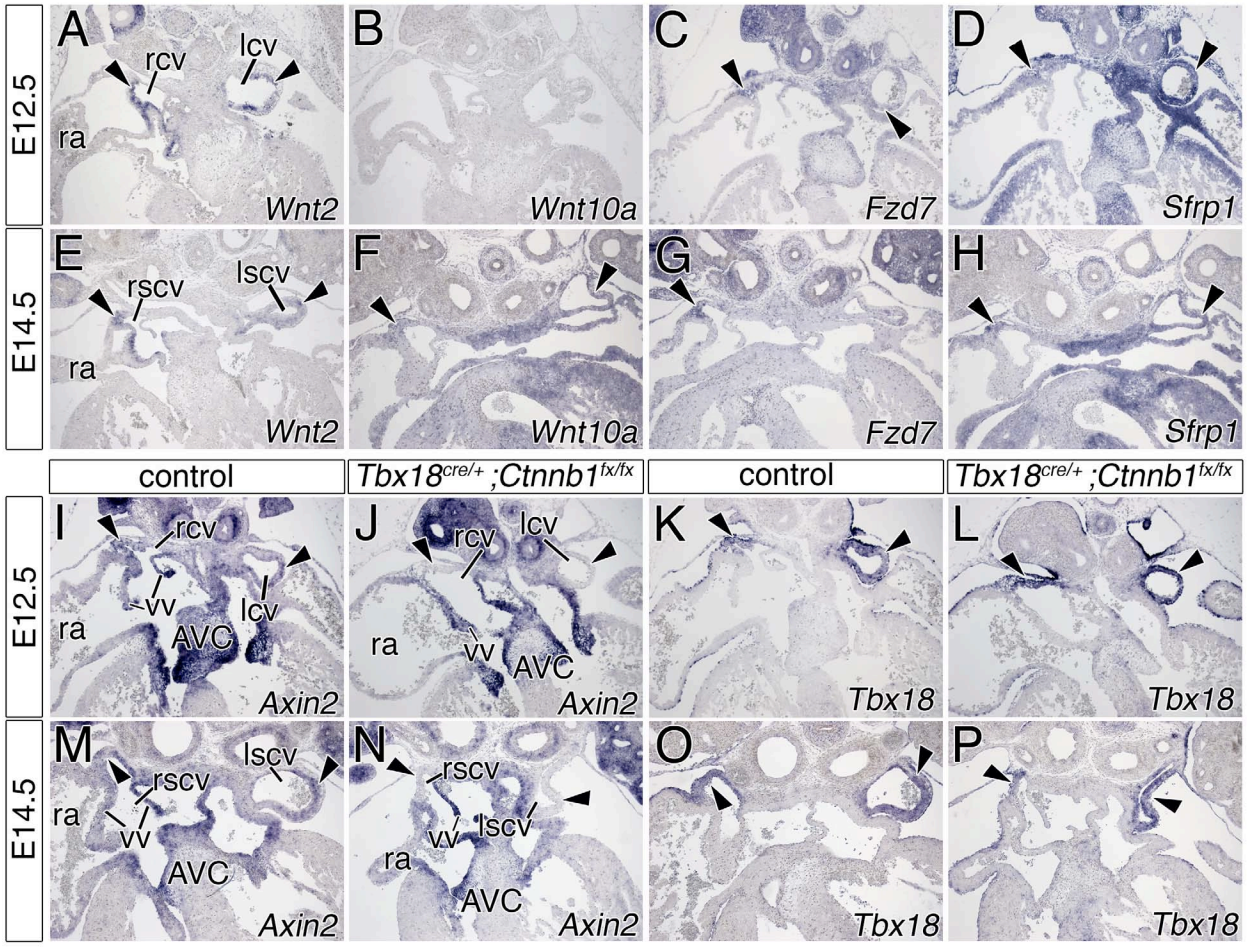

Figure 1. Wnt signaling in sinus horn development. *In situ* hybridization analysis on transverse sections through the venous pole region for expression of Wnt pathway components in wildtype embryos (**A through H**), and of *Axin2* and *Tbx18* (**I through P**) in control (genotype: *Tbx18*$^{cre/+}$*;Ctnnb1*$^{fx/+}$) and *Tbx18*$^{cre/+}$*;Ctnnb1*$^{fx/fx}$ mutant sinus horns. Arrowheads point to the intrapericardial components of the left and right cardinal vein. Stages and probes are as indicated. AVC, atrioventricular canal; lcv, left cardinal vein; lscv, left superior caval veins; ra, right atrium; rcv, right cardinal vein; rscv, right superior caval vein; vv, venous valves.

Tbx18$^{cre/+}$*;Ctnnb1*$^{fx/fx}$ mice survived embryogenesis but skeletal malformations led to respiratory failure shortly after birth. At E18.5, the mutant heart appeared normal on a gross morphological level (data not shown). Histological analysis revealed that chambers, valves, and septa were unaffected; sinus horns were positioned next to the midline and within the pericardial cavity as in control embryos (Figure 2A and 2B). However, *in situ* hybridization analysis for cardiomyocyte specific *troponin I cardiac 3*, *(Tnni3,* also known as *cTnI)* revealed a specific lack of myocardium in the dorsal part of the sinus horns next to the pleuropericardial membrane in mutant hearts (Figure 2C and 2D). Serial section analysis and subsequent three-dimensional (3D)-reconstruction of representative embryos confirmed the regional specificity of the defect, as myocardialization of atria, the pulmonary vein, and ventral sinus horns was normal (Figure 2E and 2F).

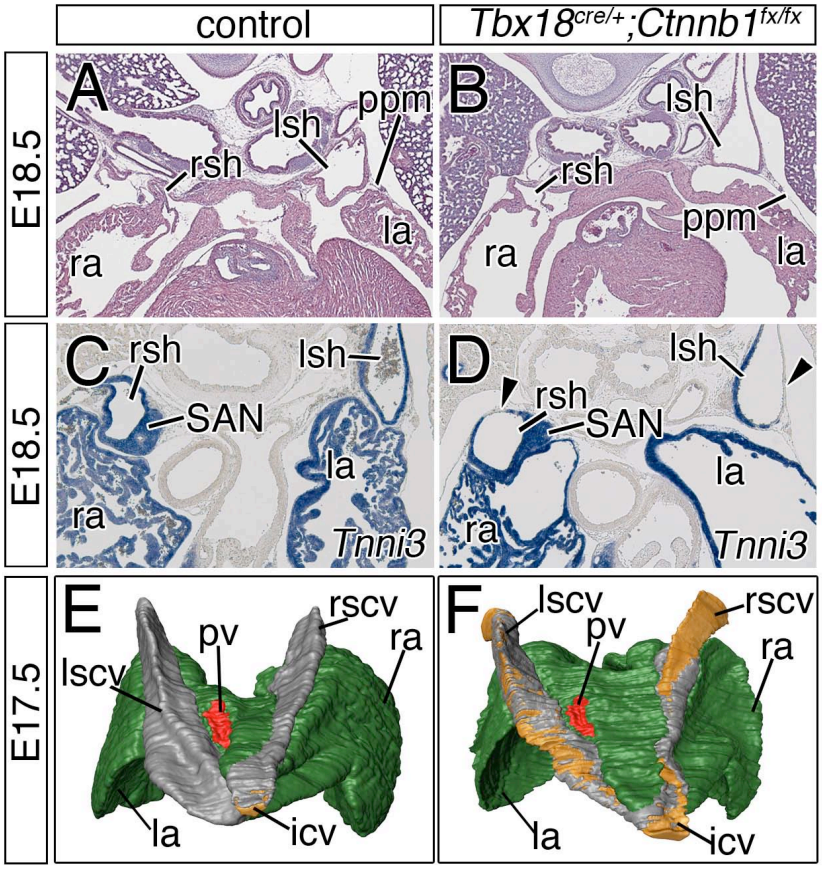

Figure 2. Myocardialization defects in the dorsal part of *Ctnnb1*-deficient sinus horns. A through D, Histological and molecular analyses of sinus horns were carried out on transverse sections through the venous pole region of E18.5 control and *Tbx18*$^{cre/+}$;*Ctnnb1*$^{fx/fx}$ hearts. Dorsal is oriented up. Histological stainings with haematoxylin and eosin (**A and B**), and *in situ* hybridization analysis of *Tnni3* expression (**C and D**). **E and F**, Morphological analysis of control and *Tbx18*$^{cre/+}$;*Ctnnb1*$^{fx/fx}$ mutant sinus horns by 3D-reconstructions of serial sections stained for *Tnni3* in a dorsal-posterior view at E17.5. Atrial myocardium is shown in green, sinus horn myocardium in grey, the lumen of the caval veins in orange, and the pulmonary vein myocardium in red. Arrowheads point to the *Tnni3*$^{-}$ domain of the left and right cardinal vein. icv, inferior caval vein; la, left atrium; lscv, left superior caval vein; lsh, left sinus horn; ppm, pleuropericardial membrane; pv, pulmonary vein; ra, right atrium; rscv, right superior caval vein; rsh, right sinus horn; SAN, sinoatrial node.

Since *Tbx18* is also expressed in the developing SAN of control and conditional *Ctnnb1*-mutant embryos (Figure 3A and 3B),[12] we analyzed the consequence of *Ctnnb1* deletion for the integrity of this tissue. *Axin2* was expressed at low levels, rarely above background, in both control and *Ctnnb1*-deficient SAN (Figure 3C and 3D), indicating if present at all, low levels of canonical Wnt signaling in this tissue. In E18.5 control embryos, the SAN expressed *T-box 3* (*Tbx3*) and *hyperpolarization-activated, cyclic nucleotide-gated K*$^{+}$ *4* (*Hcn4*). Expression of *gap junction protein, alpha 5 (Gja5*, also known as *Cx40)* was excluded from the SAN myocardium, but detectable in the *Tnni3*$^{+}$ myocardialized dorsal part of the right sinus horn, the endothelial cells of the SAN artery, and the atria. *Tbx3* and *Hcn4* expression was unaltered whereas *Tnni3* and *Gja5* expression was almost completely absent in the dorsal part of the right sinus horn in *Tbx18*$^{cre/+}$;*Ctnnb1*$^{fx/fx}$ hearts at E18.5 (Online Figure 2) and E17.5 (Figure 3E through 3H). To

determine whether the shape and volume of the SAN and right caval vein is altered in mutant embryos, we additionally performed serial sectioning and subsequent 3D-reconstruction analysis of the *Hcn4*$^{+}$ SAN and the *Gja5*$^{+}$ region of the right caval vein (Figure 3I through 3K). We detected a 93% decrease of the *Gja5*$^{+}$ domain in *Tbx18*$^{cre/+}$;*Ctnnb1*$^{fx/fx}$ mice. The lumen of the right caval vein and the volume of the SAN were only slightly decreased. The elongated comma-like structure of the SAN at the entrance to the right atrium was preserved (Figure 3J). We conclude that *Ctnnb1* and canonical Wnt signaling are dispensable for SAN development, but strongly impact on the myocardialization of the dorsal aspect of the sinus horns.

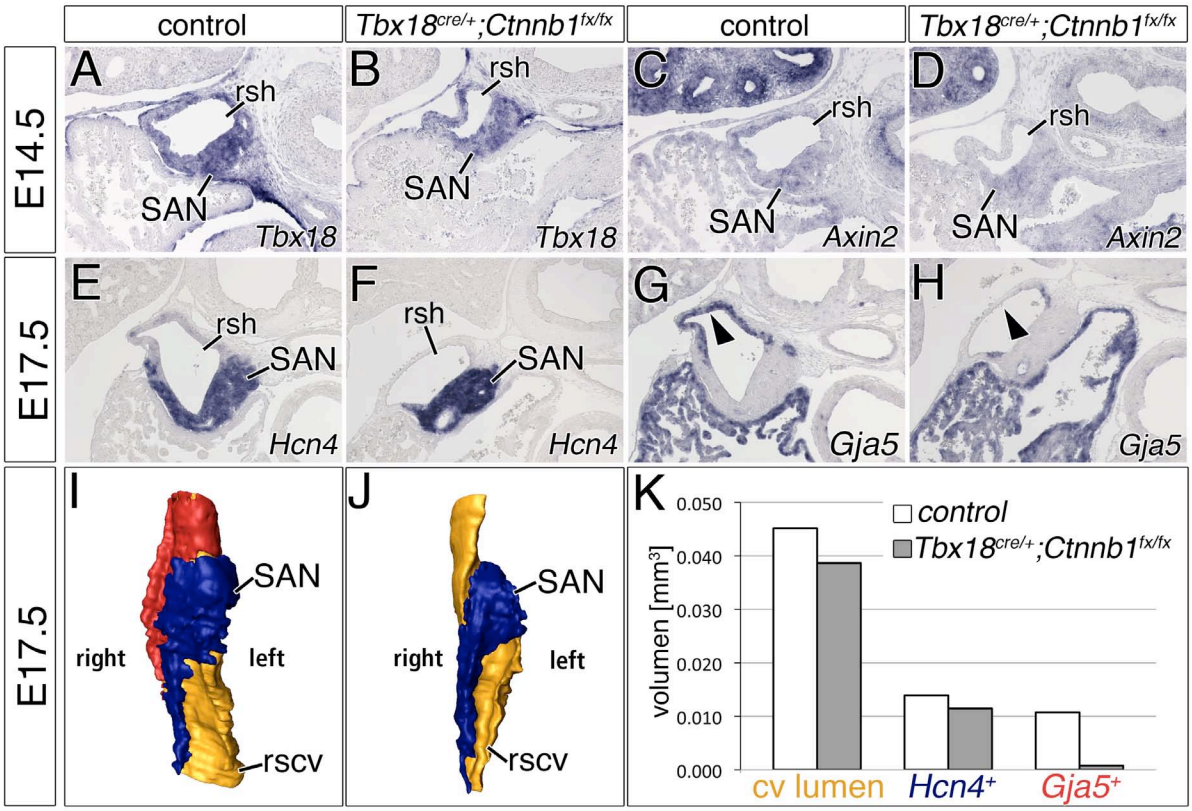

Figure 3. Morphology of the SAN in *Tbx18*$^{cre/+}$;*Ctnnb1*$^{fx/fx}$ hearts. A through H, *In situ* hybridization analysis of transverse sections through the SAN of control and *Tbx18*$^{cre/+}$;*Ctnnb1*$^{fx/fx}$ hearts for *Tbx18* (**A and B)**, the canonical Wnt signaling target *Axin2* (**C and D)**, the SAN marker *Hcn4* (**E and F)** and the atrial marker *Gja5* (**G and H**). **I through K**, 3D-reconstructions of the lumen of the right superior caval vein (orange), the *Hcn4*$^{+}$ SAN (blue), and the *Gja5*$^{+}$ myocardium of the right sinus horn (red) (**I and J**), and volume determination of the respective region using Amira software (n=1) (**K**). Note the reduction of the *Gja5*$^{+}$ domain. Arrowheads point to the dorsal domain of the right sinus horn. Genotypes and stages are as indicated. Abbreviations are as in Figure 2.

Sinus horn defects arise early in development

To determine the onset of sinus horn defects in *Tbx18*$^{cre/+}$;*Ctnnb1*$^{fx/fx}$ hearts, we analyzed embryos at earlier developmental stages. Histological analysis at E10.5 (data not shown), E12.5 and E14.5 revealed that sinus horns were released from the pericardial wall into the pericardial

cavity and positioned medially in *Tbx18*$^{cre/+}$;*Ctnnb1*$^{fx/fx}$ similar to control embryos (Figure 4A through 4D). In the latter, *Tnni3* expression, i.e. myocardialization, was restricted to the most ventral aspect of the sinus horn at E10.5 (Online Figure 6C). At E12.5, the *Tnni3*$^{+}$ domain in the control embryos expanded dorsally, and ensheathed the sinus horns at E14.5 (Figure 4E through 4L). In *Tbx18*$^{cre/+}$;*Ctnnb1*$^{fx/fx}$ embryos, myocardialization remained restricted to the ventral aspect of the sinus horn at both stages. Hence, myocardialization defects arise shortly after E10.5 when *Ctnnb1* is lost in the sinus horn lineage.

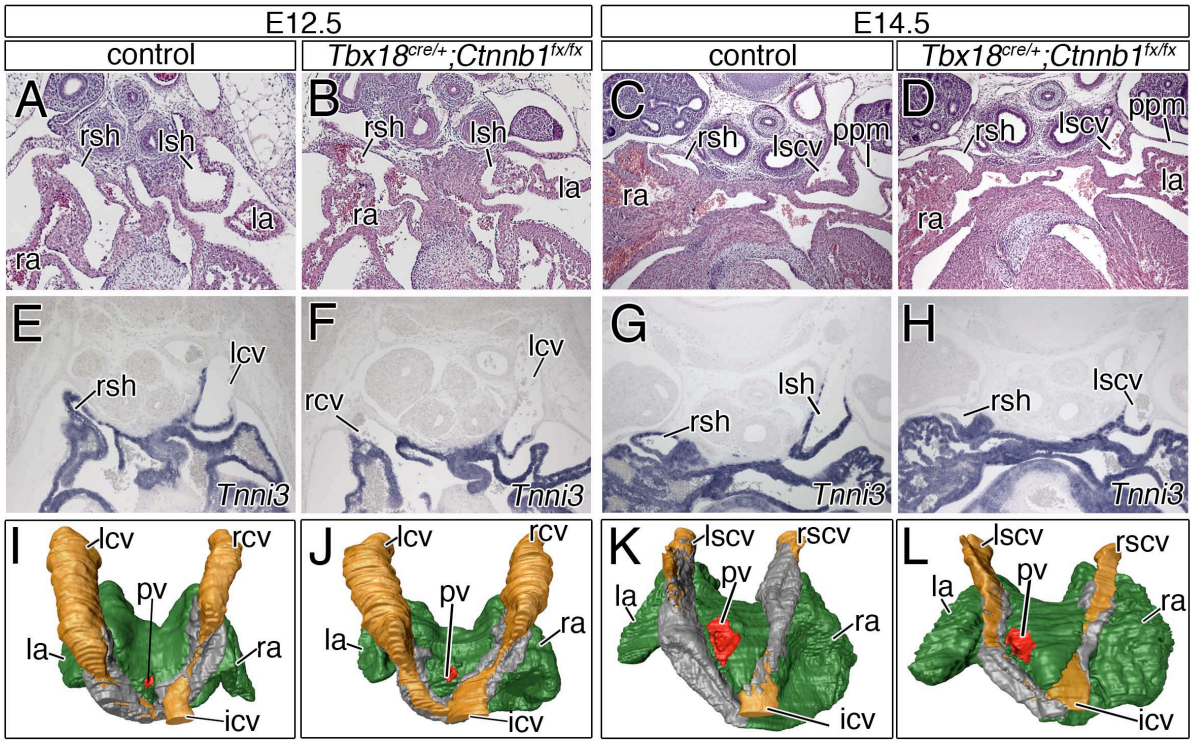

Figure 4. Developmental onset of myocardialization defects in *Ctnnb1*-deficient sinus horns. Haematoxylin and eosin staining (**A through D**), *in situ* hybridization analysis of *Tnni3* expression (**E through H**), and 3D-reconstructions of serial sections stained for *Tnni3* in a dorsal-posterior view (**I through L**) of control and *Tbx18*$^{cre/+}$;*Ctnnb1*$^{fx/fx}$ hearts at E12.5 and E14.5. Atrial myocardium is shown in green, sinus horn myocardium in grey, the lumen of the caval veins in orange, and the pulmonary vein myocardium in red (**I through L).** Stages and genotypes are as indicated. lcv: left cardinal vein; rcv, right cardinal vein; other abbreviations are as in Figure 2.

Tbx18^{+} cells do not exclusively contribute to *Ctnnb1*-deficient sinus horns

It is known that *Tbx18*$^{+}$ precursors are the source for the sinus horn myocardium in wildtype embryos.[3] To determine the fate of *Tbx18*$^{+}$ precursors in *Ctnnb1*-deficient sinus horns, we introduced an *R26*^{mTmG} reporter allele into the mutant background. In *Tbx18*$^{cre/+}$;*R26*$^{mTmG/+}$;*Ctnnb1*$^{fx/+}$ mice *Tbx18*^{cre}-expressing cells and their descendants become irreversibly labeled by expression of a bright membrane-bound green fluorescent protein (GFP). Double immunofluorescence analysis for GFP and the cardiomyocyte marker protein Tnni3 at E18.5 confirmed the derivation of the sinus horn myocardium from the *Tbx18*$^{+}$ mesenchyme of

the caval veins in control (*Tbx18$^{cre/+}$;R26$^{mTmG/+}$;Ctnnb1$^{fx/+}$)* embryos (Figure 5A through 5C). In *Tbx18$^{cre/+}$;R26$^{mTmG/+}$;Ctnnb1$^{fx/fx}$* mutant embryos, the myocardium of the SAN was GFP^{+} whereas the dorsal non-myocardialized region was not derived from *Tbx18*$^{+}$ precursors (Figure 5D through 5F). To more precisely define the character of this non-myocardialized part of the sinus horns, we expanded our immunohistochemical analysis. In control hearts the myo-fibroblast marker fibronectin 1 (Fn1) was not detectable in the *Tbx18*-derived sinus horn myocardium but was expressed in the pleuropericardial membrane and the adjacent tissue next to the dorsal mesocardium (Figure 5G through 5I). However, the GFP^{-} region of the right sinus horn in *Tbx18$^{cre/+}$;R26$^{mTmG/+}$;Ctnnb1$^{fx/fx}$* embryos stained for Fn1 as well as for actin, alpha 2, smooth muscle, aorta (Acta2) (Figure 5J through 5L, 5P through 5R). In the wildtype control, Acta2 was expressed in vascular smooth muscle cells[13] but not in the sinus horns (Figure 5M through 5O). Moreover, we verified the nearly complete loss of Gja5 in *Tbx18$^{cre/+}$;R26$^{mTmG/+}$;Ctnnb1$^{fx/fx}$* sinus horns by double immunofluorescence analysis for GFP and Gja5 (Online Figure 3A through 3F). Expression of the conduction system marker Tbx3, and the mesothelial marker Wilms tumor 1 homolog (Wt1) was unchanged in the mutant sinus horns, confirming the sinus horn specific defects after *Tbx18^{cre}* mediated inactivation of *Ctnnb1* (Online Figure 3G through 3R). In conclusion, the dorsal region of *Ctnnb1*-deficient sinus horns is composed of myofibroblasts that derive from sources other than *Tbx18*$^{+}$ precursors.

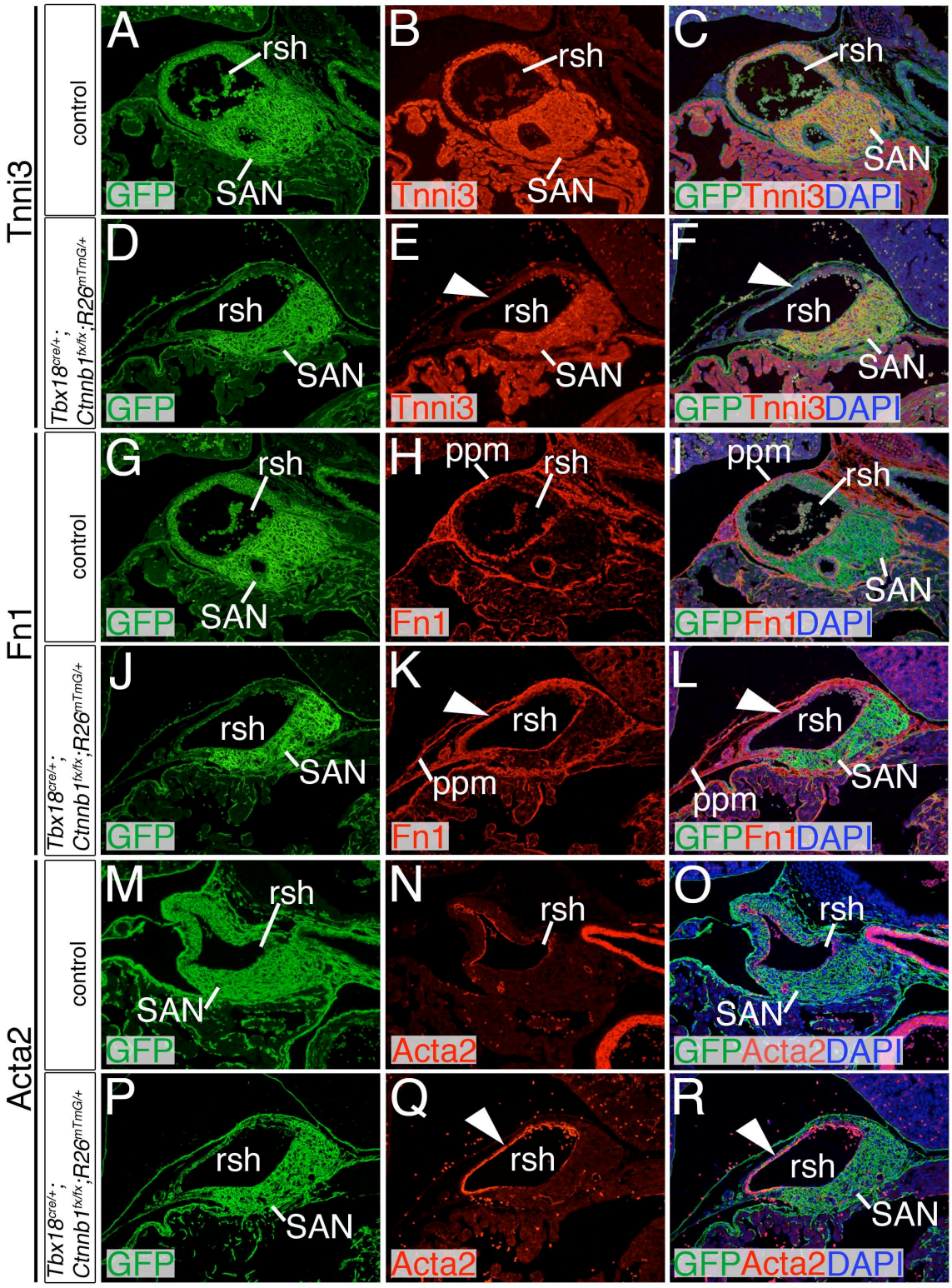

Figure 5. Cellular contributions to the *Ctnnb1*-deficient systemic venous return of the heart. **A through R**, Comparative immunofluorescence analysis of cellular derivates of the *Tbx18*$^{+}$ domain of the sinus horns, marked by GFP expression, and cardiac troponin Tnni3 (**A through F**), the fibroblast marker Fn1 (**G through H**) or the smooth muscle marker Acta2 (**M through N**) in control (genotype: *Tbx18*$^{cre/+}$;*R26*$^{mTmG/+}$;*Ctnnb1*$^{fx/+}$) and *Tbx18*$^{cre/+}$;*R26*$^{mTmG/+}$;*Ctnnb1*$^{fx/fx}$ mutant sinus venosus region of the heart at E18.5. Antibodies and genotypes are as indicated, nuclei are counterstained with DAPI. Arrowheads mark the Tnni3^{-} part of the *Tbx18*$^{cre/+}$;*R26*$^{mTmG/+}$;*Ctnnb1*$^{fx/fx}$ mutant right sinus horns. rsh; right sinus horn; SAN, sinoatrial node.

Molecular analysis of *Ctnnb1*-deficient sinus horns

We next analyzed by *in situ* hybridization analysis whether the observed defects in the *Ctnnb1*-deficient sinus horns are accompanied by altered expression of factors or pathways associated with regionalization and differentiation of the posterior cardiac pole. Expression of marker genes for the FHF (*Nkx2-5)* and the SHF (*Tbx1*, *Isl1,* and *Fgf10)* was absent from wildtype and mutant sinus horns at E12.5. *Tbx5* was expressed in the atria and sinus horns of both wildtype and *Ctnnb1*-deficient mice (Online Figure 4A through 4J). The Fgf signaling pathway promotes proliferation in the anterior SHF and is important for the development of the OFT,[14] but *Fgf8* and *Fgf10* as well as its target genes[15] *ets variant gene 4 (Etv4,* also known as *Pea3)* or *Etv5 (*also known as *Erm)* were not detectable in control or *Tbx18$^{cre/+}$;Ctnnb1$^{fx/fx}$* sinus horns (Online Figure 4I through 4L, and data not shown). Since the bone morphogenetic protein (Bmp) signaling pathway is crucial for the differentiation of cardiomyocytes in the OFT,[16] we additionally analyzed the expression of *Bmp2* and *Bmp4*, as well as its target genes *homeobox, msh-like 1* (*Msx1)* and *Msx2*, in the developing sinus horns at E12.5. *Bmp2* and *Bmp4* expression was detectable in the SAN tail, which is located in the sinus venosus, in both control and *Ctnnb1*-deficient mice (Online Figure 4M through 4R, and data not shown).[17] Loss of sonic hedgehog (Shh) signaling in *Isl1*-positive cardiac progenitors leads to OFT defects.[18] Expression of *Shh* and its target gene *patched homolog 1 (Ptch1)* were unverifiable in the intrapericardial domain of the wildtype and mutant sinus horns at E12.5 (Online Figure 4S and 4T, and data not shown). A feed-forward loop between the Wnt ligand *Wnt2* and the *GATA binding protein 6* (*Gata6)* is important for proliferation of SHF progenitors of the heart and, hence, for the development of the atria and the AVC.[6] We detected expression of *Wnt2* and *Gata6* in the developing sinus horns at E14.5 in both wildtype and mutant embryos (Online Figure 5A through 5D). Similarly, *Sfrp1* expression was unchanged, excluding a self-regulation of Wnt/Ctnnb1 signaling in this region (Online Figure 5E and 5F). Furthermore, loss of *Ctnnb1* did not affect expression of markers of the pleuropericardial membrane and its underlying mesenchyme including *Sfrp2, Wt1,* and *aldehyde dehydrogenase family 1, subfamily A2 (Aldh1a2)* (Online Figure 5G through 5L).[19] In conclusion, these results again demonstrate the distinct molecular signature of the developing sinus horns and the SAN. We could not reveal a role of Bmp, Fgf and Shh signaling during sinus horn development. Loss of *Ctnnb1* does not affect regionalization and precursor contribution at the posterior cardiac pole.

Ectopic activation of canonical Wnt signaling in the developing sinus horns

To further clarify the role of *Ctnnb1*-dependent Wnt signaling during sinus horn development, we employed a gain-of-function approach with conditional (*Tbx18^{cre}*-mediated) overexpression of a stabilized form of Ctnnb1 (*Ctnnb1$^{(Ex3)fl}$*)[9] (Figure 6).

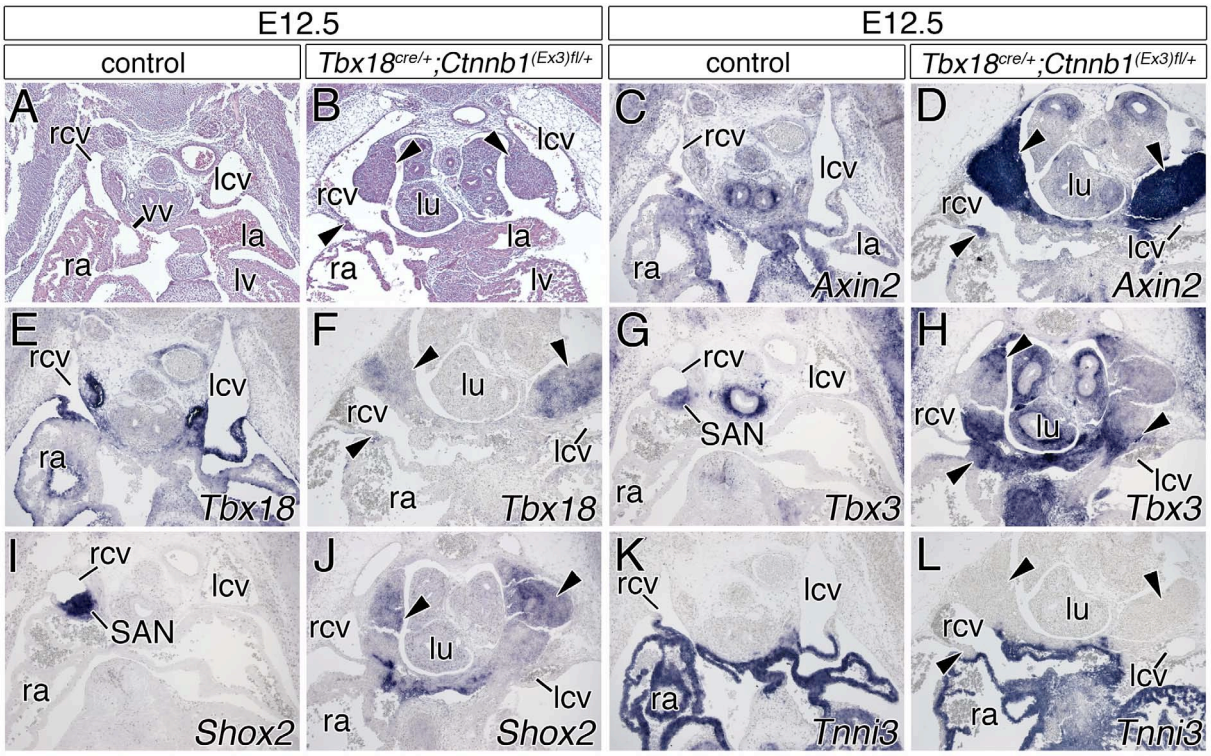

Figure 6. Ectopic activation of canonical Wnt signaling in the sinus venosus region induces cell clusters. (**A and B)** Haematoxylin and eosin staining, and (**C through L**) *in situ* hybridization analysis on transverse sections for the Wnt target gene *Axin2* (**C and D**), the sinus horn marker gene *Tbx18* (**E and F**), the SAN marker genes *Tbx3* and *Shox2* **(G trough J**), and the cardiomyocyte marker*Tnni3* (**K and L**) in control and *Tbx18$^{cre/+}$;Ctnnb1$^{(Ex3)fl/+}$* mutant cardiac venous pole region at E12.5. Genotypes are as indicated. Arrowheads point to the ectopic cell clusters in the *Tbx18$^{cre/+}$;Ctnnb1$^{(Ex3)fl/+}$* sinus venosus region. la, left atrium; lcv, left cardinal vein; lu, lung; lv, left ventricle; ra; right atrium; rcv, right cardinal vein; SAN, sinoatrial node; vv, venous valves.

Tbx18$^{cre/+}$;Ctnnb1$^{(Ex3)fl/+}$ embryos died during midgestation due to cardiovascular insufficiencies (to be described in full detail somewhere else). Histological inspection of surviving embryos at E12.5 revealed the presence of large cell aggregates in the developing sinus horns of *Tbx18$^{cre/+}$;Ctnnb1$^{(Ex3)fl/+}$* mutant embryos (Figure 6A and 6B). Strong *Axin2* expression confirmed activation of canonical Wnt signaling in these cell clusters (Figure 6C and 6D). Expression of the regional marker genes *Tbx18*, *Tbx3* and *short stature homeobox 2* (*Shox2)* was present, whereas cardiomyocyte marker expression (*Tnni3*) was absent from these cell aggregates (Figure 6E through 6L). Inspection of earlier developmental stages revealed presence of small cell aggregates from E10.5 onwards. Expression of *Etv5*, a target gene of the Fgf signaling pathway, which is known to promote proliferation in SHF progenitors, was found in the outer layers of these clusters. Also the expression of *cyclinD1* (*Ccnd1*), a direct Wnt target gene and positive regulator of cell cycle progression, was detectable in these cell clusters (Online Figure 6 and 7). We conclude that sinus horn specific expression of a stabilized form of Ctnnb1 results in formation of aggregates composed of mesenchymal precursor cells, which were not able to differentiate into cardiomyocytes.

Cellular changes in the *Tbx18*-positive region of the developing sinus horns

We next investigated whether changes in proliferation and apoptosis may underlie the observed lack of cardiomyocytes in the dorsal aspects of *Tbx18*$^{cre/+}$;*Ctnnb1*$^{fx/fx}$ sinus horns. The BrdU incorporation assay revealed decreased proliferation of *Tbx18* expressing sinus horn precursor cells between E10.5 and E14.5 (Figure 7D, Online Figure 8), reaching significant values at E10.5 (wildtype 0.274±0.0183 vs mutant 0.217±0.0341; P=0.042) and E14.5 (wildtype 0.173±0.0197 vs mutant 0.100±0.0254; P=0,018), but not at E12.5 (wildtype 0.208±0.0252 vs mutant 0.181±0.0116; P=0.175). Apoptosis was not increased in the sinus horns in any of these stages (data not shown) suggesting that decreased proliferation contributes to the observed defects in mutant embryos.

Since we noted an increasing size of the cell clusters in the *Tbx18*$^{cre/+}$;*Ctnnb1*$^{(Ex3)fl/+}$ embryos from E10.5 to E12.5, we also analyzed cell proliferation and apoptosis in these mutant mice. At E10.5, the proliferation in the *Tbx18*$^{+}$ cell aggregates was highly and significantly increased (control 0.167±0.0390 vs mutant 0.437±0.0275; P=0.002). At E11.5, proliferation rates decreased in control and mutant clusters but were maintained at a significantly higher level in the mutant (control 0.190±0.0300 vs mutant 0.235±0.0675; P<0.001) (Figure 7E and Online Figure 9). At E10.5, low levels of apoptosis was observed in *Tbx18*$^{+}$ cell aggregates, but not in the cardinal veins of both control and gain-of-function embryos (we analyzed three control and three *Tbx18*$^{cre/+}$;*Ctnnb1*$^{(Ex3)fl/+}$-mutant embryos). At E11.5 and E12.5, the whole center of these cell aggregates became largely apoptotic (we analyzed two embryos of each genotype), whereas apoptosis was not detectable in control embryos (Online Figure 10). Hence, canonical Wnt signaling is required and sufficient to maintain proliferation of mesenchymal precursor cells of the sinus horn myocardium.

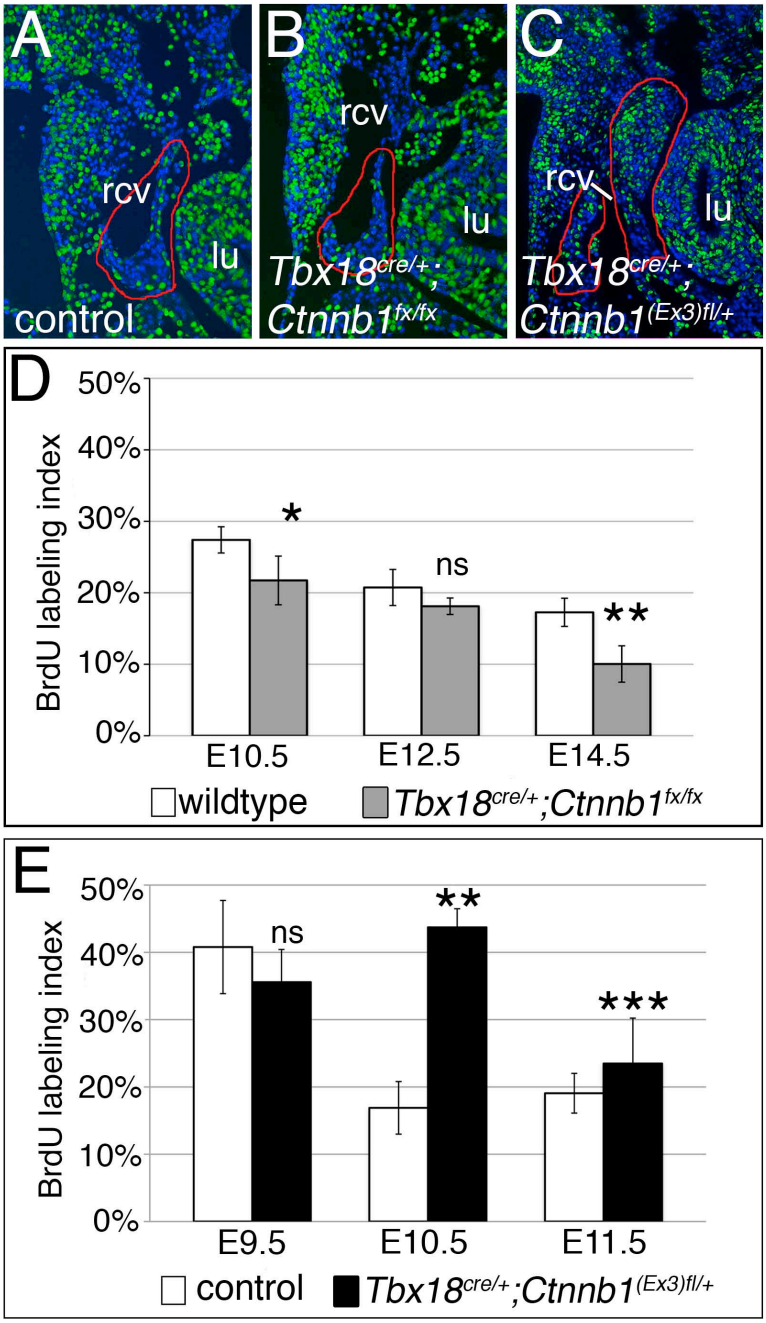

Figure 7. **Cellular changes in *Ctnnb1*-deficient sinus horns and in ectopic aggregates of *Tbx18*$^{cre/+}$;*Ctnnb1*$^{(Ex3)fl/+}$ sinus horns. A through C**, Analysis of proliferation by BrdU immunohistochemistry in the red encircled, *Tbx18*$^{+}$ intrapericardial domain of the sinus horns performed on transverse sections through the posterior systemic venous return at E10.5. BrdU positive cells are labeled in green, nuclei are counterstained with DAPI. **D and E**, Proliferation rates (% BrdU labeling index) of red encircled regions in genotypes and stages as shown. **D,** The P-values in the *Ctnnb1*-deficient sinus horns are P=0.042 (*) at E10.5, P=0.175 (not significant) at E12.5 and P=0,018 (**) at E14.5. **E**, The P-values in the *Tbx18*$^{cre/+}$;*Ctnnb1*$^{(Ex3)fl/+}$ mutant systemic venous return including the ectopic cell aggregates are P= 0.2637 (ns) at E9.5, P= 0,002 (**) at E10.5 and P<0,001 (***) at E12.5. lu, lung, rcv, right cardinal vein.

Discussion

The myocardial sleeves of the superior and inferior caval veins and the SAN myocardium derives from a distinct *Tbx18*$^{+}$*Nkx2-5*$^{-}$ mesenchymal precursor cell population. Here, we have shown that canonical Wnt signaling is required for the myocardialization of the dorsal domain of the developing sinus horns. Forced Wnt signaling is sufficient to induce high proliferation and prevent the differentiation into cardiomyocytes in this region. We suggest that Ctnnb1-dependent Wnt signaling in the intrapericardial domain of the developing caval veins is part of a signaling system that balances proliferation and cardiomyocyte differentiation of these mesenchymal precursor cells.

A regionalized requirement for canonical Wnt signaling in sinus horn development

The general significance of canonical Wnt signaling in heart development has been shown in previous studies.[1,20] Conditional loss of *Ctnnb1* in the early mesodermal progenitors of both the FHF and SHF revealed that *Ctnnb1*-dependent Wnt signaling does not affect cardiac crescent formation, which derives from the FHF, but is required for the development of SHF derived structures and cardiac looping.[21] *Wnt2* has been identified as a canonical ligand acting in the *Nkx2-5*$^{+}$*Isl*$^{+}$ inflow tract mesoderm to regulate addition of atria and AVC to the posterior pole of the growing heart tube.[6,22]

Our analysis of the expression of Wnt pathway components and the function of *Ctnnb1* expands the role of canonical Wnt signaling to sinus horn formation. Deletion of *Ctnnb1* from the sinus venosus lineage results in a specific lack of myocardialization in the dorsal aspects of the sinus horns. However, loss of *Ctnnb1* does not affect formation of the SAN that also derives from a Tbx18^{+} cell lineage. Although the SAN considerably expands between E10.5 and E14.5, increase in size may not rely on recruitment and myocardialization of mesenchymal precursor cells but may occur by division of primitive cardiomyocytes that are specified early to a SAN sub-lineage. Evidence is provided by the distinct molecular character of the developing SAN including the expression of *Tbx3*, *Shox2, Hcn4* and Bmp signaling components. Although *Tbx3* was discussed as a target of canonical Wnt signaling in cancer, unaltered expression in the *Tbx18*$^{cre/+}$*;Ctnnb1*$^{fx/fx}$ sinus venosus argues for a different regulation in this developmental context.

Ctnnb1 is not only the transcriptional effector of the canonical Wnt signaling pathway, but additionally is a key molecule in adherens junctions.[23,24] Nevertheless, its close relative plakoglobin, also known as gamma-catenin, can compensate the loss of beta-catenin in *Ctnnb1*-deficient embryos[23] as well as in adult cardiomyoctes.[24] In *Ctnnb1* loss-of-function mutants adherens junctions developed, and the cell morphology remained unchanged. Therefore, we conclude that the defects described in the *Tbx18*$^{cre/+}$*;Ctnnb1*$^{fx/fx}$ mutant sinus horns are mainly due to the loss of *Ctnnb1* as a signaling molecule.

Support for a role of canonical Wnt signaling in the developing sinus horns is provided by expression of Wnt ligands and receptors, and most importantly by expression of *Axin2* that has been described as a *bona fide* target of this pathway. Loss of expression of *Axin2* from the intrapericardial domain of the sinus horns after *Tbx18*^{cre}-mediated deletion of *Ctnnb1* function and strong induction of *Axin2* expression after stabilization of Ctnnb1 in this domain confirms the character of *Axin2* as a target of Ctnnb1 for the development of the dorsal aspect of the sinus horns and proves the efficiency of our genetic approach to manipulate canonical Wnt signaling. Our Wnt expression screen argues that canonical Wnt signaling in the developing sinus horns is mediated by Wnt2 and Wnt10a ligands and the Fzd7 receptor. Wnt signaling may be modulated (diminished) by sFRP1 that binds the ligands and prevents activation of the pathway.

In the posterior SHF, *Wnt2* works in a feed-forward transcriptional loop with *Gata6* to regulate atria and AVC development.[6] *Wnt2* as well as *Gata6* expression were unchanged in the *Tbx18*$^{cre/+}$*;Ctnnb1*$^{fx/fx}$ sinus horns, suggesting that Wnt signaling in the "third heart field" employs different downstream mediators compared to the SHF. The analysis of additional signaling pathways further emphasizes the distinct character of the *Tbx18*$^{+}$*Nkx2-5*$^{-}$ precursor pool. The Bmp, Fgf and Shh signaling pathways are important for the development of SHF-derived structures, especially the OFT region of the murine heart.[1] However, none of the analyzed components or target genes of these pathways were detectable in the developing sinus horns, nor were they de-repressed in *Ctnnb1*-deficient sinus horns.

Canonical Wnt signaling maintains proliferation of mesenchymal precursor cells

We have recently shown that the myocardialized proximal aspects of the superior and inferior caval veins form only after heart cardiac looping by recruitment and subsequent myocardial differentiation of *Tbx18*$^{+}$ pericardial precursors.[3] The lack of myocardium in the dorsal aspect of the sinus horns of *Ctnnb1*-deficient embryos can therefore be explained in at least two ways. Canonical Wnt signaling may promote the expansion of the mesenchymal precursor pool or additionally/alternatively direct the differentiation of these progenitors into cardiomyocytes.

In *Ctnnb1*-deficient sinus horns, cell proliferation was significantly reduced as early as E10.5 suggesting that the progenitor pool was strongly and quickly diminished. This is supported by the lineage analysis in these mutants that revealed that the *Tbx18*$^{+}$ sinus venosus progenitors do not contribute to the myofibroblastic tissue in the dorsal domain. Furthermore, forced activation of canonical Wnt signaling by a stabilized form of Ctnnb1 leads to hyperproliferative cell aggregates which express regional marker genes including *Tbx18* but fail to differentiate into cardiomyocytes.

Together, these findings strongly argue that canonical Wnt signaling maintains the sinus horn precursor pool. A similar mode of action was described for Wnt2 function in the posterior SHF and goes along the general line of Wnt signaling as a positive regulator of the cell cycle.[20,25] Not surprisingly, we found activation of *Ccnd1* expression, a direct Wnt target gene and positive

regulator of cell cycle progression, in the cell aggregates expressing stabilized Ctnnb1 in the sinus horns. Increased levels of canonical Wnt/Ctnnb1 signaling were also found to be sufficient to induce Fgf signaling that has been associated with increased cell proliferation in many other contexts. It remains unclear whether Fgf signaling represents an non-physiological response to enhanced Wnt signaling since we did not detect expression of the Fgf target gene *Etv5* in the wildtype sinus horns.

Our molecular analysis in the myocardium of the sinus horns did not detect Bmp signaling, a known promoter of cardiomyocyte differentiation. It therefore remains to be deciphered what other signaling pathway(s) counteract Wnt signaling to promote myocardial differentiation during sinus horns development.

Acknowledgements

We thank Rolf Kemler for providing the *Ctnnb1^{fx}*-mice and Benjamin Förthmann for help with the 3D-reconstructions.

Sources of Funding

This work was supported by grants from the European Community's Sixth Framework Programme contract ("HeartRepair" LSHM-CT-2005-018630), the German Research Foundation (DFG) for the Cluster of Excellence REBIRTH (From Regenerative Biology to Reconstructive Therapy) and for the Clinical Research Group KFO136 at Hannover Medical School (to A.K.).

References

1. Vincent SD, Buckingham ME. How to make a heart: The origin and regulation of cardiac progenitor cells. *Curr Top Dev Biol*. 2010;90:1-41
2. Anderson RH, Brown NA, Moorman AFM. Development and structures of the venous pole of the heart. *Dev Dyn*. 2006;235:2-9
3. Christoffels VM, Mommersteeg MTM, Trowe M-O, Prall OWJ, De Gier-De Vries C, Soufan AT, Bussen M, Schuster-Gossler K, Harvey RP, Moorman AFM, Kispert A. Formation of the venous pole of the heart from an nkx2-5-negative precursor population requires tbx18. *Circulation Research*. 2006;98:1555-1563
4. Mommersteeg MTM, Domínguez JN, Wiese C, Norden J, De Gier-De Vries C, Burch JBE, Kispert A, Brown NA, Moorman AFM, Christoffels VM. The sinus venosus progenitors separate and diversify from the first and second heart fields early in development. *Cardiovascular Research*. 2010; 87(1):92-101

5. Ai D, Fu X, Wang J, Lu M-F, Chen L, Baldini A, Klein WH, Martin JF. Canonical wnt signaling functions in second heart field to promote right ventricular growth. *Proc Natl Acad Sci USA*. 2007;104:9319-9324

6. Tian Y, Yuan L, Goss AM, Wang T, Yang J, Lepore JJ, Zhou D, Schwartz RJ, Patel V, Cohen ED, Morrisey EE. Characterization and in vivo pharmacological rescue of a wnt2-gata6 pathway required for cardiac inflow tract development. *Developmental cell*. 2010;18:275-287

7. Trowe M-O, Shah S, Petry M, Airik R, Schuster-Gossler K, Kist R, Kispert A. Loss of sox9 in the periotic mesenchyme affects mesenchymal expansion and differentiation, and epithelial morphogenesis during cochlea development in the mouse. *Developmental Biology*. 2010;342:51-62

8. Brault V, Moore RT, Kutsch S, Ishibashi M, Rowitch DH, McMahon AP, Sommer L, Boussadia O, Kemler R. Inactivation of the beta-catenin gene by wnt1-cre-mediated deletion results in dramatic brain malformation and failure of craniofacial development. *Development*. 2001;128:1253-1264

9. Harada N, Tamai Y, Ishikawa T, Sauer B, Takaku K, Oshima M, Taketo MM. Intestinal polyposis in mice with a dominant stable mutation of the beta-catenin gene. *EMBO J*. 1999;18:5931-5942

10. Muzumdar MD, Tasic B, Miyamichi K, Li L, Luo L. A global double-fluorescent cre reporter mouse. *genesis*. 2007;45:593-605

11. Kraus F, Haenig B, Kispert A. Cloning and expression analysis of the mouse t-box gene tbx18. *Mechanisms of Development*. 2001;100:83-86

12. Wiese C, Grieskamp T, Airik R, Mommersteeg MTM, Gardiwal A, De Gier-De Vries C, Schuster-Gossler K, Moorman AFM, Kispert A, Christoffels VM. Formation of the sinus node head and differentiation of sinus node myocardium are independently regulated by tbx18 and tbx3. *Circulation Research*. 2009;104:388-397

13. Owens GK. Regulation of differentiation of vascular smooth muscle cells. *Physiol Rev*. 1995;75:487-517

14. Watanabe Y, Miyagawa-Tomita S, Vincent SD, Kelly RG, Moon AM, Buckingham ME. Role of mesodermal fgf8 and fgf10 overlaps in the development of the arterial pole of the heart and pharyngeal arch arteries. *Circulation Research*. 2010;106:495-503

15. Brent AE, Tabin CJ. Fgf acts directly on the somitic tendon progenitors through the ets transcription factors pea3 and erm to regulate scleraxis expression. *Development*. 2004;131:3885-3896

16. Wang J, Greene SB, Bonilla-Claudio M, Tao Y, Zhang J, Bai Y, Huang Z, Black BL, Wang F, Martin JF. Bmp signaling regulates myocardial differentiation from cardiac progenitors through a microrna-mediated mechanism. *Developmental Cell*. 2010;19:903-912

17. Puskaric S, Schmitteckert S, Mori AD, Glaser A, Schneider KU, Bruneau BG, Blaschke RJ, Steinbeisser H, Rappold G. Shox2 mediates tbx5 activity by regulating bmp4 in the pacemaker region of the developing heart. *Hum Mol Genet*. 2010;19:4625-4633

18. Lin L, Bu L, Cai C-L, Zhang X, Evans S. Isl1 is upstream of sonic hedgehog in a pathway required for cardiac morphogenesis. *Dev Biol*. 2006;295:756-763

19. Norden J, Grieskamp T, Lausch E, Van Wijk B, van den Hoff MJB, Englert C, Petry M, Mommersteeg MTM, Christoffels VM, Niederreither K, Kispert A. Wt1 and retinoic acid signaling in the subcoelomic mesenchyme control the development of the pleuropericardial membranes and the sinus horns. *Circulation Research*. 2010:1212 - 1220

20. Grigoryan T, Wend P, Klaus A, Birchmeier W. Deciphering the function of canonical wnt signals in development and disease: Conditional loss- and gain-of-function mutations of beta-catenin in mice. *Genes & Development*. 2008;22:2308-2341

21. Klaus A, Saga Y, Taketo MM, Tzahor E, Birchmeier W. Distinct roles of wnt/beta-catenin and bmp signaling during early cardiogenesis. *Proc Natl Acad Sci USA*. 2007;104:18531-18536

22. Sousa KM, Villaescusa JC, Cajanek L, Ondr JK, Castelo-Branco G, Hofstra W, Bryja V, Palmberg C, Bergman T, Wainwright B, Lang RA, Arenas E. Wnt2 regulates progenitor proliferation in the developing ventral midbrain. *J Biol Chem*. 2010;285:7246-7253

23. Huelsken J, Vogel R, Brinkmann V, Erdmann B, Birchmeier C, Birchmeier W. Requirement for beta-catenin in anterior-posterior axis formation in mice. *J Cell Biol*. 2000;148:567-578

24. Zhou J, Qu J, Yi XP, Graber K, Huber L, Wang X, Gerdes AM, Li F. Upregulation of gamma-catenin compensates for the loss of beta-catenin in adult cardiomyocytes. *Am J Physiol Heart Circ Physiol*. 2007;292:H270-276

25. Gessert S, Kühl M. The multiple phases and faces of wnt signaling during cardiac differentiation and development. *Circulation Research*. 2010;107:186-199

Supplemental Online Materials and Methods

Mice and genotyping

Mice with a knock-in of the *cre* recombinase gene into the *Tbx18* locus (*Tbx18*$^{tm4(cre)Akis}$, synonym: *Tbx18*^{cre}),[1] mice with two *loxP* sites flanking the *Ctnnb1* locus from exon 2 to exon 6 (*Ctnnb1*^{tm2Kem}, synonym: *Ctnnb1*^{fx}),[2] mice with two *loxP* sites flanking exon 3 of the *Ctnnb1* locus (*Ctnnb1*^{tm1Mmt}, synonym: *Ctnnb1*$^{(Ex3)fl}$),[3] and the fluorescent reporter line *(Gt(ROSA)26Sor*$^{tm4(ACTB-tdTomato,-EGFP)Luo}$/J, synonym: *R26*^{mTmG})[4] were all described before. All lines were maintained on an outbred (NMRI) background. The sinus horns specific *Ctnnb1* loss-of-function mutants (*Tbx18*$^{cre/+}$*;Ctnnb1*$^{fx/fx}$ and *Tbx18*$^{cre/+}$*;R26*$^{mTmG/+}$*;Ctnnb1*$^{fx/fx}$) were obtained from matings of *Tbx18*$^{cre/+}$*;Ctnnb1*$^{fx/+}$ and *Tbx18*$^{cre/+}$*;R26*$^{mTmG/+}$*;Ctnnb1*$^{fx/+}$ males, respectively, with *Ctnnb1*$^{fx/fx}$ (*Ctnnb1*^{tm2Kem})[2] females. Sinus horns specific *Ctnnb1* gain-of-function mice *(Tbx18*$^{cre/+}$*;Ctnnb1*$^{(Ex3)fl/+}$ *and Tbx18*$^{cre/+}$*;R26*$^{mTmG/+}$*;Ctnnb1*$^{(Ex3)fl/+}$*)* were derived from matings of *Tbx18*$^{cre/+}$ and *Tbx18*$^{cre/+}$*;R26*$^{mTmG/+}$ males, respectively, with *Ctnnb1*$^{(Ex3)fl/(Ex3)fl}$ (*Ctnnb1*^{tm1Mmt})[3] females.

Vaginal plugs were checked in the morning after mating, for timed pregnancies noon was taken as embryonic day (E) 0.5. After harvesting the embryos in PBS, they were fixed in 4% paraformaldehyde overnight and stored in 100% methanol at –20°C before further use. For the analysis of the conditional *Ctnnb1* loss-of-function phenotype, heterozygous animals (*Tbx18*$^{cre/+}$*;Ctnnb1*$^{fx/+}$) were used as control embryos. For the *Ctnnb1* gain-of-function analysis *Tbx18*$^{+/+}$*;Ctnnb1*$^{(Ex3)fl/+}$ embryos were used as control. Genomic DNA prepared from yolk sacs or tail biopsies was used for genotyping by PCR (protocols upon request). H. Hedrich, state head of the animal facility, approved the care of animals and experiments at Medizinische Hochschule Hannover.

Histological analysis

For histological stainings embryos were fixed overnight in 4% paraformaldehyde, paraffin embedded, and sectioned to 10-μm. Sections were stained with haematoxylin and eosin, following standard procedures. At least two embryos of each genotype were used for each analysis.

In situ hybridization analysis

Nonradioactive *in situ* hybridization analysis with digoxigenin-labeled antisense riboprobes was performed as described.[5] At least two embryos of each genotype were used for each analysis. Details of used probes upon request.

Documentation

Sections were photographed using a Leica DM5000 microscope with Leica DFC300FX digital camera and afterwards processed in Adobe Photoshop CS3.

Three-dimensional reconstruction

For three-dimensional visualization and geometry reconstruction 10-μm serial sections of the whole heart of representative embryos of each genotype were used for *in situ* hybridization and documented as described. Further analysis was performed using the software “Amira” (Version 4.1.1, Mercury Computer Systems Inc) as described previously.[6] After documentation, the pictures were aligned, and regions for reconstruction were labeled. A three-dimensional model was obtained after surface conversion. Based on this reconstruction the volume of the different labels was calculated by the software “Amira”.

Immunohistochemistry

For immunofluorescence analysis, mouse monoclonal antibody against GFP (1:250, 11814460001, Roche), mouse monoclonal antibody against Fn-1 (1:300, F7387, Sigma), mouse monoclonal antibody against Acta2, FITC conjugate (1:250, F3777, Sigma), goat polyclonal antibody against Tbx3 (1:200, sc-31656, Santa-Cruz), rabbit polyclonal antibody against Gja5

(1:50, AB1726, Millipore), goat monoclonal antibody against Tnni3 (1:300, 4T21/2, HyTest), and rabbit polyclonal antibody against Wt1 (1:400, C-19, Santa Cruz Biotechnology) were used as primary antibodies.
Alexa488 goat-anti-rabbit (1:250, Invitrogen), Alexa488 donkey-anti-mouse (1:250, Invitrogen), biotinylated goat-anti-rabbit (1:250, 111-065-003, Dianova) and biotinylated donkey-anti-goat (1:250, 705-065-003, Dianova) were used as secondary antibodies. Nuclei were stained with 4',6-diamidino-2-phenylindol (DAPI) (Roth). All used paraffin sections were pressure cooked for 3 min in antigen unmasking solution (H-3300, Vector Laboratories Inc). Endogenous peroxidase activity was blocked by 3% H_2O_2. The signal was amplified using either the Tyramide Signal Amplification (TSA) system from Perkin-Elmer (NEL702001KT, Perkin Elmer LAS) or the Mouse-on-mouse (M.O.M.) immunodetection kit from Vector Laboratories (PK-2200, Vector Labs). The anti-GFP staining was performed in a second experiment directly after the first immunodetection was finished and followed the published protocols.

Proliferation and apoptosis assays
Cell proliferation in E9.5 to E14.5 embryos was investigated by detection of incorporated 5-bromo-2-deoxyuridine (BrdU) on 5-μm sections of paraffin-embedded specimens similar to previously published protocols.[7] Wildtype littermates were used as controls for each genotype and stage. Both the left cardinal vein and right cardinal veins were counted. For analysis of *Tbx18*$^{cre/+}$*;Ctnnb1*$^{fx/fx}$ hearts, five sections each of four embryos of each genotype at E10.5, and five sections each of three embryos of each genotype at E12.5 and E14.5 were used for quantification. The quantification of proliferation in *Tbx18*$^{cre/+}$*;Ctnnb1*$^{(Ex3)fl/+}$ and control hearts was performed with six sections each of four embryos of each genotype at E9.5, and six sections of each of three embryos of each genotype and stage at E10.5 and E11.5. The BrdU-labeling index was defined as the number of BrdU-positive nuclei relative to the total number of nuclei, as detected by DAPI counterstain, in the *Tbx18* expressing region of the left and right cardinal veins. Statistical analyses were performed using the 2-tailed Student's t-test. Data were expressed as mean ± SEM. Differences were considered not significant when the P-value was higher than 0.05, significant (*) when the P-value was below 0.05, highly significant (**) when the P-value was below 0.01, and extremely significant (***) if P<0.001.
Detection of apoptotic cells on 10-μm paraffin sections of wildtype and *Tbx18*$^{cre/+}$*;Ctnnb1*$^{(Ex3)fl/+}$ mutant embryos was based on modification of genomic DNA utilizing terminal deoxynucleotidyl transferase (TUNEL assay) and indirect detection of positive cells by fluorescein-conjugated anti-digoxigenin antibody. The procedure followed the recommendation of the manufacturer (Serologicals Corp.) of the ApopTag kit used. Four sections each of three embryos of each genotype at E10.5, E11.5, and E12.5 were analyzed.

Supplemental References

1. Trowe M-O, Shah S, Petry M, Airik R, Schuster-Gossler K, Kist R, Kispert A. Loss of Sox9 in the periotic mesenchyme affects mesenchymal expansion and differentiation, and epithelial morphogenesis during cochlea development in the mouse. *Developmental Biology.* 2010;342(1):51-62.

2. Brault V, Moore RT, Kutsch S, Ishibashi M, Rowitch DH, McMahon AP, Sommer L, Boussadia O, Kemler R. Inactivation of the beta-catenin gene by Wnt1-Cre-mediated deletion results in dramatic brain malformation and failure of craniofacial development. *Development.* 2001;128(8):1253-1264.

3. Harada N, Tamai Y, Ishikawa T, Sauer B, Takaku K, Oshima M, Taketo MM. Intestinal polyposis in mice with a dominant stable mutation of the beta-catenin gene. *EMBO J.* 1999;18(21):5931-5942.

4. Muzumdar MD, Tasic B, Miyamichi K, Li L, Luo L. A global double-fluorescent Cre reporter mouse. *genesis.* 2007;45(9):593-605.

5. Moorman AF, Houweling AC, de Boer PA, Christoffels VM. Sensitive nonradioactive detection of mRNA in tissue sections: novel application of the whole-mount in situ hybridization protocol. *J Histochem Cytochem.* 2001;49(1):1-8.

6. Soufan AT, Ruijter JM, van den Hoff MJ, de Boer PA, Hagoort J, Moorman AF. Three-dimensional reconstruction of gene expression patterns during cardiac development. *Physiol Genomics.* 2003;13(3):187-195.

7. Bussen M, Petry M, Schuster-Gossler K, Leitges M, Gossler A, Kispert A. The T-box transcription factor Tbx18 maintains the separation of anterior and posterior somite compartments. *Genes Dev.* 2004;18(10):1209-1221.

Supplemental Online Figures

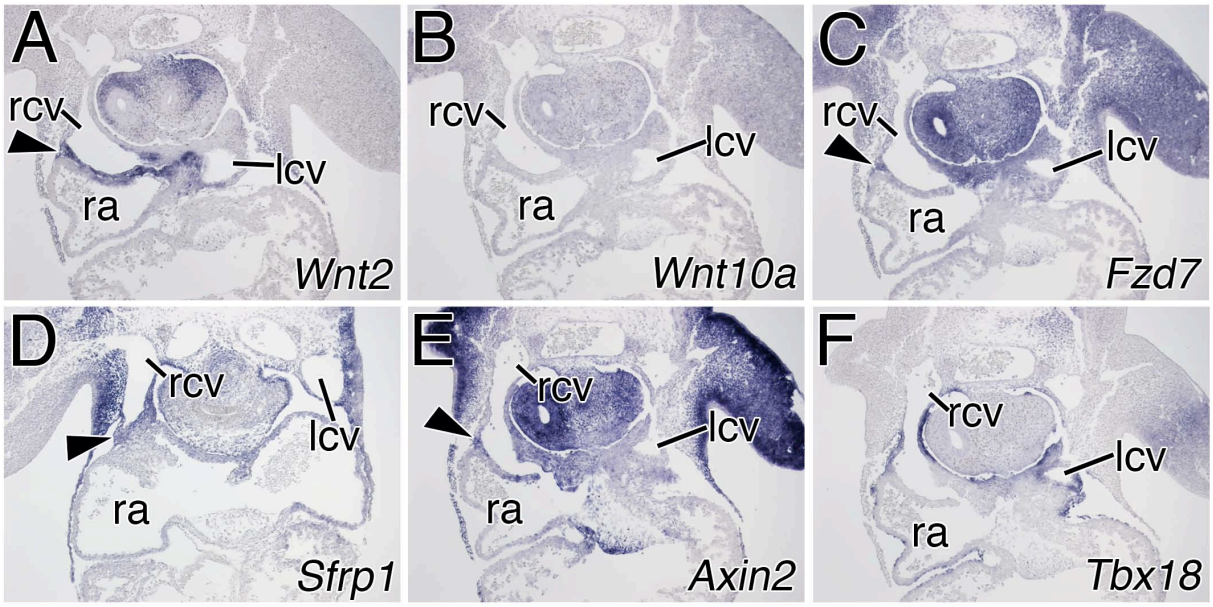

Online Figure 1. Wnt signaling in sinus horn development. *In situ* hybridization analysis on transverse sections through the venous pole region for expression of Wnt pathway components *Wnt2*, *Wnt10a*, *Fzd7* and *Sfrp1* **(A through D)**, and of *Axin2* and *Tbx18* **(E and F)** in wildtype embryos at E10.5. Arrowheads point to the intrapericardial components of the left and right cardinal vein. Probes are as indicated. lcv, left caval vein; ra, right atrium; rcv, right caval vein.

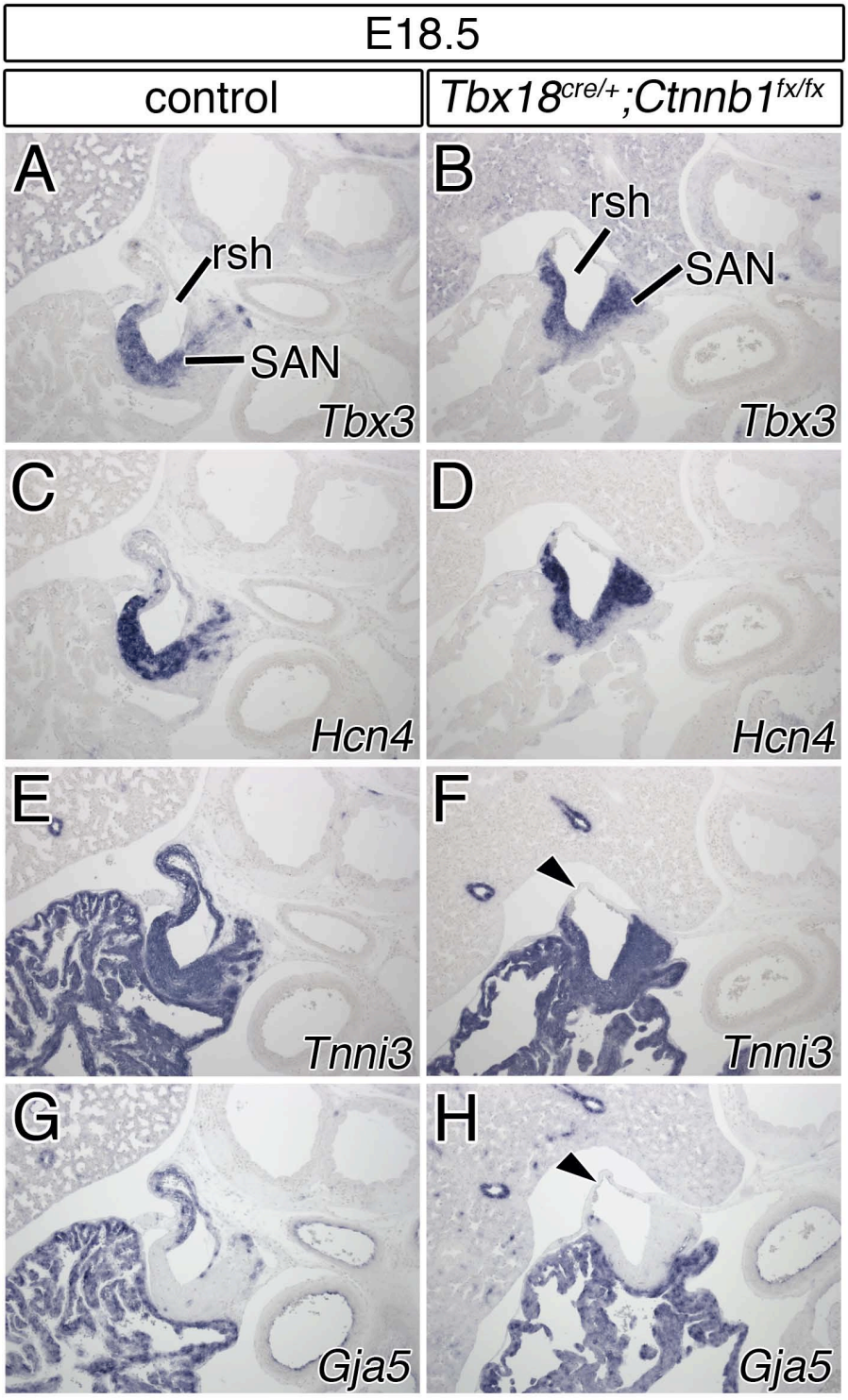

Online Figure 2. Absence of the *Gja5*$^{+}$ myocardium in the dorsal domain of the right sinus horn in *Tbx18*$^{cre/+}$*;Ctnnb1*$^{fx/fx}$ hearts. A through H, *In situ* hybridization analysis for SAN expression of *Tbx3, Hcn4,* cardiomyocyte specific *Tnni3,* and *Gja5* in E18.5 hearts of control (**left column**) and *Tbx18*$^{cre/+}$*;Ctnnb1*$^{fx/fx}$ (**right column**) embryos on transverse sections trough the base of the caval vein. Arrowheads point to the *Tnni3*$^{-}$ domain of the right sinus horn. rsh, right sinus horn; SAN, sinoatrial node.

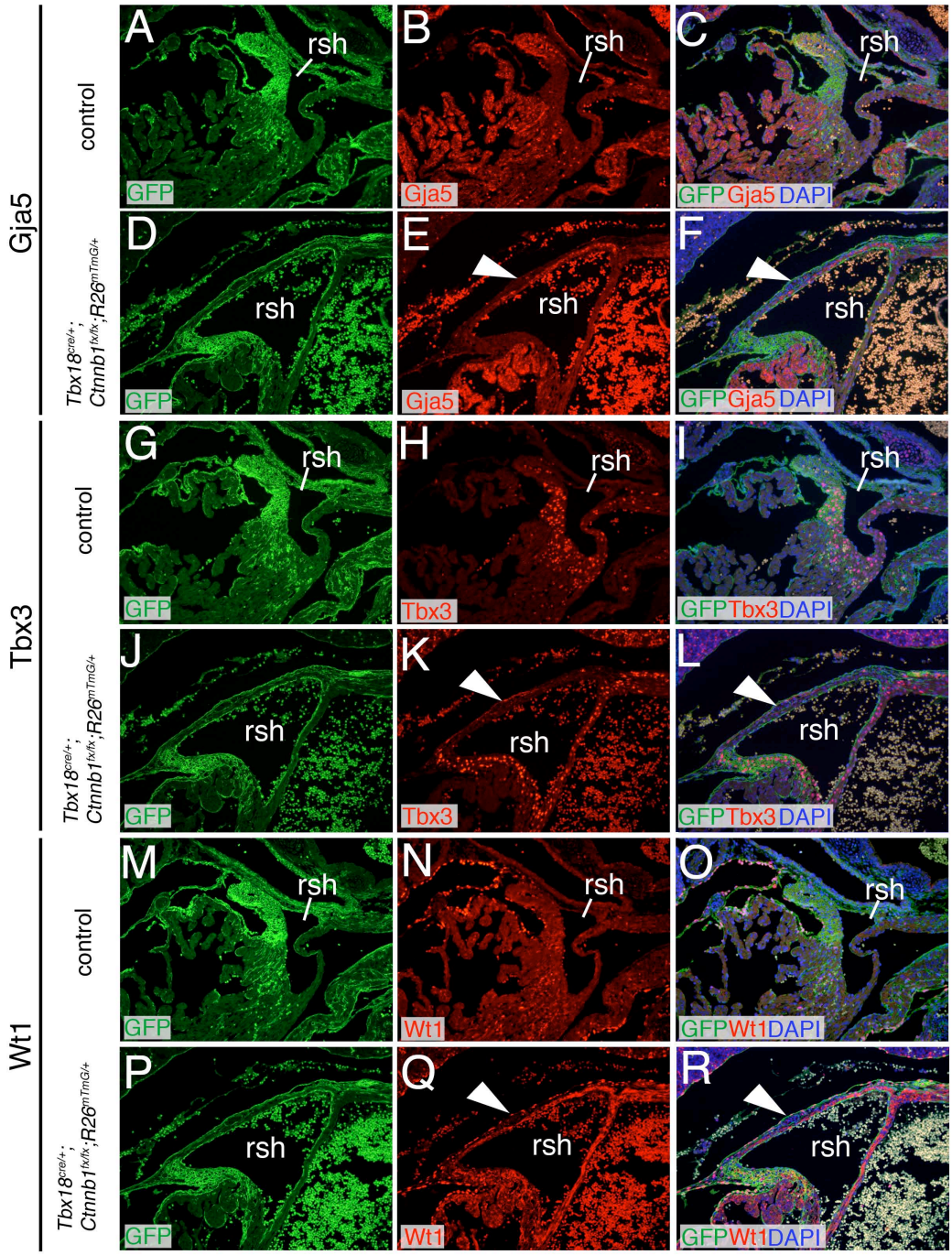

Online Figure 3. Cellular contribution to systemic venous return in E18.5 embryos with conditional deletion of *Ctnnb1*. A through R, Comparative immunofluorescence analysis on transverse sections through the sinus venosus region of control (genotype: *Tbx18*$^{cre/+}$;*R26*$^{mTmG/+}$;*Ctnnb1*$^{fx/+}$) and *Tbx18*$^{cre/+}$;*R26*$^{mTmG/+}$;*Ctnnb1*$^{fx/fx}$ mutant hearts. Cellular derivates of the *Tbx18*$^{+}$ domain of the sinus horns are marked by GFP expression and compared to the gap junction protein Gja5 (**A through F**), the conduction system marker Tbx3 (**G through L**) and the mesothelial marker Wt1 (**M through R**). Arrowheads mark the Tnni3^{-} part of the *Tbx18*$^{cre/+}$;*R26*$^{mTmG/+}$;*Ctnnb1*$^{fx/fx}$ mutant right sinus horns. Genotypes are as indicated. rsh, right sinus horn.

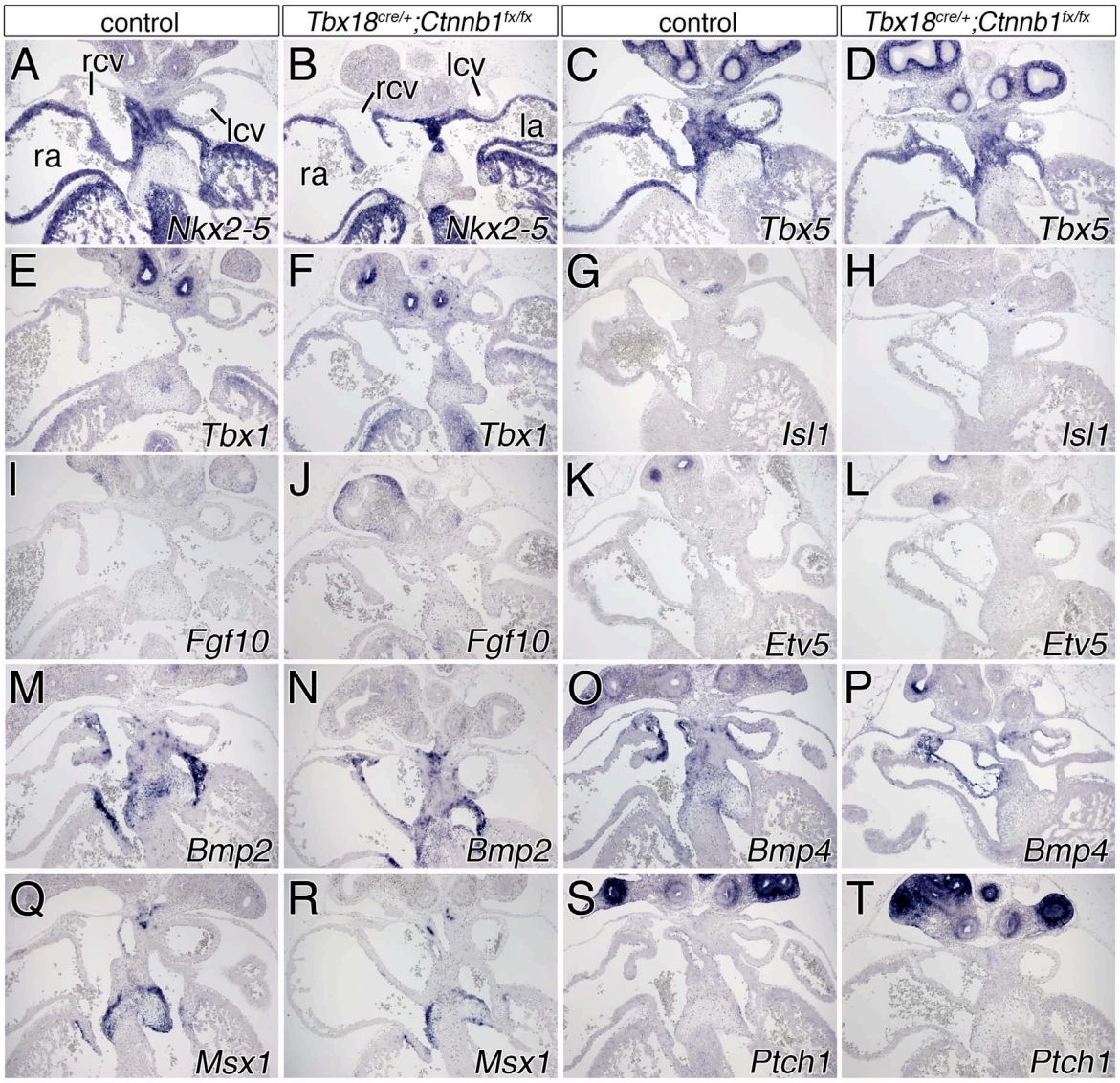

Online Figure 4. Analysis of FHF and SHF marker genes and signaling pathways in *Ctnnb1*-deficient sinus horns. A through T, *In situ* hybridization analysis of the FHF marker genes *Nkx2-5* and *Tbx5* (**A through D**), the SHF genes *Tbx1*, *Isl1* and *Fgf10* (**E through J**), the target of Fgf signaling *Etv5* (**K and L**), the Bmp signaling components *Bmp2*, *Bmp4* and its target gene *Msx1* (**M trough R**) and the Shh signaling target gene *Ptch1* (**S and T**) on transverse sections through the systemic venous return of control (genotype: *Tbx18$^{cre/+}$;Ctnnb1$^{fx/+}$)* and *Tbx18$^{cre/+}$;Ctnnb1$^{fx/fx}$* mutant embryos at E12.5. Probes and genotypes are as indicated. lcv, left caval vein; ra, right atrium; rcv, right caval vein.

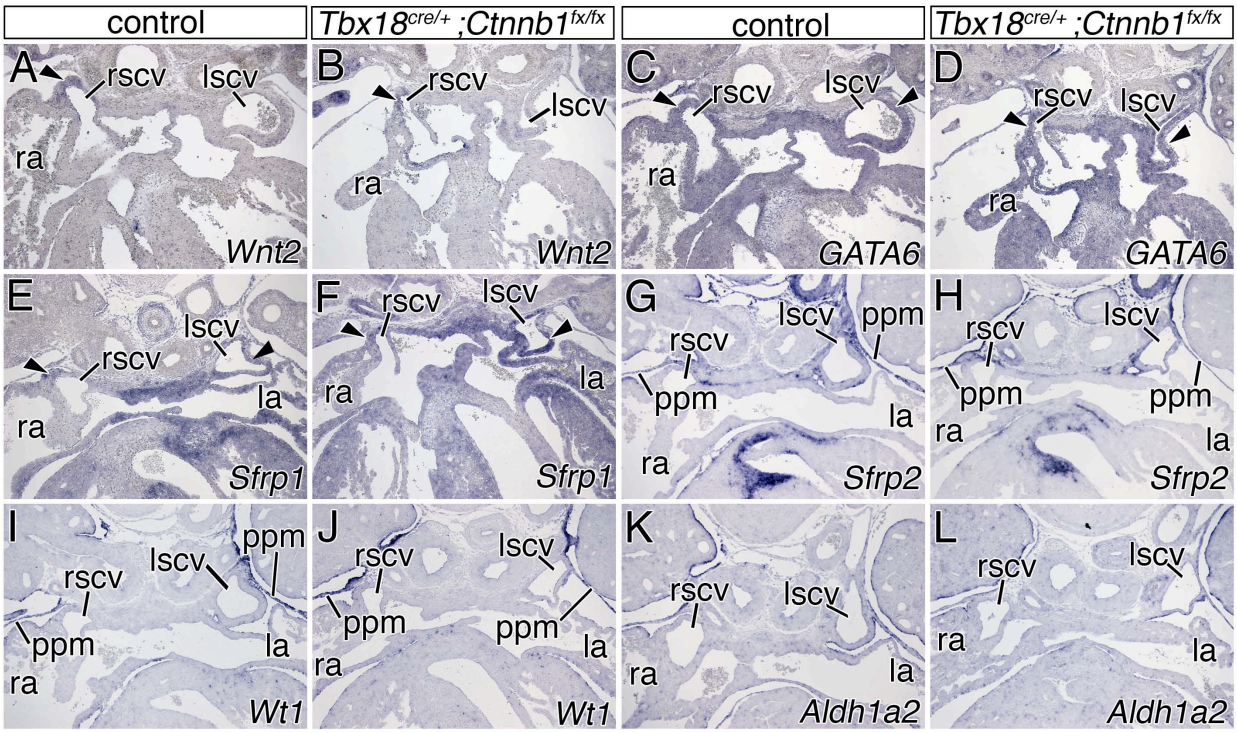

Online Figure 5. Analysis of molecular changes in the *Tbx18*$^{cre/+}$*;Ctnnb1*$^{fx/fx}$ venous pole region of the heart. A through L, *In situ* hybridization analysis of the Wnt ligand *Wnt2* (**A and B**), *Gata6* (**C and D**), the Wnt antagonists *Sfrp1* (**E and F**) and *Sfrp2* (**G and H**), and the mesothelial marker genes *Wt1* (**I and J**) and *Aldh1a2* (**K and L**) on transverse sections through the systemic venous return of control and *Tbx18*$^{cre/+}$*;Ctnnb1*$^{fx/fx}$ mutant embryos at E14.5. Probes and genotypes are as indicated. Arrowheads mark gene expression in the intrapericardial domain of the caval veins. la, left atrium; lscv, left superior caval vein; ppm, pleuro-pericardial membrane; ra, right atrium, rscv, right superior caval vein.

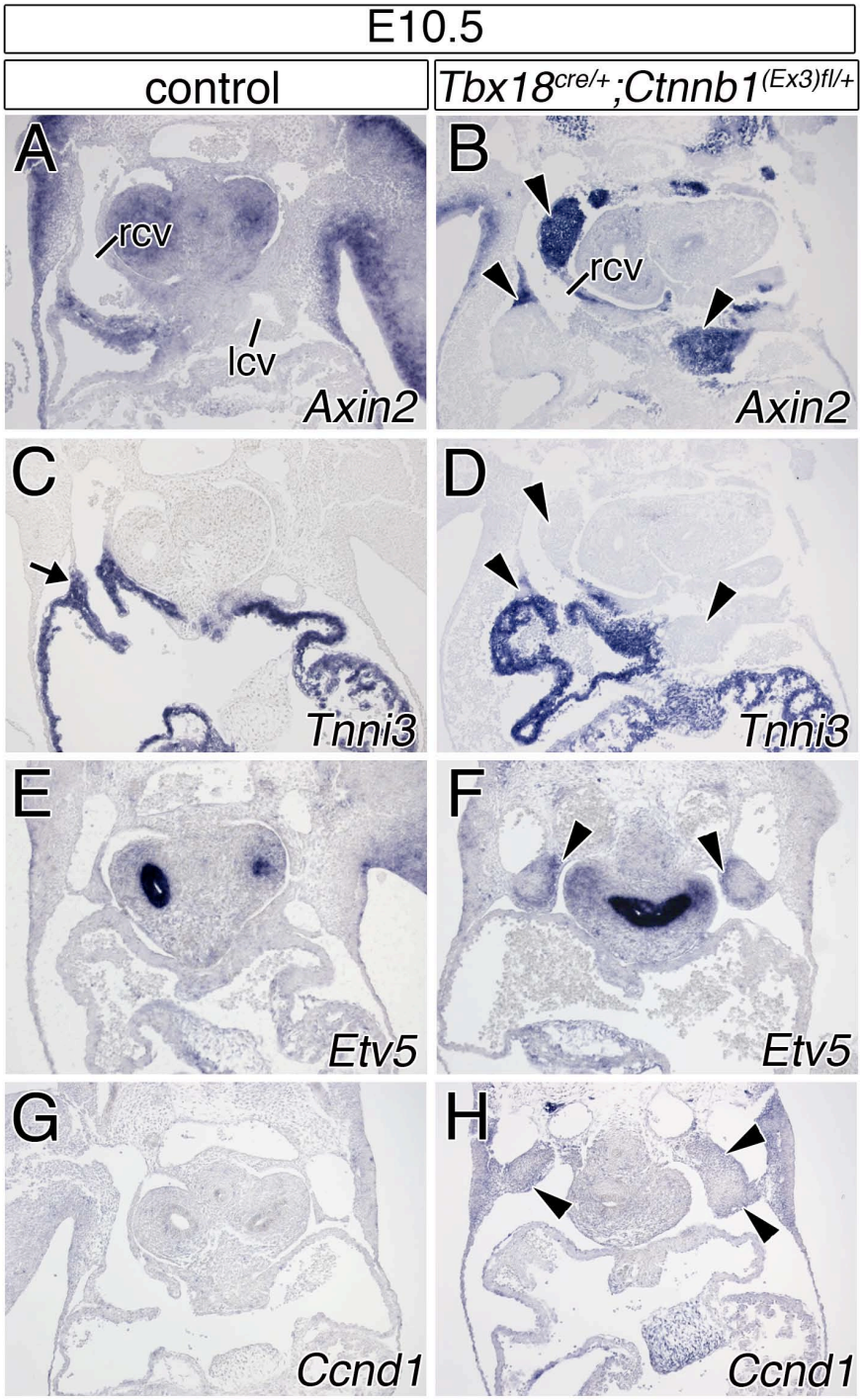

Online Figure 6. Ectopic cell aggregates in *Tbx18*$^{cre/+}$;*Ctnnb1*$^{(Ex3)fl/+}$ mutant sinus horns are detectable at E10.5. A through H, *In situ* hybridization analysis on transverse sections for the canonical Wnt signaling target gene *Axin2* (**A and B**), the cardiomyocyte marker *Tnni3* (**C and D**), the target gene of Fgf signaling *Etv5* (**E and F**) and the direct Wnt target gene and positive regulator of cell cycle progression *Ccnd1* (**G and H**) in the venous pole region of control (left column, genotype: *Tbx18*$^{+/+}$;*Ctnnb1*$^{(Ex3)fl/+}$) and *Tbx18*$^{cre/+}$;*Ctnnb1*$^{(Ex3)fl/+}$ mutant (right column) hearts at E10.5. The arrow points to the Tnni3^{+} ventral domain of the right sinus horn. Arrowheads highlight the ectopic cell clusters in *Tbx18*$^{cre/+}$;*Ctnnb1*$^{(Ex3)fl/+}$ sinus venosus region. lcv, left cardinal vein; rcv, right cardinal vein.

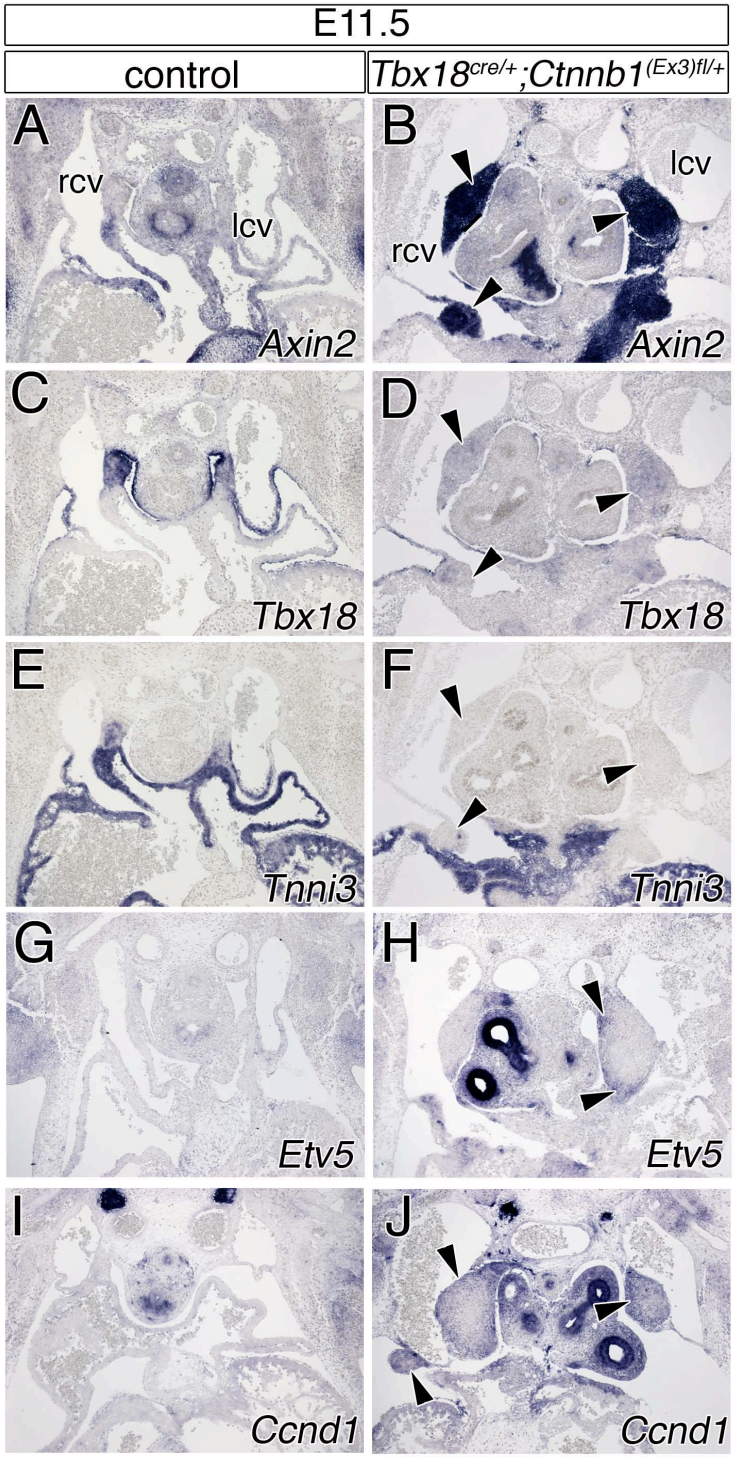

Online Figure 7. Developmental onset of ectopic cell aggregate formation in the *Tbx18*$^{cre/+}$*;Ctnnb1*$^{(Ex3)fl/+}$ sinus venosus region of the heart. A through J, *In situ* hybridization analysis on transverse sections for the Wnt target gene *Axin2* (**A and B**), the sinus horn marker gene *Tbx18* (**C and D**), the cardiomyocyte marker *Tnni3* (E and F), the target gene of Fgf signaling *Etv5* (**G and H**), and the direct Wnt target gene and positive regulator of cell cycle progression *Ccnd1* (**I and J***)* in the venous pole region in control (**left column**) and *Tbx18*$^{cre/+}$*;Ctnnb1*$^{(Ex3)fl/+}$ (**right column**) embryos at E11.5. Arrowheads point to the ectopic cell aggregates in the mutant sinus venosus region. lcv, left cardinal vein; rcv, right cardinal vein.

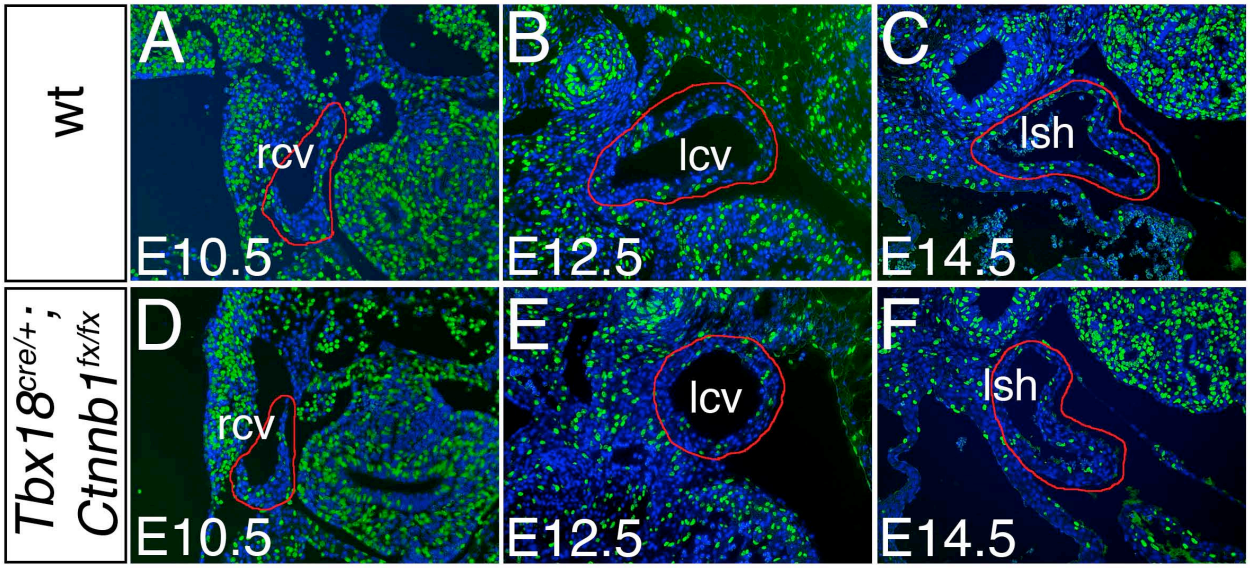

Online Figure 8. **Cellular changes in *Ctnnb1*-deficient sinus horns. A through F**, Analysis of proliferation in the red encircled, *Tbx18*$^{+}$ intrapericardial domain of the sinus horns performed on transverse sections through the posterior systemic venous return by BrdU immunohistochemistry. BrdU positive cells are labeled in green, nuclei are counterstained with DAPI. lcv, left cardinal vein; lsh, left sinus horn; rcv, right cardinal vein.

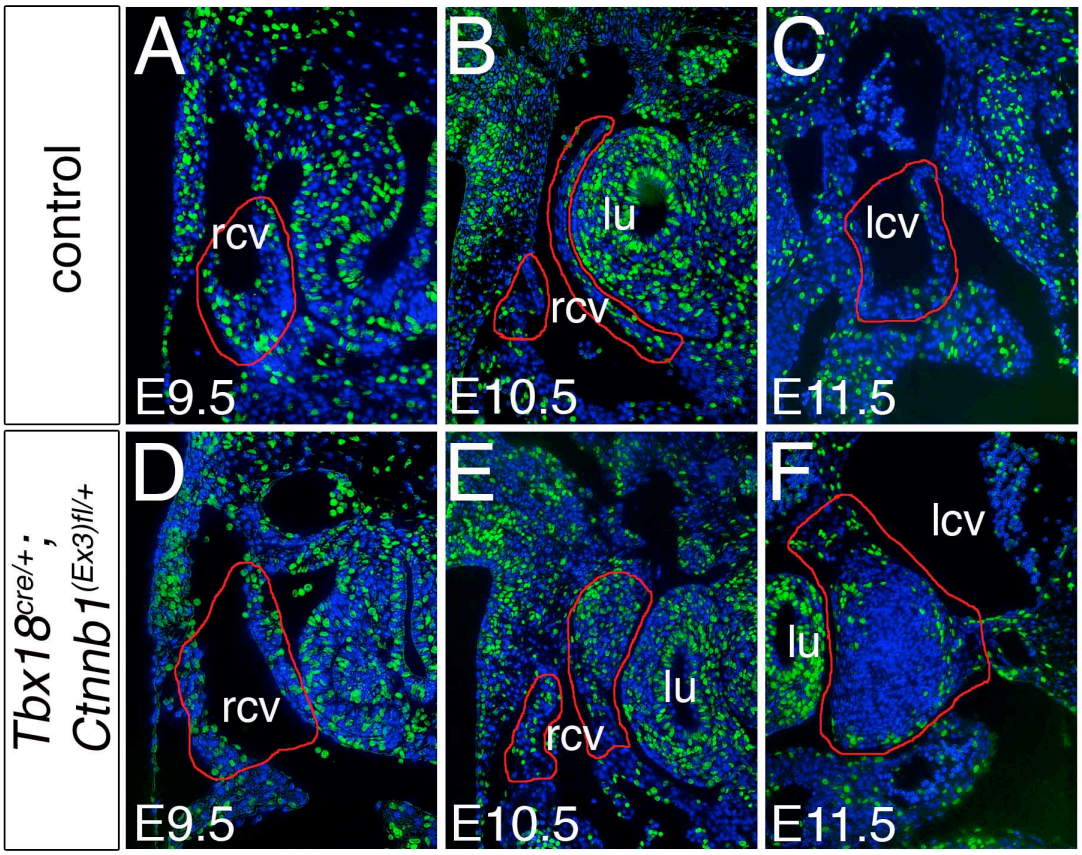

Online Figure 9. Increased cell proliferation in ectopic aggregates of *Tbx18*$^{cre/+}$;*Ctnnb1*$^{(Ex3)fl/+}$ sinus horns. A through F, Analysis of cell proliferation in the red encircled, *Tbx18*$^{+}$ intrapericardial domain of the sinus horns in control hearts and the corresponding intrapericardial domain of the sinus horns in *Tbx18*$^{cre/+}$;*Ctnnb1*$^{(Ex3)fl/+}$ mutant systemic venous return including the ectopic cell aggregates by BrdU immunohistochemistry. BrdU positive cells are labeled in green, nuclei are counterstained with DAPI. lu, lung; other abbreviations are as in Online Figure 8.

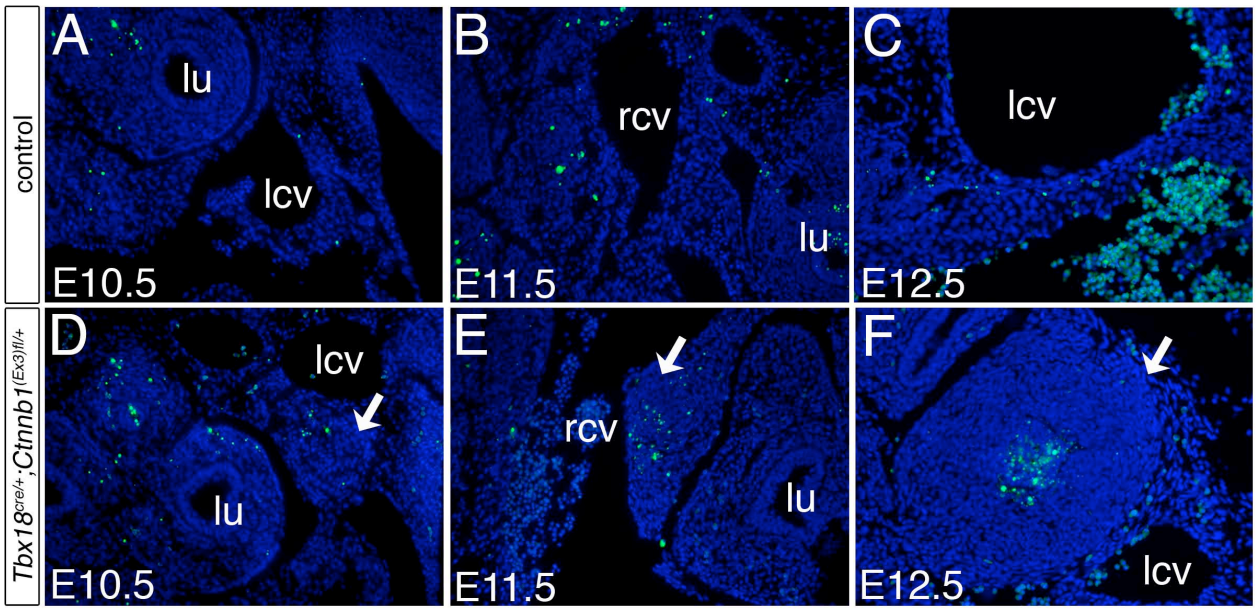

Online Figure 10. Apoptosis is detectable in the ectopic cell aggregates in the sinus venosus region of *Tbx18*$^{cre/+}$*;Ctnnb1*$^{(Ex3)fl/+}$ hearts at different embryonic stages. A through F, Analysis of apoptosis in control (A through C) and *Tbx18*$^{cre/+}$*;Ctnnb1*$^{(Ex3)fl/+}$ (D through F) sinus horns. Stages are as indicated. White arrows mark the mutant cell aggregates. lcv, left cardinal vein; lu, lung; rcv, right cardinal vein.

Concluding remarks

This study contributes significant new insides into the processes that are involved in the development of the cardiac venous pole and its mesothelial lining. I demonstrate that sinus horn and pericardial development are coupled and that both depend on *Wt1* and downstream retinoic acid signaling (part 1) as well as on canonical Wnt/beta-catenin signaling (part 3 and 4). Furthermore, this work includes the first characterization of the mechanisms involved in murine pericardial development and identifies the T-box transcription factor *Tbx18* as a crucial gene partly regulating these processes (part 2).

This work illustrates that two independent steps are essential for the development of a complete pericardium. On the one hand, the pleuropericardial membranes detach from the lateral body wall, a process that requires the disintegration of the subcoelomic mesenchyme. I discovered important factors (*Wt1* and retinoic acid signaling, canonical Wnt signaling) regulating the loss of the subcoelomic mesenchyme and the associated increase of the pleural cavity. However, most of the genetic circuit that regulates the disappearance of the subcoelomic mesenchyme is still unidentified. In a comparable cavitation process during middle ear development apoptosis is partly responsible for the loss of mesenchymal cells, but most of these mesenchymal cells are reallocated over the increasing surface of the growing cavity.[34,35] Throughout the analysis of *Wt1*-deficient embryos, I also detected low rates of apoptosis in the subcoelomic mesenchyme of wildtype embryos which was specifically lost in *Wt1*-deficient embryos. Further work will concentrate on the quantification of apoptosis, and the characterization of the fate of these subcoelomic mesenchymal cells by lineage tracing experiments. Additionally, I will enforce the identification of genes that regulate the fate of these mesenchymal cells and the pleuropericardial membranes. A first approach by a gene expression screen in the subcoelomic mesenchyme and the developing pleuropericardial membranes was already performed, and its results may point to the direction of prospective experiments.

A second mechanism that is involved in pericardial development is the closure of the pleuropericardial ducts by a *Tbx18*-positive mesenchymal protrusion within these canals. I conclude that the closure of the pleuropericardial ducts is partly required for the medial positioning of the caval veins next to the hilus of the lung. In the absence of sinus horn attachment to their medial fixation point, the tensile force of the increasing embryonic size onto the pleuropericardial membranes leads to the their lateral positioning. This tension might also be partly essential for the detachment of the pleuropericardial membranes from the lateral body wall, a mechanism that was already proposed for human pericardial development,[11] but neither cellular nor genetically analyzed. Therefore, the underlying mechanisms need to be further examined, as molecular insides into these processes are unidentified so far.

In *Wt1*-deficient embryos the sinus horns are positioned laterally within the persisting subcoelomic mesenchyme and not myocardialized. At this time I speculated that a medial

positioning of the sinus horns next to the hilus of the lung and thus to sources of differentiation signals is a prerequisite for their myocardialization. However, my analysis in conditional beta-catenin gain- and loss-of-function embryos questioned my earlier statements, as the caval veins are myocardialized although they are embedded in a persisting subcoelomic mesenchyme. However, in addition to the known significance of *Tbx18* for the myocardialization of the sinus horns, my analysis demonstrated the importance of canonical Wnt signaling specifically in the *Tbx18*-positive domain of the sinus horn for their myocardialization. In this specific domain of the sinus horns the beta-catenin mediated Wnt signaling pathway is required to maintain the proliferation of progenitor cells. Also in general, canonical Wnt/beta-catenin signaling is known to be important for precursor cell proliferation and additionally it inhibits the terminal differentiation of these cells in various developmental processes, one of them is the elongation of the heart tube by the progenitor cells of the second heart field.[20] Whether this signaling pathway has a similar function in pericardial development remains unanswered so far.

Recent publications emphasized the evolutionary conservation of genetic mechanisms regulating embryonic cardiac development.[36] In both human and murine venous pole development the myocardialized caval veins are positive for *Tbx18* and negative for *Nkx2-5* expression. Furthermore, human pericardial development is described as an active ingrowth of two pleuropericardial folds, which will form the pleuropericardial membranes and later the mature pericardium.[37] I was not able to verify an active ingrowth of two folds into the pleuropericardial ducts during murine pericardial development. In my opinion this interpretation of human pericardial development may be the result of limited human embryonic material available. The genetic background of human pericardial defects is completely missing at the moment, but a sporadic familiar accumulation of this defect points to inherited genetic defects.[38] Future analysis might reveal more similarities between murine and human cardiac development, therefore my research in this so far insufficiently examined region of the heart will continue.

References

1. Stennard F, Harvey R. T-box transcription factors and their roles in regulatory hierarchies in the developing heart. *Development*. 2005 Nov 1;132(22):4897-910.
2. Harvey R. Patterning the vertebrate heart. *Nat Rev Genet*. 2002 Juli 1;3(7):544-56.
3. Anderson R, Brown N, Moorman A. Development and structures of the venous pole of the heart. *Dev Dyn*. 2006 Jan 1;235(1):2-9.
4. Gruber PJ, Epstein JA. Development Gone Awry: Congenital Heart Disease. *Circ Res*. 2004 Feb 20;94(3):273-283.
5. Bruneau B. The developmental genetics of congenital heart disease. *Nature*. 2008 Feb 21;451(7181):943-8.
6. Nemer M. Genetic insights into normal and abnormal heart development. *Cardiovasc Pathol*. 2008 Jan 1;17(1):48-54.
7. Moorman A, Christoffels V, Anderson R. Anatomic substrates for cardiac conduction. *Heart rhythm*. 2005;2(8):875-86.
8. Sadler TW, Langman J. Medizinische Embryologie. Die normale menschliche Entwicklung und ihre Fehlbildungen. 10. Aufl. Thieme, Stuttgart; 2003.
9. Persaud TVN, Moore KL. Embryologie. 5. Aufl. München [u.a.]: Elsevier, Urban & Fischer; 2007.
10. Salzer GM. Der Verschluss der pleuroperikardialen Verbindung bei menschlichen Embryonen. *Z Anat Entwickl Gesch*. 1959;121(2):54-70.
11. Salzer GM. Die Topogenese der Pleurahoehlen. *Z. Anat. Entwickl. Gesch.* 1960;122(3):232-240.
12. Buckingham M, Meilhac S, Zaffran S. Building the mammalian heart from two sources of myocardial cells. *Nat Rev Genet*. 2005 Nov 1;6(11):826-35.
13. Rosenthal N, Harvey RP. Heart Development and Regeneration. Elsevier Science & Technology; 2010.
14. Vincent S, Buckingham M. How to make a heart: the origin and regulation of cardiac progenitor cells. *Curr Top Dev Biol*. 2010 Jan 1;90:1-41.
15. van den Berg G, Abu-Issa R, de Boer BA, Hutson MR, de Boer PAJ, Soufan AT, Ruijter JM, Kirby ML, van den Hoff MJB, Moorman AFM. A Caudal Proliferating Growth Center Contributes to Both Poles of the Forming Heart Tube. *Circ Res*. 2009 Jan 30;104(2):179-188.
16. Chen L, Fulcoli FG, Tang S, Baldini A. Tbx1 Regulates Proliferation and Differentiation of Multipotent Heart Progenitors. *Circ Res*. 2009 Okt 23;105(9):842-851.
17. Tirosh-Finkel L, Zeisel A, Brodt-Ivenshitz M, Shamai A, Yao Z, Seger R, Domany E, Tzahor E. BMP-mediated inhibition of FGF signaling promotes cardiomyocyte differentiation of anterior heart field progenitors. *Development*. 2010;137(18):2989 -3000.
18. Hutson MR, Zeng XL, Kim AJ, Antoon E, Harward S, Kirby ML. Arterial pole progenitors interpret opposing FGF/BMP signals to proliferate or differentiate. *Development*. 2010;137(18):3001 -3011.
19. Tian Y, Yuan L, Goss A, Wang T, Yang J, Lepore J, Zhou D, Schwartz R, Patel V, Cohen E, Morrisey E. Characterization and In Vivo Pharmacological Rescue of a Wnt2-Gata6 Pathway Required for Cardiac Inflow Tract Development. *Developmental cell*. 2010 Feb 16;18(2):275-287.
20. Gessert S, Kühl M. The multiple phases and faces of wnt signaling during cardiac differentiation and development. *Circulation Research*. 2010 Juli 23;107(2):186-99.

21. Christoffels V, Mommersteeg M, Trowe M, Prall O, De Gier-De Vries C, Soufan A, Bussen M, Schuster-Gossler K, Harvey R, Moorman A, Kispert A. Formation of the venous pole of the heart from an Nkx2-5-negative precursor population requires Tbx18. *Circulation Research*. 2006 Juni 23;98(12):1555-63.

22. Mommersteeg MTM, Domínguez JN, Wiese C, Norden J, de Gier-de Vries C, Burch JBE, Kispert A, Brown NA, Moorman AFM, Christoffels VM. The sinus venosus progenitors separate and diversify from the first and second heart fields early in development. *Cardiovascular Research*. 2010 Juli 1;87(1):92 -101.

23. Greulich F, Rudat C, Kispert A. Mechanisms of T-box gene function in the developing heart. *Cardiovasc Res*. 2011 Apr 14; *In press*.

24. Grieskamp T, Rudat C, Lüdtke TH-W, Norden J, Kispert A. Notch signaling regulates smooth muscle differentiation of epicardium-derived cells. *Circ. Res*. 2011 Apr 1;108(7):813-823.

25. Wiese C, Grieskamp T, Airik R, Mommersteeg M, Gardiwal A, De Gier-De Vries C, Schuster-Gossler K, Moorman A, Kispert A, Christoffels V. Formation of the sinus node head and differentiation of sinus node myocardium are independently regulated by Tbx18 and Tbx3. *Circulation Research*. 2009 Feb 13;104(3):388-97.

26. Christoffels V, Grieskamp T, Norden J, Mommersteeg M, Rudat C, Kispert A. Tbx18 and the fate of epicardial progenitors. *Nature*. 2009 Apr 16;458(7240):E8-10.

27. Gittenberger-De Groot A, Mahtab E, Hahurij N, Wisse L, DeRuiter M, Wijffels M, Poelmann R. Nkx2.5-negative myocardium of the posterior heart field and its correlation with podoplanin expression in cells from the developing cardiac pacemaking and conduction system. *Anatomical record (Hoboken, NJ : 2007)*. 2007 Jan 1;290(1):115-22.

28. Mahtab E, Vicente-Steijn R, Hahurij N, Jongbloed M, Wisse L, DeRuiter M, Uhrin P, Zaujec J, Binder B, Schalij M, Poelmann R, Gittenberger-De Groot A. Podoplanin deficient mice show a RhoA-related hypoplasia of the sinus venosus myocardium including the sinoatrial node. *Dev Dyn*. 2009 Jan 1;238(1):183-93.

29. Blaschke R, Hahurij N, Kuijper S, Just S, Wisse L, Deissler K, Maxelon T, Anastassiadis K, Spitzer J, Hardt S, Schöler H, Feitsma H, Rottbauer W, Blum M, Meijlink F, Rappold G, Gittenberger-De Groot A. Targeted mutation reveals essential functions of the homeodomain transcription factor Shox2 in sinoatrial and pacemaking development. *Circulation*. 2007 Apr 10;115(14):1830-8.

30. Moore A, McInnes L, Kreidberg J, Hastie N, Schedl A. YAC complementation shows a requirement for Wt1 in the development of epicardium, adrenal gland and throughout nephrogenesis. *Development*. 1999 Mai 1;126(9):1845-57.

31. Kreidberg J, Sariola H, Loring J, Maden M, Pelletier J, Housman D, Jaenisch R. WT-1 is required for early kidney development. *Cell*. 1993;74(4):679-91.

32. Discenza M, Pelletier J. Insights into the physiological role of WT1 from studies of genetically modified mice. *Physiological Genomics*. 2004 Feb 13;16(3):287-300.

33. Mutsaers S, Wilkosz S. Structure and function of mesothelial cells. *Cancer Treat Res*. 2007 Jan 1;134:1-19.

34. Richter CA, Amin S, Linden J, Dixon J, Dixon MJ, Tucker AS. Defects in middle ear cavitation cause conductive hearing loss in the Tcof1 mutant mouse. *Human Molecular Genetics*. 2010 Apr 15;19(8):1551 -1560.

35. Piza J, Northrop C, Eavey RD. Embryonic middle ear mesenchyme disappears by redistribution. *The Laryngoscope*. 1998 Sep 1;108(9):1378-1381.

36. Sizarov A, Anderson R, Christoffels V, Moorman A. Three-dimensional and molecular analysis of the venous pole of the developing human heart. *Circulation*. 2010;122(8):798-807.

37. Faridah Y, Julsrud P. Congenital absence of pericardium revisited. *The international journal of cardiovascular imaging*. 2002 Feb 1;18(1):67-73.

38. Verloes A, Perrin L, Delbecque K, Gonzales M, Demarche M, Dekoster G. Congenital absence of the left pericardium and diaphragmatic defect in sibs. *Eur J Med Genet.* 2010 Juni;53(3):133-135.

Acknowledgements

First, I thank my supervisor Prof. Dr. Andreas Kispert for the great opportunity to work on these fascinating projects in his laboratory. Furthermore, I thank him for his continuous and enthusiastic support during the last years.

I would like to thank Prof. Dr. Hans-Jörg Jacobsen and PD Dr. Florian P. Limbourg for their kind acceptance as a referee during my dissertation.

And thanks to everyone all over the world who make my research possible by providing mice, plasmids, or technical help.

Thanks to all my colleagues in the laboratory of Andreas Kispert, and the whole IfM for discussions, help, and a nice working atmosphere.

In particular I wish to thank Franziska Greulich, Dr. Thomas Grieskamp, and Carsten Rudat for special support in my research projects.
Additionally, I thank Anna Foik and Anna-Carina Weiss for personal encouragement during the last years.

Curriculum vitae

Name:	Julia Norden
Date of birth:	18/05/1978
Place of birth:	Walsrode
Citizenship:	German
E-mail:	norden.julia@mh-hannover.de

School education:

1984 – 1988	Grundschule Kirchboitzen
1988 – 1990	Orientierungsstufe Rethem
1990 – 1997	Gymnasium Walsrode

Apprenticeship and previous work experience:

1997 – 2000	professional education as laboratory assistant ("Milchwirtschaftliche Laborantin"), Nordmilch eG, Zeven, Germany
2000	employed as laboratory assistant ("Milchwirtschaftliche Laborantin") Uelzena eG, Uelzen, Germany

University studies:

2000 – 2002	Undergraduate studies of Biotechnology ("Vordiplom") at the Technical University of Braunschweig
2002 – 2006	Graduate studies of Biotechnology ("Diplom") at the Technical University of Braunschweig
2005 – 2006	Diploma thesis in the Institute for Microbiology at the Technical University of Braunschweig, under supervision of Prof. Dr. Dieter Jahn, Title of diploma thesis: "Chromosomale Integration in *Bacillus megaterium*"
2006 – 2011	Research assistant in the laboratory of Prof. Dr. Andreas Kispert in the Institute for Molecular Biology at Hannover Medical School

List of publications

Wnt/beta-catenin signaling maintains the mesenchymal precursor pool for murine sinus horn formation.
Norden J. , Greulich F., Rudat C., Taketo M. M., Kispert A.
Circ Res. 2011, *in press*

Notch signaling regulates smooth muscle differentiation of epicardium-derived cells.
Grieskamp T, Rudat C, Lüdtke THW, **Norden J**, Kispert A.
Circ Res. 2011 Apr 1;108(7):813-23.

Developmental origin, growth, and three-dimensional architecture of the atrioventricular conduction axis of the mouse heart.
Aanhaanen WT, Mommersteeg MT, **Norden J**, Wakker V, de Gier-de Vries C, Anderson RH, Kispert A, Moorman AF, Christoffels VM.
Circ Res. 2010 Sep 17;107(6):728-36.

The sinus venosus progenitors separate and diversify from the first and second heart fields early in development.
Mommersteeg MT, Domínguez JN, Wiese C, **Norden J**, de Gier-de Vries C, Burch JB, Kispert A, Brown NA, Moorman AF, Christoffels VM.
Cardiovasc Res. 2010 Jul 1;87(1):92-101.

Wt1 and retinoic acid signaling in the subcoelomic mesenchyme control the development of the pleuropericardial membranes and the sinus horns.
Norden J, Grieskamp T, Lausch E, van Wijk B, van den Hoff MJ, Englert C, Petry M, Mommersteeg MT, Christoffels VM, Niederreither K, Kispert A.
Circ Res. 2010 Apr 16;106(7):1212-20.

Tbx20 interacts with smads to confine tbx2 expression to the atrioventricular canal.
Singh R*, Horsthuis T*, Farin HF, Grieskamp T**, Norden J**, Petry M, Wakker V, Moorman AF, Christoffels VM, Kispert A.
Circ Res. 2009 Aug 28;105(5):442-52, *contributed equally to this work.

The Tbx2+ primary myocardium of the atrioventricular canal forms the atrioventricular node and the base of the left ventricle.
Aanhaanen WT, Brons JF, Domínguez JN, Rana MS, **Norden J**, Airik R, Wakker V, de Gier-de Vries C, Brown NA, Kispert A, Moorman AF, Christoffels VM.
Circ Res. 2009 Jun 5;104(11):1267-74.

Tbx18 and the fate of epicardial progenitors.

Christoffels VM, Grieskamp T, **Norden J**, Mommersteeg MT, Rudat C, Kispert A.

Nature. 2009 Apr 16;458(7240):E8-9; discussion E9-10.

Declaration

I hereby declare and confirm that this thesis is entirely the result of my own work except where otherwise indicated. This thesis has not been used as part of any other examination.

Julia Norden
Hannover, 06/05/2011

Erklärung zur Dissertation

Hiermit erkläre ich, dass ich die Dissertation “Molecular programs in the venous pole of the developing murine heart” selbständig verfasst habe und alle benutzten Hilfsmittel sowie evtl. zur Hilfeleistung herangezogenen Institutionen vollständig angegeben habe.

Die Dissertation wurde nicht schon als Diplom- oder ähnliche Prüfungsarbeit verwendet.

Julia Norden
Hannover, den 06.05.2011